# LIGHT ALKANE CONVERSION TO VALUABLE LIQUID HYDROCARBONS ON BIFUNCTIONAL CATALYSTS IN A SINGLE STEP

by

**Che-Wei Chang**

**A Dissertation**

*Submitted to the Faculty of Purdue University*

*In Partial Fulfillment of the Requirements for the degree of*

**Doctor of Philosophy**


Davidson School of Chemical Engineering

West Lafayette, Indiana

May 2022

# THE PURDUE UNIVERSITY GRADUATE SCHOOL
# STATEMENT OF COMMITTEE APPROVAL

**Dr. Jeffrey T. Miller, Chair**

Davidson School of Chemical Engineering, Purdue University

**Dr. Abhaya K. Datye**

Department of Chemical and Biological Engineering, University of New Mexico

**Dr. Rajamani Gounder**

Davidson School of Chemical Engineering, Purdue University

**Dr. Jeffrey P. Greeley**

Davidson School of Chemical Engineering, Purdue University

**Dr. Christina W. Li**

Department of Chemistry, Purdue University

**Approved by:**

Dr. John A. Morgan

*To my family, for their unconditional love and support*

# ACKNOWLEDGMENTS

It has been an amazing journey for my Ph.D. experience at Purdue. I have learned and grown a lot regarding research, engineering, and presentation skills. I would like to thank all the people that I worked with for their mentoring, help and support.

First of all, I would like to express my gratitude to my advisor, Professor Jeff Miller. It is always inspiring and fun to talk about science with Jeff. Jeff's mentoring has helped me learn how to identify and solve the most important problems effectively. I will remember those stories he always told, such as turn lead into gold and lake Michigan, which are interesting and rich in philosophy. I feel appreciative and fortunate to work with and learn from Jeff.

Additionally, I would like to thank my committee members, Dr. Abhaya Datye, Dr. Raj Gounder, Dr. Jeff Greeley, and Dr. Christina Li for offering useful feedbacks and suggestions in my Ph.D. research journey. I am always excited to present my research progress to Dr. Datye during CISTAR meeting and listening to his insightful comments about the metal catalysis. The feedbacks that Dr. Gounder gave me always motivates me to dive deeper into the fundamental of kinetic and diffusion of the bifunctional catalyst system. I am grateful that Dr. Greeley suggests me to investigate reaction pathway by cofeeding reaction intermediates. Dr. Li's advanced inorganic chemistry class has given me a more profound understanding of molecular orbital interaction between the reactant and the metal. These valuable conversations have helped me to come up with new ideas and think in different perspectives.

I would like to thank all the past and current members of Miller group: Dr. Nicole Libretto, Dr. Johnny Zhu Chen, Dr. Laryssa Cesar, Matt Conrad, Kurt Russel, Junxian Gou, David Dean, Christian Becker, Wenqing Zhang, Jiajing Kuo and Hamta Bardool. Nicole and Johnny have mentored me how to solve technical and research problems and helped me prepare my qualifying exam presentation. It was such a fun experience to work with two of you in the beamline at APS. I will remember all the helpful conversations and laughter we shared. Thank Matt and David for helping me fix high pressure reactors and GC.

I would like to express my gratitude to my collaborators, Ryan Alcala and Dr. Hien Pham, for conducting TEM and EDX for my samples very efficiently. I also would like to thank David and Ryan for getting me involved in the project of the stability and regeneration of Pt alloy for propane dehydrogenation. I feel so lucky being able to work with all of you and have learned so much from our collaborative work.

Finally, I would like to acknowledge my family and friends who have always been supportive throughout the highs and lows during my Ph.D. life. Their accompany and encouragement makes me pursue my passion toward scientific research adamantly. I would like to thank my parents for their unconditional love and support.

I appreciate all the moments that made me feel uncomfortable because it showed me the limit and possibility.

# TABLE OF CONTENTS

# LIST OF TABLES

# LIST OF FIGURES

# ABSTRACT

Cyclar process was previously developed to convert propane and butane into aromatics using gallium-promoted ZSM-5 zeolites (Ga/ZSM-5). However, it has two major limitations. Firstly, light gases (methane and ethane) limit the yield of higher molecular weight hydrocarbons for propane conversion. Secondly, ethane is unreactive on Ga/ZSM-5 catalysts. Relative rates and selectivity for propane conversion on two components, gallium ($Ga/Al_2O_3$) and acid ZSM-5 (H-ZSM-5) were investigated, and the results suggest that light gas was produced by propane monomolecular cracking on ZSM-5 due to the imbalance of alkane dehydrogenation and olefin conversion rates on two catalytic functions. A PtZn alloy catalyst, which has >99% propene selectivity and 30 times higher rate than Ga, was used for the dehydrogenation function. The bifunctional $PtZn/SiO_2$+ZSM-5 catalyst has high yields of aromatics with low methane selectivity (<5%) at ~70% propane conversion. The results suggest methane can be minimized by utilizing the PtZn alloy and lowering the monomolecular cracking rate by ZSM-5. In addition, PtZn alloy increases aromatics selectivity. Aromatics formation pathway was investigated by studying the rate and selectivity of a model intermediate (cyclohexene) on ZSM-5, $PtZn/SiO_2$ and $Ga/Al_2O_3$. Benzene is formed at similar rates on $Ga/Al_2O_3$ and ZSM-5 but cracking of cyclohexene on the latter is two orders of magnitude higher than the benzene formation rate, indicating cracking of cyclic hydrocarbons leads to low aromatization rate on Ga/ZSM-5. The benzene formation rate on the $PtZn/SiO_2$ is 200 times higher than that on ZSM-5, suggesting aromatics are formed by the metal pathway on $PtZn/SiO_2$+ZSM-5.

Unlike Ga/ZSM-5 catalysts, $PtZn/SiO_2$+ZSM-5 catalysts also convert propane to aromatics at low temperature (350 ℃). The temperature effect on propane dehydroaromatization pathways on the $PtZn/SiO_2$+ZSM-5 bifunctional catalysts was investigated to develop strategies for propane conversion to valuable liquid hydrocarbons. At high temperature (550 ℃), high dehydrogenation rates and lower monomolecular cracking rates are required to minimize methane formation, leading to primarily propene and BTX (benzene, toluene, and xylenes). By recycling propene in the propane conversion range of 30-45%, >80% BTX yields is likely achievable at full recycle. At mid temperature (400-450 ℃), the product has high selectivity to gasoline-blending hydrocarbons (butanes, $C_5^+$ hydrocarbons, toluene, and xylenes) at 15-25% propane conversions because

dehydrogenation rates are moderately high, and oligomerization is more favored than cracking. At low temperature (350℃), ~25% propane conversion is achieved and has high selectivity (~60%) to butanes, but the propane conversion rates are likely too low to be practical. While methane formation by monomolecular cracking limits liquid yields at high reaction temperature, at mid and low temperatures, hydrogen co-produced at high propane conversions saturates light olefins to make undesired ethane, which becomes major yield-loss reaction on the PtZn/$SiO_2$+ZSM-5.

Finally, PtZn/$SiO_2$+ZSM-5 catalysts can convert ethane to $C_3^+$ and aromatics but the methane selectivity increases rapidly at high ethane conversion. The roles of two catalytic function (Pt-Zn alloy and ZSM-5) in the dehydroaromatization pathways of ethane and propane will be further studied and their product distribution will be compared to have better understandings on the differences in the dominant yield-loss reaction and dehydroaromatization pathways.

# 1. INTRODUCTION

## 1.1 The U.S Shale Gas Boom

Shale gas production in the U.S has increased the supply of light alkanes, especially methane, ethane, and propane. Particularly, ethane and propane could be converted to ethene and propene and further transformed into other higher molecular weight hydrocarbons for production of polymers, chemicals, and fuels.[1] However, many of the light alkanes production sites are distributed in the remote areas distant from most chemical processing facilities at the East, West and Gulf coast regions (Figure 1), which requires costly transportation over long distances by a pipeline. Direct transformation of $C_2$-$C_3$ light alkane into chemicals and/or high-octane gasoline blending components, including $C_3^+$ olefins, oligomers and aromatics could become an attractive option.[1]

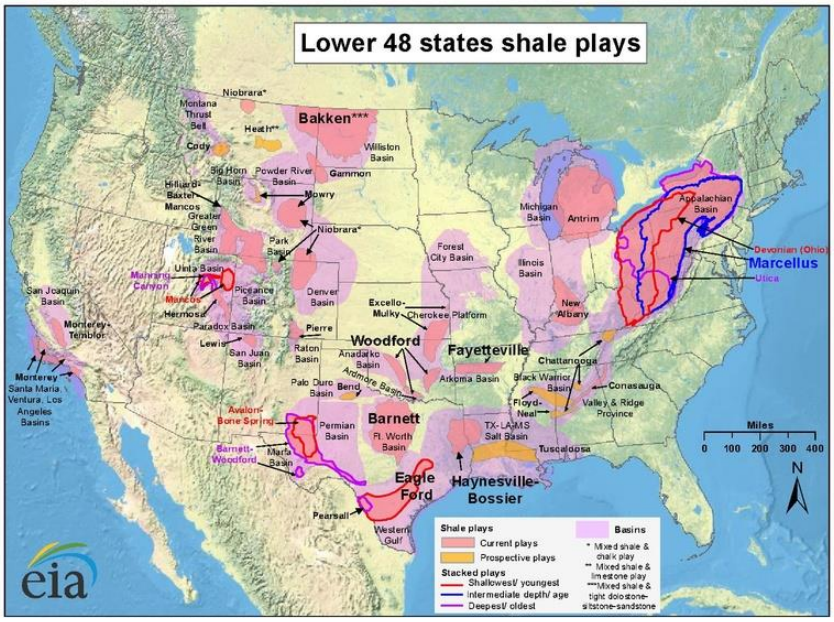


Figure 1. The map of shale gas in the United States

## 1.2 Propane Dehydroaromatization

In early studies, Csicsery has reported the dehydrocyclodimerization of $C_3$-$C_5$ alkanes over the bifunctional $Pt/Al_2O_3$ catalysts (with acid and dehydrogenation activities) and proposed a mechanism for the reactions involving alkane dehydrogenation, olefin dimerization, cracking, and aromatization.[2–5] However, $Pt/Al_2O_3$ suffers from light gas formation (methane and ethane) and fast deactivation. Instead, ZSM-5 was developed at the time and widely investigated for transformation of light paraffin and the corresponding olefins to aromatics due to its activity for acid-catalyzed reactions and resistance to deactivation.[6,7] Extensive efforts have been made to understand the reaction pathways of light alkane conversion over the ZSM-5 catalysts.[8–12] Gusinet et al. discussed the mechanism of alkane activation and the reaction scheme of $C_2$-$C_4$ alkanes aromatization on ZSM-5.[13] Due to complexity of reaction networks, reaction pathways are mostly established based on the observed product distribution (Figure 2).[14] For example, the primary products of propane on ZSM-5 are methane and ethene in equal molar amounts as well as propene and hydrogen at high temperature (reaction 1 and 1', Figure 2), which cannot be explained by typical bimolecular cracking mechanism. Instead, Haag and Dessau reported the monomolecular cracking pathway for activation of alkanes, through which pentacoordinated carbonium ions are formed which crack the feed to give hydrogen, alkanes and olefins.[15,16] Although it is generally accepted that the activation of alkanes might proceed via both the bimolecular hydride abstraction and monomolecular cracking over the ZSM-5, it is inferred that the monomolecular pathway dominates when olefin concentration becomes low and might account for formation of methane.[9,17,18] In Figure 2, the generated ethene and propene from reaction 1 and 1' oligomerize (reaction 2), and these higher molecular weight olefins crack into $C_2$-$C_5$ olefins (reaction 3) or undergo cyclization (reaction 4) followed by aromatization (reaction 5).[9]

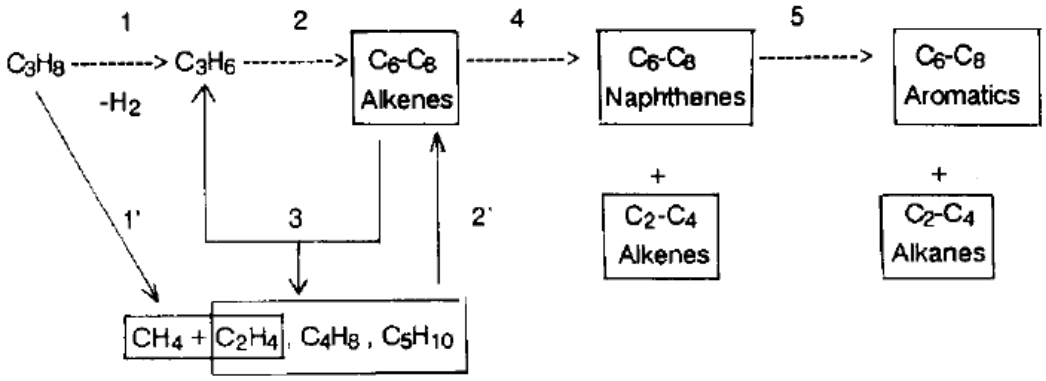


Figure 2. Reaction pathway of propane dehydroaromatization on H-ZSM-5. [14] Reprinted from Applied Catalysis A: General, 89, M. Guisnet, N.S. Gnep, F. Alario, Aromatization of short chain alkanes on zeolite catalysts, 1-30, Copyright (2022) with permission from Elsevier.

Reaction 2, 2' and 3 in Figure 2 occur through carbenium ion intermediates, which subsequently react with other olefins to produce higher molecular weight olefins. Once higher molecular weight olefins are formed, they will rapidly isomerize via hydride or alkyl transfer reactions and crack via β-scission.[9] The cyclization (reaction 4 in Figure 2) is more complex. Firstly, it involves the formation of an olefinic carbenium ion and a paraffin through a hydride transfer from an olefin to a carbenium ion ($R^+$). Subsequently, the olefinic carbenium forms a cyclic carbenium ion. The formation of aromatics from the cyclic carbenium ions occurs through successive proton elimination and hydride transfer to carbenium ion.[9]

Gnep et al. have compared the conversion of propane and propene over ZSM-5 and concluded alkane dehydrogenation is the rate-limiting step in the conversion to aromatics.[13] To enhance the rate of light alkane transformation, metals with dehydrogenation activity (i.e. Pt, Zn, Ga) were utilized as promoters with HZSM-5 for light alkane conversion.[14,16,19–23] Gnep et al. have investigated the product distribution on Pt/ZSM-5 and ZSM-5 for catalytic conversion of propane and propene to aromatics.[24] The distinct difference in the product yield suggested that propane aromatization occurred through a bifunctional process. Introduction of Pt enhanced not only propane dehydrogenation but also the propene aromatization process. Unfortunately, light gas formation and fast deactivation make Pt/ZSM-5 impractical for industrial purposes. Although Pt has the highest dehydrogenation activity, Zn and Ga containing ZSM-5 give higher selectivity to aromatics for propane conversion possibly due to high dehydrogenation rates of alkanes and

cycloalkanes and display higher stability than Pt.[14,16,19–23] Particularly, Ga/ZSM-5 catalysts have been reported to produce the highest yield to aromatics among all the metal-promoted ZSM-5 catalysts for propane.[25–31] There has been significant interest in investigating the catalytic function of Ga in the aromatization of light alkanes especially propane over the Ga/HMFI catalysts. Kitagawa et al. discussed the modification of gallium loading to the mechanistic pathway of propane over ZSM-5 and concluded that Ga species do not directly participate in the activation of propane, but provide for the efficient transformation of the olefin intermediate species into aromatic hydrocarbons.[10] In contrast, Gnep et al. studied the product distribution as a function of propane conversion over Ga/ZSM-5, and concluded that Ga species might be responsible for alkane to olefin, olefin to diene, cycloalkane to cycloalkene to aromatics (Figure 3).[16,32] Although it is believed that a synergic effect exists over the bifunctional catalyst, the detailed nature of the bifunctional pathways remains uncertain.

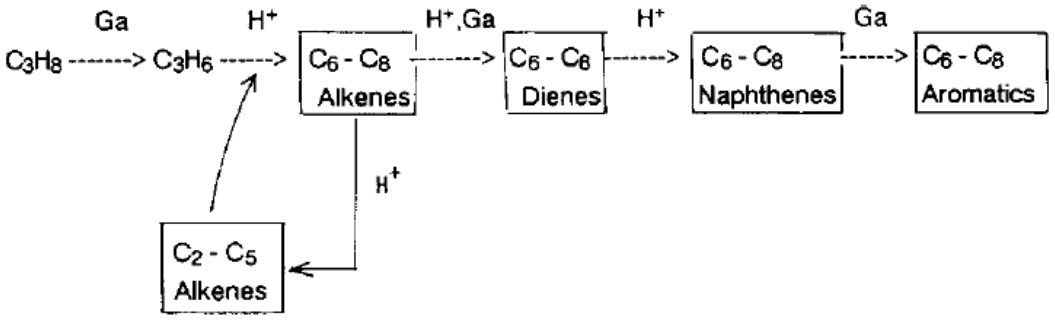


Figure 3. Reaction pathway of propane dehydroaromatization on Ga/H-ZSM-5. [14] Reprinted from Applied Catalysis A: General, 89, M. Guisnet, N.S. Gnep, F. Alario, Aromatization of short chain alkanes on zeolite catalysts, 1-30, Copyright (2022) with permission from Elsevier.

Additionally, since the rate and equilibrium conversion of each elementary step in propane dehydroaromatization is different, the reaction pathways are highly dependent on temperature. For example, propane dehydrogenation is highly endothermic, and therefore, temperature of 550-650℃ is required to achieve high propane conversion (>50%) at 1bar. On the contrary, propene oligomerization typically has higher rates at milder temperatures (200-300℃). At lower temperatures from 350-450℃, propane dehydrogenation rates and equilibrium are lower, while the olefin oligomerization on MFI is favored over cracking producing higher molecular weight olefin hydrocarbons. As temperature increases, the olefin conversion rates increase but cracking

becomes significant, which decreases the selectivity to higher molecular weight hydrocarbons. Studies on the product selectivity for propane dehydroaromatization, particularly at mid and low temperatures (<450°C), is scarce. Choudhary et al. investigated the influence of temperature (400-600°C) on the product selectivity and aromatics distribution in propane aromatization over H-GaAlMFI zeolite.[33] The aromatics selectivity decreased, and the benzene selectivity increased whereas the toluene and $C_8$ aromatics selectivity decreased as temperature increased. Since aromatics formation is favored at higher temperature thermodynamically, the results suggest that aromatics selectivity is controlled by kinetics not thermodynamics. However, the propane conversion reported at 400°C is less than 5%, which offer little insight on reaction pathways.

### 1.3 Ethane Dehydroaromatization

Compared to propane, ethane conversion is much more challenging since high temperature is required to activate C-H bond in ethane. The most promising results regarding the conversion, product distribution and reaction mechanism in the literature for ethane dehydroaromatization are mostly obtained on Zn-modified ZSM-5 catalysts.[34–38] Ono et al. studied the ethane conversion on H-ZSM-5 and Zn-ZSM-5 at 873K and ethane pressure of 20 kPa and proposed that the presence of metal cations is essential for the formation of aromatics from ethane.[39] The effect of zinc cations content in the zeolite on the ethene yield was also examined, which indicates the first step of the aromatization is ethane dehydrogenation over the Zn species. The ethene formed may be oligomerized to higher-molecular weight olefins over acidic sites. However, Hagen et al. has discussed the activation steps and reactions proceeding at zeolitic Bronsted and/or Lewis acid sites on H-ZSM-5 and Zn-ZSM-5 for ethane in nitrogen and hydrogen and proposed that a direct ethane aromatization process is preferred on zinc species and Bronsted acid sites are not necessarily involved.[40] On substitution of nitrogen by hydrogen, the conversion of ethane and formation of aromatics decrease significantly. Consequently, they concluded that reactions with release of molecular hydrogen are reversible on Zn-ZSM-5. Mehdad et al. has also investigated the effect of zinc content and Si/Al in H-ZSM-5 for ethane and ethene dehydroaromatization and concluded that increasing Zn/BAS resulted in an increase in both ethane conversion and selectivity to aromatics, while low Zn/BAS forms more aromatics for ethene aromatization.[41] More recently, bimetallic Pt−Sn, Pt−Ge, Pt−Ga, and Pt−Fe modified H-ZSM-5 catalysts were recently patented by the Shell Oil Company.[42–44] However, the BTX yields for ethane conversion are low due to

methane formation. Irrespective of the type of metal promoters, the proposed reaction pathway is almost identical for ethane to aromatics in the prior work. It remains unclear how methane is produced and how to improve the BTX yields for ethane conversion.

### 1.4 Industrial Processes and Their Limitations

Multiple industrial processes have been developed to convert light alkanes, e.g., M-2 forming,[45] aroforming, Cyclar and Z-forming, which are summarized in Table 1.[46] Among them, the Cyclar process appears as the most relevant and significant industrial process for propane dehydroaromatization. In the Cyclar process, Ga/ZSM-5 was utilized to convert propane and butane directly to BTX in a single reactor at high temperature (500-600℃) and atmosphere pressure in conjunction with a continuous catalyst regeneration (CCR) technique to maintain the catalyst lifetime (Figure 4).[46,47] With promotion by Ga, the yield of aromatics in the Cyclar process can reach 60-65%.

Table 1. Summary of industrial processes for light alkane conversion. [46]

| process | M2 forming | Aroforming | Cyclar | Z-forming |
|---|---|---|---|---|
| feedstock | light olefins, FCC gasoline or naphatha | LPG-light naphtha | $C_3$-$C_4$ paraffins | LPG-light naphtha |
| catalysts | ZSM-5 | Ga/ZSM-5 | Ga/ZSM-5 | Ga/ZSM-5 |
| aromatics yields | 44% | 55% | 60-65% | 60% |
| mode of regeneration | Swing oxidative reactor | Swing reactor | Continuous catalyst regeneration | Switching reactor regeneration |

*Reproduced from ref 46, S. M. Al-Zahrani, Catalytic Conversion of LPG to High-Value Aromatics: The Current State of the Art and Future Predictions, Asia-Pacific Journal of Chemical Engineering, copyright (2022) with permission from John Wiley and Sons

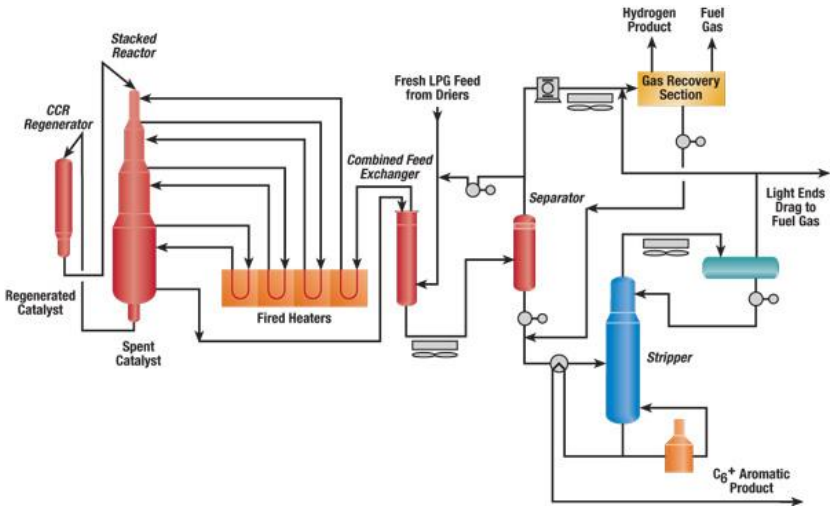


Figure 4. UOP Cyclar process

Unfortunately, there are two major limitations for the Cyclar process. Firstly, the liquid yield is low for propane feed. The yield to aromatics reported in literatures is limited by concurrent formation of light gas, particularly methane and ethane, which can't be further transformed into BTX. Although several potential pathways for light gas formation in the dehydroaromatization process were proposed, including alkane monomolecular cracking, hydrogenolysis and aromatic dealkylation,[48,49] the most problematic reaction pathway has never been explicitly identified. Therefore, catalysts with improved liquid yield have not been reported. In addition, since propane dehydrogenation is the rate-limiting step (r.l.s), the product selectivity and reaction pathways were mostly studied at temperatures above 550℃ on Ga/ZSM-5 catalysts. The understandings of the intertwined effect of catalyst functions and process conditions on propane dehydroaromatization pathways are limited in previous studies.

Secondly, ethane is not practically reactive, and the aromatics yield is low due to high methane selectivity. Consequently, there is no industrial process for ethane dehydroaromatization. The methane formation pathway for ethane and the differences in the light gas formation pathways between the dehydroaromatization of ethane and propane have never been systematically discussed. As a result, the improved liquid yields for ethane have not been reported and the strategies to convert ethane to higher molecular hydrocarbons remain unclear.

# 2. EXPERIMENTAL

## 2.1 Catalyst Synthesis

*$PtZn/SiO_2$*

Strong electrostatic adsorption method (SEA) was firstly used on 5 g of commercially available silica (Sigma- Aldrich, Davisil Grade 646) to prepare $Zn/SiO_2$.[50] 0.68g $Zn(NO_3)_2 \cdot 6H_2O$ (Sigma-Aldrich) was dissolved in 50 mL deionized water (DI water) to obtain 3% Zn weight loading assuming all the Zn was loaded onto $SiO_2$. Subsequently, ammonium hydroxide ($NH_4OH$, Sigma-Aldrich) was added to $Zn(NO_3)_2$ solution to adjust to pH to 11-12. The $SiO_2$ was added to the Zn solution and stirred for 10 minutes. The sample was vacuum filtered and washed with 50 mL DI water for three times. The wet powder was dried overnight at 125℃ and calcined at 300℃ for 3 h (10℃ /min).[51]

Pt was then added to the $Zn/SiO_2$ by pH adjusted incipient wetness impregnation method (IWI) to give 2% Pt weight loading in the final $PtZn/SiO_2$ catalyst. Its impregnation volume was calculated to be 1.16 mL/g by adding $H_2O$ dropwise to 1g of $SiO_2$ until it was saturated. 0.2g $Pt(NH_3)_4(NO_3)_2$ (Sigma-Aldrich) was dissolved in about 2mL DI water. 1 mL $NH_4OH$ was added to Pt solution and stirred until all crystals dissolved and the pH of the Pt solution was about 11-12. Additional DI water was added to the solution to bring the overall volume to impregnation volume of $SiO_2$. The solution was added dropwise to the $Zn/SiO_2$ support. The catalyst was dried overnight at 125℃, calcined at 200℃ for 3 h (5℃ /min ramp) and reduced at 225 °C in 5 % $H_2/N_2$ at 100 $cm^3$/min for 30 min.

*$Ga/Al_2O_3$*

$Ga/Al_2O_3$ was prepared by IWI method on 5g of $\gamma$-$Al_2O_3$ (Alfa Aesar). 0.41g of citric acid (Sigma-Aldrich) was added to 1.5g of $Ga(NO_3)_3$ solution (Alfa Aesar, 9-10 wt% Ga) to obtain 3% Ga weight loading assuming all Ga was loaded onto the support. Concentrated $NH_4OH$ was added to the solution to adjust to a pH of 11-12. The solution was then diluted with DI water up to the impregnation volume and added dropwise onto $Al_2O_3$. The pre-catalyst was dried overnight at 125 °C and calcined at 550 °C for 3 h (10℃/min).

*PtZn/$SiO_2$+ZSM-5 bifunctional catalysts*

Commercial ZSM-5 extrudes (CBV5524G, 80wt% zeolite and 20wt% alumina binder, $SiO_2/Al_2O_3$=50) were obtained from Zeolyst Inc. The ZSM-5 extrudes were firstly ground, pelleted, and sieved to retain 180-400 μm particle size and then calcined in air at 550℃ for 3h to obtain its acidic form, which will be referred as ZSM-5 catalysts. The bifunctional catalysts were prepared by physical mixing of PtZn/$SiO_2$ and ZSM-5 and referred as PtZn/$SiO_2$+ZSM-5 catalysts. The Z/PA ratio in the latter context will be defined as the weight loading ratio of ZSM-5 (Z) and PtZn/$SiO_2$ (PA).

## 2.2 Catalytic Performance Test

The catalytic performance was evaluated in a quartz tube fixed bed reactor (10.5 mm i.d.) equipped with mass flow rate controllers (Parker Porter, CM400) for atmospheric pressure conditions. A furnace (Applied Test Systems series 3210) was connected to a temperature controller to supply the heat and maintain the desired temperature. The gases used in this work are dilute (5%) and pure (99.99%) $C_3H_8$ (Indiana Oxygen), 3% $C_3H_6$ (Indiana Oxygen). The cyclohexene vapor is supplied by purging ultra-high purity $N_2$ (99.99%, Indiana Oxygen) into cyclohexene solution (Sigma-Aldrich, 99%) through a bubbler (Ace Glass), which is maintained at 0°C with ice bath in a Dewar flask.

The catalysts were supported on quartz wool with a K-type thermocouple placed in the center bottom of the catalyst bed to monitor the temperature in the bed. Reactor effluent was discharged through a line heated to 170°C using heating tapes (Omega) and wrapped woth insulation and introduced to a gas chromatograph (Agilent 7890A) equipped with a flame ionization detector (Agilent J&W HP-AL/S column, 0.320 mm i.d. × 25m) for reactant and product quantification. PtZn/$SiO_2$ and PtZn/$SiO_2$+ZSM-5 catalysts were pretreated with $N_2$ for 15 min to remove any adsorbed moisture and reduced in 5% $H_2/N_2$ (Indiana Oxygen) at 550°C for 30 min before the reaction was performed, while Ga/$Al_2O_3$ and ZSM-5 were only pretreated with $N_2$ at 550°C for 30 min. The catalytic performances were evaluated at 350-600°C and atmospheric pressure. Fresh catalysts were loaded for each experiment. The conversion and product selectivity were obtained at different space velocities. PtZn/$SiO_2$+ZSM-5 bifunctional catalysts showed minor deactivation

over about 5 h. As an example, propane conversion as a function of time on stream over the PtZn/$SiO_2$+ZSM-5 catalyst (Z/PA=1) is shown in Figure S1.

### 2.3 X-ray Absorption Spectroscopy (XAS)

*In situ* XAS experiments were performed at the 10-BM-B beamline at the APS for the Pt L3 edge (11.564 keV) and Ga K edge (10.375 keV) to correlate the catalytic performance with the structure information on the PtZn/SiO2 and Ga/Al2O3. Samples were loaded in a six-shooter, placed in the middle of a glass tube sealed with leak-tight end caps, The PtZn/SiO2 catalyst was reduced in 5% H2/N2 at 550°C and cooled in He. The measurement for the PtZn/SiO2 was accompanied by a Pt foil scan which was obtained through a third ion chamber and used for calibration. The as-synthesized Ga/Al2O3 catalyst and gallium acetylacetonate (Ga(AcAc)3) reference were scanned in air at room temperature. The X-ray absorption near edge structure (XANES) spectra were used to identify the chemical state and valence of Pt or Ga, while extended X-ray absorption fine structure (EXAFS) provided information of coordination number (CN) and bond distacne (R). XANES and EXAFS data were obtained and interpreted using WinXAS v 3.1 software.52 Feff6 calculations were performed using Pt1Zn1 phase (RPt-Zn=2.66, CNPt-Zn=8, RPt-Pt=2.85, CNPt-Pt=6). The final EXAFS fit was performed based on the fitting of calculated Pt−Zn and Pt−Pt scattering of the Pt1Zn1 structure to determine the coordination number and bond distance on the PtZn/SiO2.53 The coordination number and bond distance of Ga/Al2O3 was determined for Ga-O scattering based on experimental obtained Ga(AcAc)3 spectra (RGa−O=1.95 Å, CNGa−O=6).

### 2.4 Transmission Electron Microscope (TEM)

Samples were dispersed in ethanol and mounted on holey carbon grids for examination in a JEOL NEOARM 200CF transmission electron microscope equipped with spherical aberration correction to allow atomic resolution imaging, and an Oxford Aztec Energy Dispersive System (EDS) for elemental analysis. The microscope is equipped with two large area JEOL EDS detectors for higher throughput in acquisition of x-ray fluorescence signals. Images were recorded in annular dark field (ADF) mode.

# 3. THE DIFFERENCE IN DEHYDROAROMATIZATION PATHWAYS OF PROPANE ON BIFUNCTIONAL CATALYSTS

This chapter is reproduced from C.-W. Chang, H.N. Pham, R. Alcala, A.K. Datye, J.T. Miller, "Dehydroaromatization Pathway of Propane on PtZn/$SiO_2$+ZSM-5 Bifunctional Catalyst", ACS Sustainable Chem. & Eng. 2022, 10, 1, 394–409 by permission from American Chemical Society. DOI: 10.1021/acssuschemeng.1c06579

## 3.1 Introduction

The Cyclar process utilized Ga/ZSM-5 bifunctional catalysts to convert propane and butanes to aromatic chemicals but the BTX yields are low (60-65%). Significant amounts of light gas, majorly methane, are produced and remain unreactive in the product mixture. Due to the complexity of reaction networks on dual sites, which are dictated by relative kinetics of elementary steps and thermodynamic equilibrium of multiple hydrocarbon species, it remains challenging to identify the dominant yield-loss reaction on the Ga/ZSM-5 catalysts and develop optimal strategies for formulating bifunctional catalyst compositions to obtain improved BTX yields.

## 3.2 Objective

The objective of chapter three is to determine the light gas formation pathway in the dehydroaromatization of propane on Ga/ZSM-5 bifunctional catalysts and develop a strategy to minimize the light gas selectivity, thus, increasing the aromatic yields by utilizing PtZn/$SiO_2$+ZSM-5 bifunctional catalysts. The product distribution was determined at different propane conversions and ratios of ZSM-5 to PtZn/$SiO_2$ (Z/PA) to identify the individual role of two catalytic functions in the dehydroaromatization pathway of propane. The reaction pathways of cyclic hydrocarbons (cyclohexene) are studied to understand the differences in the aromatization pathway of MFI, Ga/MFI and PtZn alloy-MFI catalysts.

## 3.3 Results

### 3.3.1 XAS Characterization of $Ga/Al_2O_3$

The structure of $Ga/Al_2O_3$ catalyst characterized by *in situ* XAS is reported in Figure 5. Figure 5a shows that the XANES energy of the $Ga(AcAc)_3$ reference and $Ga/Al_2O_3$ is 10.377 keV and 10.375 keV, respectively, which is consistent with 6-coordinate octahedral $Ga^{3+}$ and 4-coordinate $Ga^{3+}$ reported in prior studies.[54–56] The EXAFS spectra were fitted to determine the coordination number and bond distance of the catalysts. The lower intensity of first shell Ga-O scattering of $Ga/Al_2O_3$ compared with that of $Ga(AcAc)_3$ is suggestive of lower coordination (Figure 5b).

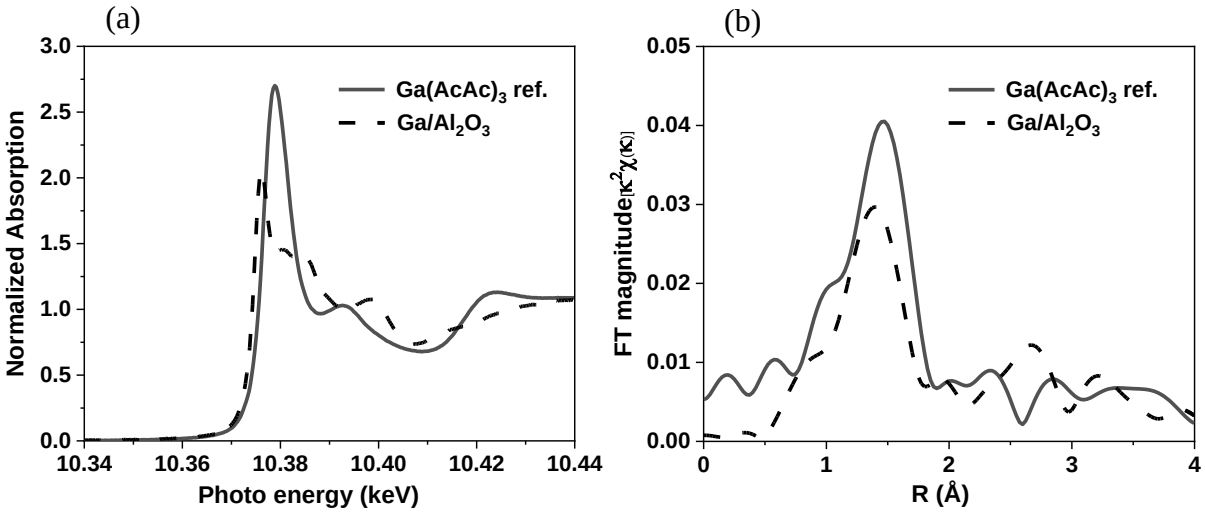


Figure 5. (a) XANES and (b) EXAFS of $Ga(AcAc)_3$ (solid) and $Ga/Al_2O_3$ (dash)

Table 2. Coordination number and bond distance from in situ EXAFS simulation of $Ga/Al_2O_3$ and $Ga(AcAc)_3$

| Sample | XANES energy (keV) | Coordination Number | Bond Distance (Å) | $\Delta\sigma^2$ |
|---|---|---|---|---|
| $Ga(AcAc)_3$ ref. | 10.377 | 6.0 | 1.95 | 0.005 |
| $Ga/Al_2O_3$ | 10.375 | 4.2 | 1.85 | 0.003 |

Table 2 shows the $k^2$-weighted EXAFS fitting parameters. The $Ga(AcAc)_3$ reference compound has a coordination number of 6 and a bond distance (Ga-O) of 1.95 Å, while $Ga/Al_2O_3$ has a coordination number of 4.2 and a bond distance of 1.85 Å. 4-coordinate $Ga^{3+}$ has a lower XANES energy by 2 eV and a shorter bond distance than 6-coordinate $Ga^{3+}$ by about 0.1 Å. The results

indicate the active site is a single-site, 4-coordinate $Ga^{3+}$ ion on alumina. Similar XANES and EXAFS have been reported for $Ga/SiO_2$ propane dehydrogenation catalysts.[54,55]

### 3.3.2 Light Gas Formation on $Ga/Al_2O_3$+ZSM-5

Two catalytic components, $Ga/Al_2O_3$ and ZSM-5, were investigated for their individual contribution to light gas formation for the propane dehydroaromatization process.

***propane conversion over ZSM-5 and 3% $Ga/Al_2O_3$***

The product selectivity of 5% propane at 550℃ over $Ga/Al_2O_3$ and ZSM-5 is shown in Table 3. The carbon selectivity to methane is approximately 26% on the ZSM-5. At 44.4% propane conversion, the selectivities to methane, ethane and ethene are 26.0%, 3.3% and 40.4%, indicating most of light gas are methane and ethene. Propene and higher molecular weight hydrocarbons, including butanes, butenes, $C_5^+$ oligomers and aromatics, are also formed on the ZSM-5. $Ga/Al_2O_3$ demonstrates 0.5% selectivity to methane and 0.2 % selectivity to ethane at 20.0% propane conversion. The propene selectivity is 89.7%, showing that it is moderately selective for propane dehydrogenation. However, 3.9% ethene and 5.7% butenes are also observed in the products, which are likely formed by the secondary reactions of propene.13,57 The light gas selectivity is 3.3% (1.4% methane, 1.9% ethane) at 42.9% propane conversion. As the propane conversion increases, the propene selectivity decreases to 81.6%; while the selectivity to ethene and butenes increases to 7.5% and 7.6%, respectively, which further implies that decreasing propene selectivity is attributed to the secondary reactions.

The rates on each catalyst are estimated based to the carbon number of reactants consumed or products generated per gram of the catalyst (Table 3). For example, the methane formation rates are estimated by multiplying propane conversion rate and methane selectivity. The average rates at different propane conversions on two catalysts in Table 3 were utilized for comparison. Although 3% $Ga/Al_2O_3$ has higher olefin selectivity than that on ZSM-5, the average propane conversion rates on ZSM-5 ($3.0\times10^{-6}$ (mol $C_3H_8$)(g ZSM-5)$^{-1}s^{-1}$) are about 1.5 times higher than on the $Ga/Al_2O_3$ ($2.1\times10^{-6}$ (mol $C_3H_8$)(g $Ga/Al_2O_3$)$^{-1}s^{-1}$). As a result, the methane formation rates on ZSM-5 ($7.8\times10^{-7}$ (mol $CH_4$)(g ZSM-5)$^{-1}s^{-1}$) are around 40 times higher than on $Ga/Al_2O_3$

($2.0\times10^{-8}$ (mol $CH_4$)(g $Ga/Al_2O_3$)$^{-1}s^{-1}$). The ethene formation rates on ZSM-5 ($1.3\times10^{-6}$ (mol $C_2H_4$)(g ZSM-5)$^{-1}s^{-1}$) are around 10 times higher than on $Ga/Al_2O_3$ ($1.2\times10^{-7}$ (mol $C_2H_4$)(g $Ga/Al_2O_3$)$^{-1}s^{-1}$). Due to high dehydrogenation rates of Ga, the propene formation rates on the $Ga/Al_2O_3$ ($1.8\times10^{-6}$ (mol $C_3H_6$)(g $Ga/Al_2O_3$)$^{-1}s^{-1}$) are 3.5 times higher than on ZSM-5 ($5.3\times10^{-7}$ (mol $C_3H_6$)(g ZSM-5)$^{-1}s^{-1}$). The results indicate that propane conversion occurs at similar rates on ZSM-5 and $Ga/Al_2O_3$. The former makes methane and ethene on Brønsted acid sites by monomolecular cracking, while the latter makes propene by dehydrogenation. Subsequently, low molecular weight olefins (light olefins) are transformed into higher molecular weight hydrocarbons over ZSM-5; while methane remains unreactive.

Table 3. Propane conversion on ZSM-5 and $Ga/Al_2O_3$.

| | ZSM-5 | | 3% $Ga/Al_2O_3$ | |
|---|---|---|---|---|
| Conversion (%) | 21.8 | 44.4 | 20.0 | 42.9 |
| WHSV ($h^{-1}$) | 0.72 | 0.36 | 0.60 | 0.22 |
| Selectivity (%) | | | | |
| Methane | 25.5 | 26.0 | 0.5 | 1.4 |
| Ethane | 2.5 | 3.3 | 0.2 | 1.9 |
| Ethene | 45.6 | 40.4 | 3.9 | 7.5 |
| Propene | 18.7 | 16.8 | 89.7 | 81.6 |
| Butanes, butenes | 2.7 | 3.0 | 5.7 | 7.6 |
| $C_5^+$ paraffins, olefins and aromatics | 5.0 | 10.5 | trace[a] | trace[a] |
| Propane conversion rate ((mol $C_3$)(g catalyst)$^{-1}s^{-1}$) | $3.0\times10^{-6}$ | $3.0\times10^{-6}$ | $2.3\times10^{-6}$ | $1.9\times10^{-6}$ |
| Methane formation rate ((mol $C_1$)(g catalyst)$^{-1}s^{-1}$) | $7.7\times10^{-7}$ | $7.8\times10^{-7}$ | $1.2\times10^{-8}$ | $2.7\times10^{-8}$ |
| Ethene formation rate ((mol $C_2^=$)(g catalyst)$^{-1}s^{-1}$) | $1.4\times10^{-6}$ | $1.2\times10^{-6}$ | $9.0\times10^{-8}$ | $1.4\times10^{-7}$ |
| Propene formation rate ((mol $C_3^=$)(g catalyst)$^{-1}s^{-1}$) | $5.6\times10^{-7}$ | $5.0\times10^{-7}$ | $2.0\times10^{-6}$ | $1.6\times10^{-6}$ |

Reaction conditions: temperature, 550°C, pressure, 101 kPa, 5% $C_3H_8/N_2$
[a] Trace indicates <0.1% selectivity

***propene conversion over ZSM-5***

Propene, as one of primary olefins produced by propane, was chosen as the representative olefin to demonstrate the selectivity and rate for olefin conversion over ZSM-5 using 3% propene at 550℃. Figure 6a shows the propene conversion rate as a function of propene conversion over ZSM-5. The propene rates are also compared to the propane conversion rates at the same temperature to understand the difference in rate and product selectivity between alkanes and olefins on the acid sites. The average propene conversion rate is $7.2\times10^{-5}$ (mol $C_3H_6$)(g ZSM-5)$^{-1}$s$^{-1}$, higher than the propane conversion rate ($3.6\times10^{-6}$(mol $C_3H_8$)(g ZSM-5)$^{-1}$s$^{-1}$)) by a factor of about 20, indicating olefins are significantly more reactive than alkanes.[13,57] Figure 6b shows that the product distribution of propene conversion is composed of primarily ethene, $C_3$-$C_6^+$ hydrocarbons and BTX with low methane selectivity at high propene conversion (74%). Methane selectivity remains less than 1% at 20% and 32% propene conversion and increases to 4% (methane 3%, ethane 1%) at 74% conversion. At 20% propene conversion, major products are ethene (38%) and butenes (41%); while small amount of $C_5^+$ hydrocarbons (9%) and BTX (6%) are also observed.

Generally, formation of ethene by the cracking reaction is less favored because of the stability of primary carbenium ions. However, it has previously been suggested that due to the small pore size of ZSM-5, steric confinement between the zeolite surface and adsorbed carbenium ions could stabilize the primary carbenium intermediates and likely facilitate ethene formation.[58–60] This may explain why high ethene selectivity is observed in the product mixture for propene conversion on ZSM-5 catalysts. As propene increases from 20% to 74%, the butenes and $C_5^+$ hydrocarbons decrease to 9% and 1%, respectively; while the BTX selectivity increases significantly to 33%, suggesting butenes and $C_5^+$ oligomers are formed by propene as intermediates and eventually converted to aromatics on ZSM-5 as proposed in the previous studies.[8–12] Meanwhile, the selectivity to propane and butanes increases from 6% to 10%, which is believed to form along with aromatics.[61] The ethene selectivity is highest (45%) at the intermediate conversions (32%), implying that it is generated from propene at low propene conversion and slowly converted to higher molecular weight olefins at high propene conversion. The detailed product selectivity is shown in Table S1. These results are consistent with other studies for propene conversion on MFI catalysts.[13,57]

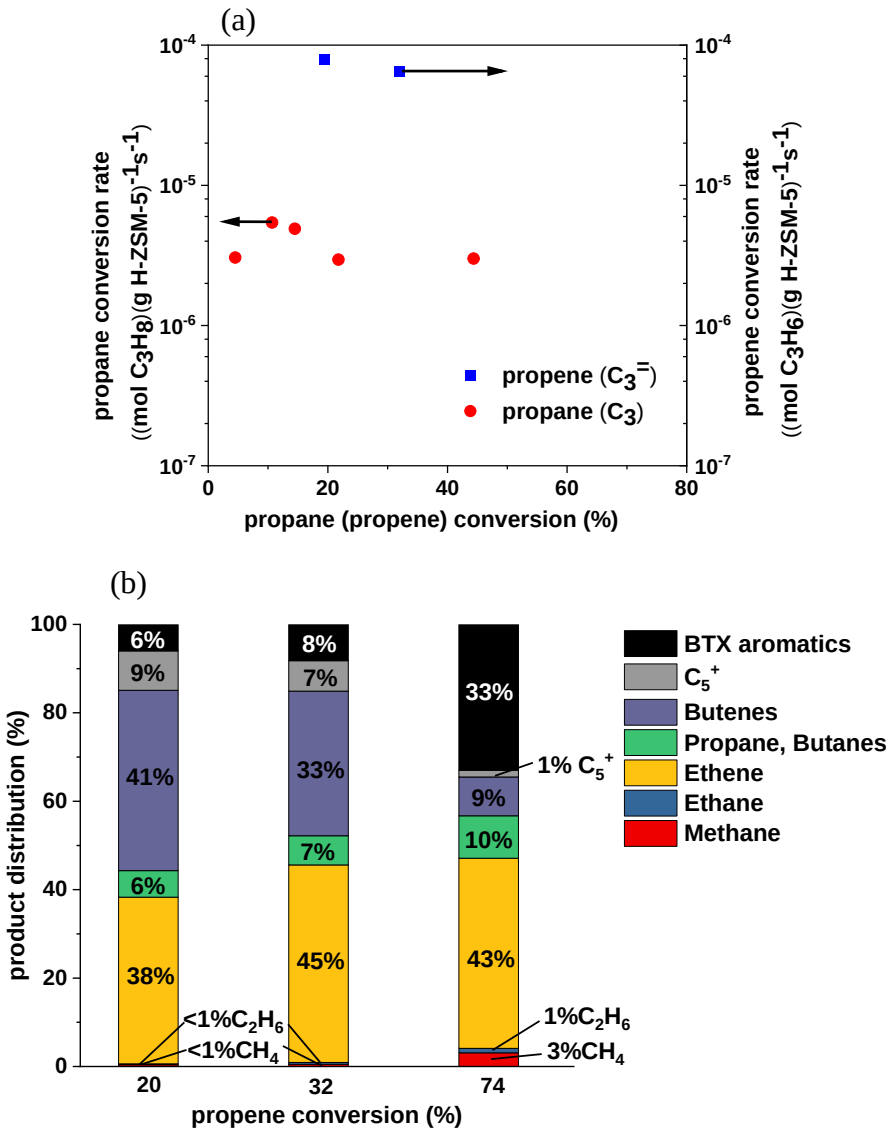


Figure 6. (a) the rates of propane[a] and propene[b] conversion (b) product distribution of propene conversion on ZSM-5. Reaction conditions: temperature, 550 °C, pressure, 101 kPa. [a] cat., 0.1-0.5 g; 5% $C_3H_8/N_2$; WHSV=0.2-4 $h^{-1}$. [b] cat., 0.005-0.1 g; 3% $C_3H_6/N_2$; WHSV=1-20 $h^{-1}$

### 3.3.3 Catalytic Performance and Structure Characterization of PtZn/$SiO_2$

PtZn intermetallic alloy was reported to be nearly 100% selective to ethene with a high rate for ethane conversion.[53] As a result, the PtZn alloy was utilized as a high activity dehydrogenation function in the bifunctional catalyst for propane conversion. The structure of the synthesized PtZn/$SiO_2$ catalyst was characterized by *in situ* XAS to ensure the formation of the PtZn alloy. Figure 7a shows the normalized absorption as a function of energy from 11.540 to 11.600 keV on Pt foil, Pt/$SiO_2$ and PtZn/$SiO_2$. Comparing the XANES of Pt/$SiO_2$ and PtZn/$SiO_2$ catalyst with the

Pt foil standard at Pt $L_3$ edge, the edge energy of Pt catalyst is 11.5640 keV, same as Pt foil. The change in the shape of the XANES of $Pt/SiO_2$ is attributed to small particle size.[62] The XANES of the $PtZn/SiO_2$ is slightly different from Pt foil and increases by 0.9 eV because of the formation of PtZn intermetallic nanoparticles.[53] Figure 7b shows the magnitude of the $k^2$-weighted FT plot. The three peaks of $Pt/SiO_2$ are characteristic peaks of metallic Pt, which has the similar shape to that of Pt foil. However, $PtZn/SiO_2$ is significantly different from metallic Pt, which suggests a PtZn intermetallic alloy was formed.

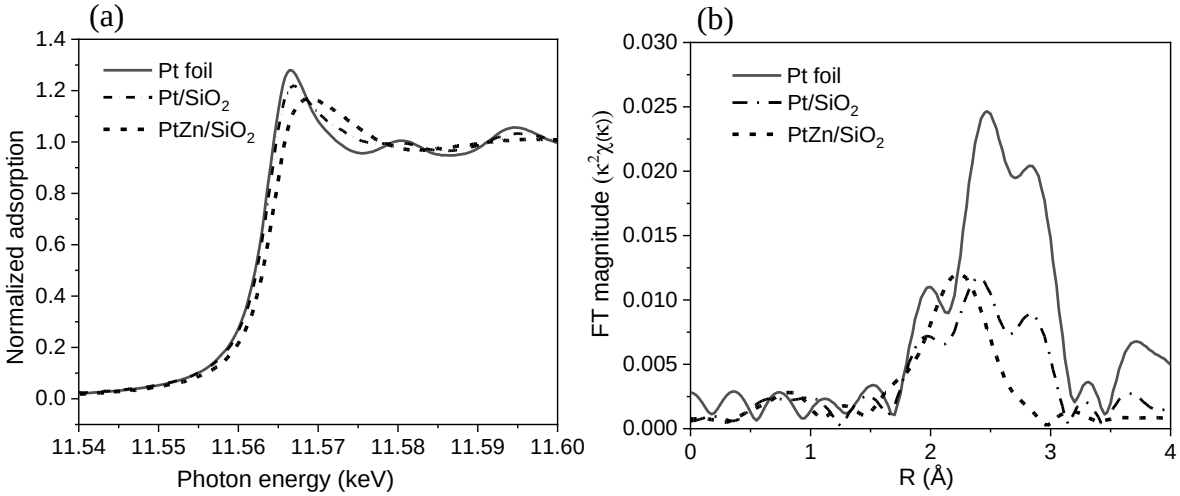


Figure 7. (a) XANES and (b) EXAFS of Pt foil (solid), $Pt/SiO_2$ (dash dot) and $PtZn/SiO_2$ (dash)
*Samples were pre-treated with 5% $H_2/N_2$ at 550°C for 1 hr and purged with He when cooling to room temperature before scanned

The $k^2$-weighted EXAFS at Pt edge of all samples was fitted to acquire the average coordination number and bond distance between Pt and the nearest neighbor atoms (Table 4). Pt-Pt with an average bond distance of 2.73 Å and coordination number of 8.6 was confirmed on $Pt/SiO_2$. On the $PtZn/SiO_2$, the average Pt-Zn bond distance of 2.56 Å with coordination number of 3.1 and average Pt-Pt bond distance of 2.71 Å with coordination number of 2.4 were obtained. The coordination number of Pt-Zn to Pt-Pt on the $PtZn/SiO_2$ is approximately 1.3, which is consistent with the $Pt_1Zn_1$ phase with a tetragonal AuCu structure.[53] In comparison to bulk Pt and $Pt_1Zn_1$, the coordination number of both samples are smaller, implying small particles are formed. The bond distance of Pt-Zn and Pt-Pt is ~0.1 Å smaller than those reported for $Pt_1Zn_1$ phase, which can be

attributed to lattice contraction as the particle size decreases.[62] The result of structure characterization is indicative of the formation of the $Pt_1Zn_1$ alloy with small particle size.

Table 4. Coordination number and bond distance from *in situ* EXAFS simulation of $Pt/SiO_2$ and $PtZn/SiO_2$

| Sample | XANES energy (keV) | Scattering Pair | Coordination Number | Bond Distance (Å) | $\Delta\sigma^2$ |
|---|---|---|---|---|---|
| 2%$Pt/SiO_2$ | 11.5640 | Pt-Pt | 8.6 | 2.73 | 0.007 |
| 2%Pt-3%$Zn/SiO_2$ | 11.5649 | Pt-Zn | 3.1 | 2.56 | 0.007 |
| | | Pt-Pt | 2.4 | 2.71 | 0.007 |

Figure 8 shows AC-STEM images of the pre-reduced $PtZn/SiO_2$ catalyst and the corresponding particle size distribution with an average particle size of 4.7 ± 3.0 nm. EDS elemental mapping was done to show the alloying of PtZn particles. Figure 9 shows elemental maps of Si $K\alpha_1$, O $K\alpha_1$, Zn $K\alpha_1$, and Pt $M\alpha_1$ corresponding to the AC-STEM image. The maps show that the particles are rich in Pt, with Zn co-existing with Pt in the particles and on the silica support. The weight ratio of Pt:Zn is close to 1:1, with excess Zn in the sample. Figure 10b and 10c show another elemental mapping of Pt $M\alpha_1$ and Zn $K\alpha_1$ corresponding to a portion of the AC-STEM image (Figure 10a). The two regions from the Pt map were then extracted to obtain the compositions. Results show that the particles contain Pt and Zn, whereas the region devoid of particles contains only Zn on the silica support. The EDS map suggests that Pt is also present in the region devoid of any particles, but the signal is at the background noise level, hence we concluded that while Zn is dispersed on the support, the Pt is only present in the form of particles.

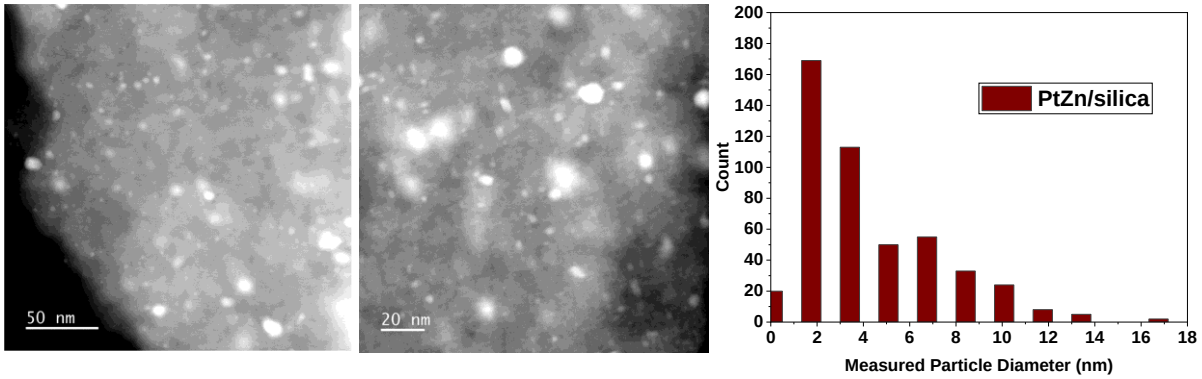


Figure 8. AC-STEM images of $PtZn/SiO_2$ pre-reduced in $H_2$, and the corresponding particle size distribution.

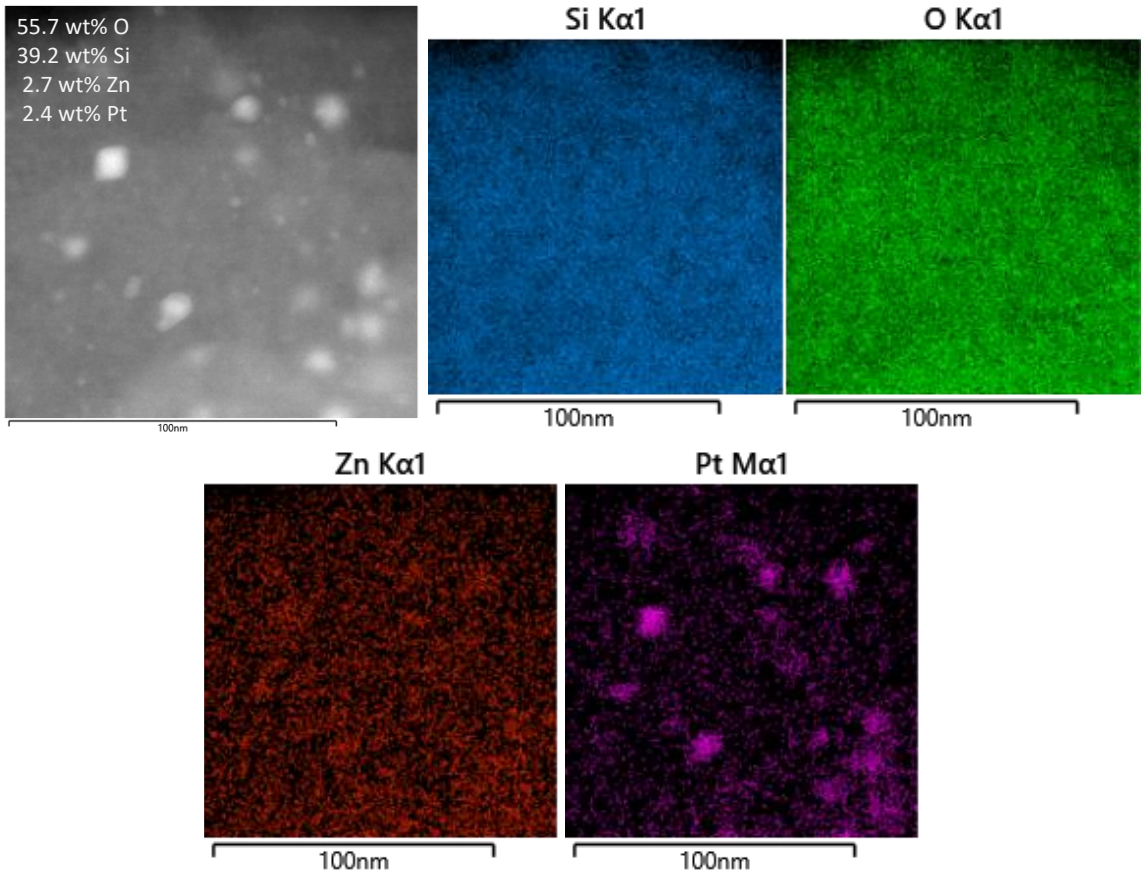


Figure 9. EDS elemental maps of Si $K\alpha_1$, O $K\alpha_1$, Zn $K\alpha_1$, and Pt $M\alpha_1$ corresponding to the AC-STEM image.

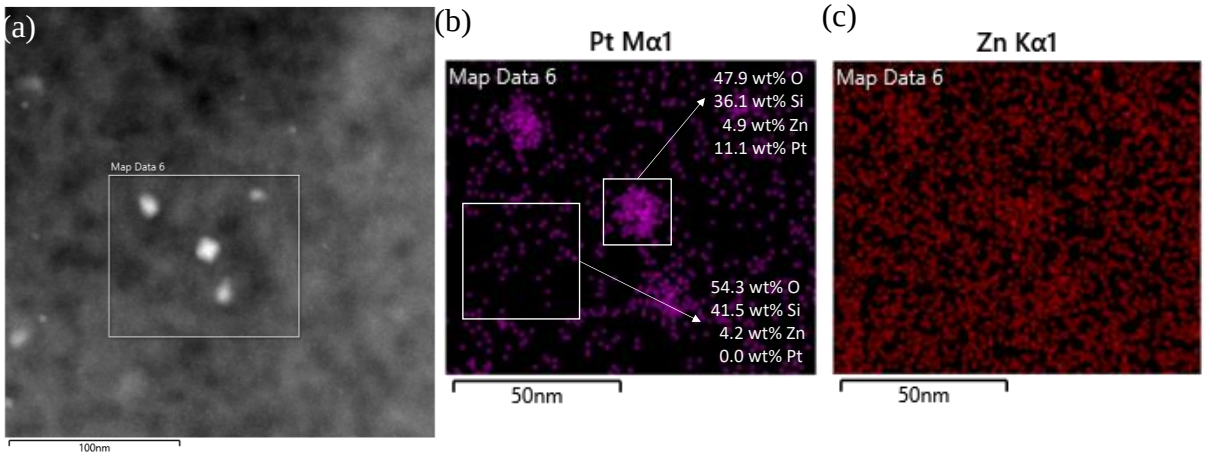


Figure 10. (a) AC-STEM image of Pt-Zn/$SiO_2$ catalyst and EDS elemental maps of (b) Pt $M\alpha_1$ and (c) Zn $K\alpha_1$ corresponding to the region shown in the AC-STEM image (a). The two regions indicated in the white box were analyzed obtain compositions.

The catalytic performance of $PtZn/SiO_2$ was evaluated for propane dehydrogenation to estimate propane conversion rate and propene selectivity in comparison with $Ga/Al_2O_3$. Figure 11a and 14b show propene selectivity and propane conversion rates as a function of propane conversion, respectively, using 2.5% propane with 2.5% $H_2$ at 550 °C and atmosphere pressure over $PtZn/SiO_2$ and $Ga/Al_2O_3$. The purpose of cofeeding $H_2$ is to evaluate the extent of hydrogenolysis on each catalyst. $PtZn/SiO_2$ can achieve nearly 100% selectivity to propene within 10-55% propane conversion even with hydrogen, which suggests that methane formation by hydrogenolysis is nearly suppressed on the $PtZn/SiO_2$. $Ga/Al_2O_3$ has demonstrated 78-88% selectivity to propene and 5-13% selectivity to methane and ethane within 18-40% propane conversion, suggesting that hydrogenolysis can be a contributor to light gas formation at high propane conversion with Ga-MFI catalysts. The propane conversion rates on $PtZn/SiO_2$ ($2.5\times10^{-5}$ (mol $C_3H_8$)(g $PtZn/SiO_2$)$^{-1}s^{-1}$) are 25 times higher than on $Ga/Al_2O_3$ ($9.8\times10^{-7}$ (mol $C_3H_8$)(g $Ga/Al_2O_3$)$^{-1}s^{-1}$). $Ga/Al_2O_3$ is moderately selective for propane dehydrogenation, but its dehydrogenation rate is significantly lower than that of $PtZn/SiO_2$. The catalytic performance results confirm that synthesized $PtZn/SiO_2$ catalyst demonstrates high dehydrogenation rate and high olefin selectivity even in the presence of hydrogen, which indicates that olefins can be produced at higher rate and selectivity than with Ga or MFI zeolite.

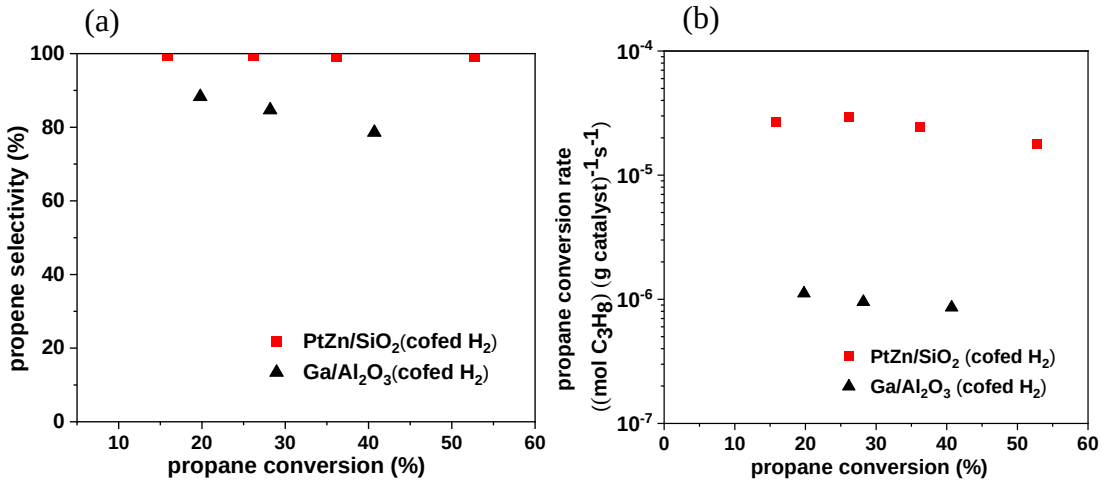


Figure 11. Propane kinetics for $PtZn/SiO_2$ and $Ga/Al_2O_3$ (a) $C_3H_6$ selectivities as a function of $C_3H_8$ conversion (b) the propane conversion rates as a function of $C_3H_8$ conversion.
Reaction conditions: cat., 0.01-0.8 g; temperature, 550 °C, pressure, 101 kPa; 2.5% $C_3H_8$, 2.5% $H_2$ balanced with $N_2$; WHSV=7-442 $h^{-1}$

### 3.3.4 Product Selectivity and Conversion Rates of Propane Conversion on Bifunctional PtZn/$SiO_2$+ZSM-5 Catalysts

PtZn/$SiO_2$+ZSM-5 bifunctional catalyst composed of PtZn/$SiO_2$ (PA) and ZSM-5 (Z) were studied for propane conversion in this work. The product distribution at different propane conversions was determined for bifunctional catalysts with different weight ratios in gram of ZSM-5 to PtZn/$SiO_2$ (Z/PA) to understand the role of two catalytic functions in the reaction pathways of propane conversion. Figure 12a-12f show product selectivity as a function of propane conversion and Z/PA ratio using 5% propane at 550 °C. The ZSM-5 product distribution was also determined for comparison.

On ZSM-5, the methane selectivity remains at 25-28% in the range of 5-65% propane conversion (Figure 12a). The ethene selectivity is approximately 50% at 5% propane conversion (Figure 12b) and the ratio of ethene selectivity to methane is approximately 2, which is consistent with formation by propane monomolecular cracking. As propane conversion increases, the ethene selectivity decreases, indicating ethene undergoes secondary reactions. The propene selectivity is 20% at low conversion and decreases as propane conversion increases (Figure 12c). Propene selectivity decreases faster than ethene, suggesting propene is more reactive than ethene on ZSM-5.[6] The non-zero selectivities to methane, ethene and propene at conversion close to zero are indicative that these are primary products. On the contrary, the butenes selectivity is low and approaches zero at the conversion less than 5%. As propane conversion increases, the butenes selectivity increases and goes through a maximum (Figure 12d). The results indicate that butenes are secondary products generated from ethene and propene through the oligomerization-cracking cycle and are further transformed into aromatics. The aromatics selectivity gradually increases as propane conversion increases (Figure 12e). The product selectivity as a function of propane conversion over ZSM-5 is in agreement with prior studies, suggesting that propane undergoes monomolecular cracking, oligomerization, β-scission and aromatization reactions on acid sites.[10] PtZn/$SiO_2$+ZSM-5 catalysts with different Z/PA ratio are further investigated to understand how Z/PA ratio contributes to product selectivity. Higher Z/PA ratio indicates that the bifunctional catalyst has a higher weight loading of ZSM-5, while low Z/PA ratio is indicative of increasing amounts of PtZn/$SiO_2$ and higher dehydrogenation rates. With Z/PA=50, the methane selectivity is 20% and the ethene selectivity is 40% at 6% propane conversion (Figure 12a-12b). The ratio of

ethene to methane selectivity is close to 2, indicating methane and ethene are mostly formed by propane monomolecular cracking on PtZn/$SiO_2$+ZSM-5. However, the lower methane and ethene selectivity and the higher propene selectivity than those on ZSM-5 (Figure 12c), suggesting propane is partly converted by dehydrogenation on the PtZn/$SiO_2$. As propane conversion increases to 55%, the methane selectivity decreases to 15%. This suggests that the mode of the monomolecular cracking of propane by acid sites may by partially inhibited. The maximum butenes selectivity is 4% and slightly higher than that on the ZSM-5 (Figure 12d). The BTX selectivity is low at 10% propane conversion and increases to approximately 37% at 67% propane conversion (Figure 12e). The 15% higher BTX selectivity on the PtZn/$SiO_2$+ZSM-5 (Z/PA=50) compared to ZSM-5 at the same conversion suggests that the addition of the PtZn/$SiO_2$ enhances BTX formation.

With a decrease in the Z/PA ratio to 6, the methane selectivity decreases to 4% at propane conversion from 15-80% (Figure 12a). The methane selectivity is significantly lower than 25% on ZSM-5 and 20% on PtZn/$SiO_2$+ZSM-5 (Z/PA=50). The ethene selectivity behaves differently depending on the conversion (Figure 12b). At less 15% propane conversion, decrease in the ethene selectivity may be attributed to less monomolecular cracking due to the lower levels of ZSM-5 in the catalyst. In the range of 15-80% propane conversion, ethene slightly increases from 10% to 15% and is likely formed by secondary cracking reactions of higher molecular weight olefins. Eventually, the ethene selectivity decreases to 8% likely due to acid catalyzed conversion to higher molecular weight hydrocarbons, which is consistent with what has been shown for propene conversion on ZSM-5 (Figure 6b). For the PtZn/$SiO_2$+ZSM-5 catalyst with Z/PA=6, the BTX selectivity increases to 52% at 82% propane conversion (Figure 12e).

Further decreasing Z/PA ratio to 1, the methane selectivity remains nearly constant at less than 1% up to propane conversions of almost 70% (Figure 12a). The ethene selectivity is lower than 5% (Figure 12b). The propene selectivity at low propane conversion (<5%) is 95% (Figure 12c), which is close to the dehydrogenation selectivity (99%) on the PtZn/$SiO_2$. The results indicate that propane is primarily converted into propene on the PtZn/$SiO_2$ catalyst, rather than by monomolecular cracking on ZSM-5. As propane conversion increases to 72%, the propene selectivity decreases from 95% to 42%, which is attributed to secondary reactions on acid sites.

The maximum of the butenes selectivity (4%) appears at higher propane conversion (50%), implying that the consumption rate of butenes is lower (Figure 12d). The BTX selectivity as a function of propane conversion is higher on all PtZn/$SiO_2$+ZSM-5 catalysts than ZSM-5 regardless of Z/PA ratio, but it is surprising to find that the BTX selectivity with Z/PA=1 is lower than, for example, Z/PA=6 (Figure 12e). By comparing the BTX selectivity at similar propane conversions (40-47%) on ZSM-5 and PtZn/$SiO_2$+ZSM-5 catalysts, it is shown that the BTX selectivity on the former is 10%; while it is 20% and 35% on the latter with Z/PA ratio equal to 50 and 6, respectively. This suggests that increasing dehydrogenation rates can improve aromatics formation, which is consistent with previous results where the dehydrogenation step is rate limiting step for propane aromatization on ZSM-5.[13] However, the BTX selectivity decreases to 20% on the PtZn/$SiO_2$+ZSM-5 catalyst (Z/PA=1) suggesting that the limiting step of aromatics formation is no longer limited by dehydrogenation but is now limited by oligomerization and cyclization by ZSM-5.

Some general trends of product distribution are observed on the PtZn/$SiO_2$+ZSM-5 catalysts regardless of Z/PA ratio. The methane and ethene selectivities on the bifunctional catalysts are lower than those over ZSM-5, while the propene selectivity is higher (Figure 12a-12c). The butenes selectivity over the bifunctional catalysts undergoes a similar trend as that over ZSM-5, going through a maximum as a function of propane conversion increases (Figure 12d). The BTX selectivity on both ZSM-5 and PtZn/$SiO_2$+ZSM-5 catalysts are low at propane conversion below 15% and increases rapidly as the propane conversion increases. At higher propane conversion (>15%), the BTX aromatics selectivity is higher on the bifunctional catalysts than ZSM-5 (Figure 12e). Significant amounts of ethane are observed at propane conversion higher than 40% on the-ZSM-5 and PtZn/$SiO_2$+ZSM-5 catalysts, but ethane selectivity approaches zero at <5% propane conversion, suggesting ethane is a secondary product. (Figure 12f). The results show that addition of the PtZn/$SiO_2$ helps decrease formation of methane and ethene but increases propene, aromatics, and ethane yields.

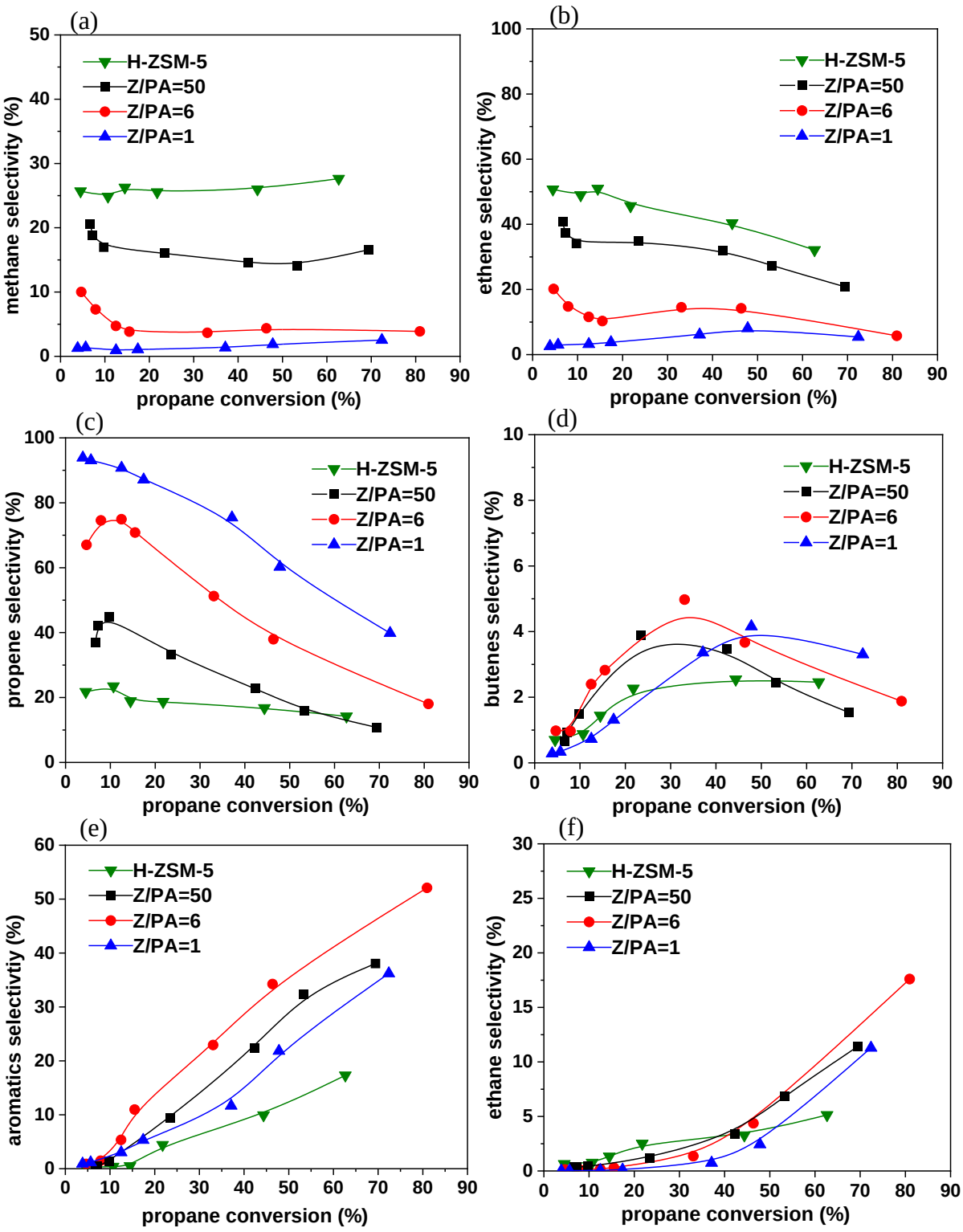


Figure 12. selectivities of (a) methane, (b) ethene, (c) propene, (d) butenes, (e) BTX aromatics (benzene, toluene, xylenes), (f) ethane as a function of propane conversion with a series of Z/PA ratio
Reaction conditions: cat., 0.005-0.7g, temperature, 550°C; pressure, 101 kPa; WHSV, 4-88 $h^{-1}$

The BTX distribution at different propane conversions on ZSM-5 and PtZn/$SiO_2$+ZSM-5 catalysts were also determined in Figure 13. On ZSM-5, the BTX distribution slightly changes with propane conversions and dominant aromatics are benzene (~49%) and toluene (~38%). On the PtZn/$SiO_2$+ZSM-5, benzene percentage is higher compared to ZSM-5 at low propane conversions (10-13%), and benzene percentage increases as Z/PA ratio decreases. For example, with Z/PA=1, aromatics majorly consist of benzene (79%) at 13% propane conversion. These results imply that increasing loading of PtZn catalyst may enhance the dehydrogenation of $C_6$ cyclic hydrocarbons formed by propene dimerization-cyclization and increase the benzene percentage in the BTX distribution at low propane conversions. At medium propane conversions (43-46%), benzene percentage decreases and toluene percentage increases as Z/PA decreases to 6. However, with further decrease in Z/PA ratio to 1, the BTX distribution is similar to that on ZSM-5.

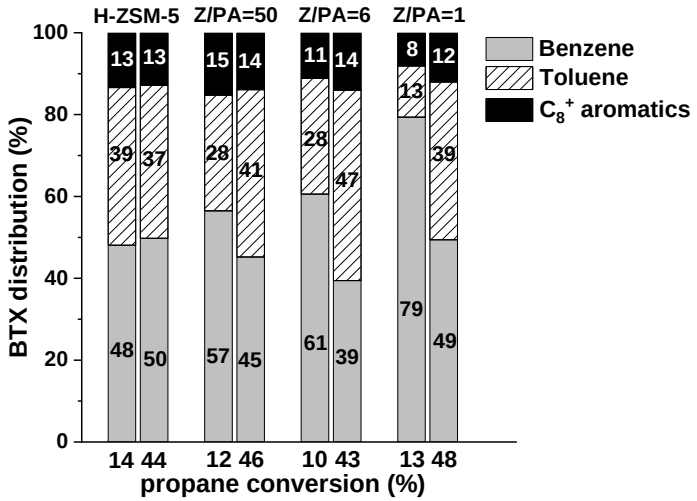


Figure 13. BTX distribution at different propane conversions on ZSM-5 and PtZn/$SiO_2$+ZSM-5 (Z/PA=50, 6, 1) catalysts

To further understand the correlation between Z/PA ratio and selectivity to methane and BTX, the formation rates of methane and BTX as a function of propane conversion on ZSM-5 and PtZn/$SiO_2$+ZSM-5 catalysts were determined in Figure 14. The methane formation rates slightly decrease as propane conversion decreases on both catalysts (Figure 14a). As a result, the average methane formation rates at different conversions on ZSM-5 and PtZn/$SiO_2$+ZSM-5 catalysts are used for comparison. On ZSM-5, the average methane formation rate normalized by the amounts of ZSM-5 in the evaluated propane conversion range is about $4.6\times10^{-7}$ (mol $CH_4$)(g ZSM-5)$^{-1}s^{-1}$.

On the bifunctional catalysts with Z/PA ratio of 50, 6 and 1, the average methane formation rates normalized by the amounts of ZSM-5 are $2.6\times10^{-7}$, $3.1\times10^{-7}$, $3.5\times10^{-7}$ (mol $CH_4$)(g ZSM-5)$^{-1}s^{-1}$, respectively. Within the scatter of the data, the methane formation rates are independent of Z/PA ratio, suggesting methane is formed primarily by monomolecular cracking and lower methane selectivity in PtZn/$SiO_2$+ZSM-5 is due to the lower loading of ZSM-5. For catalyst with lower Z/PA ratio, the propene selectivity increases (Figure 12c). Therefore, monomolecular cracking and formation of methane is independent of propene concentration. The slight decrease in methane with increasing conversion may, therefore, be due to inhibition of monomolecular cracking by BTX, which increases with increasing propane conversion.

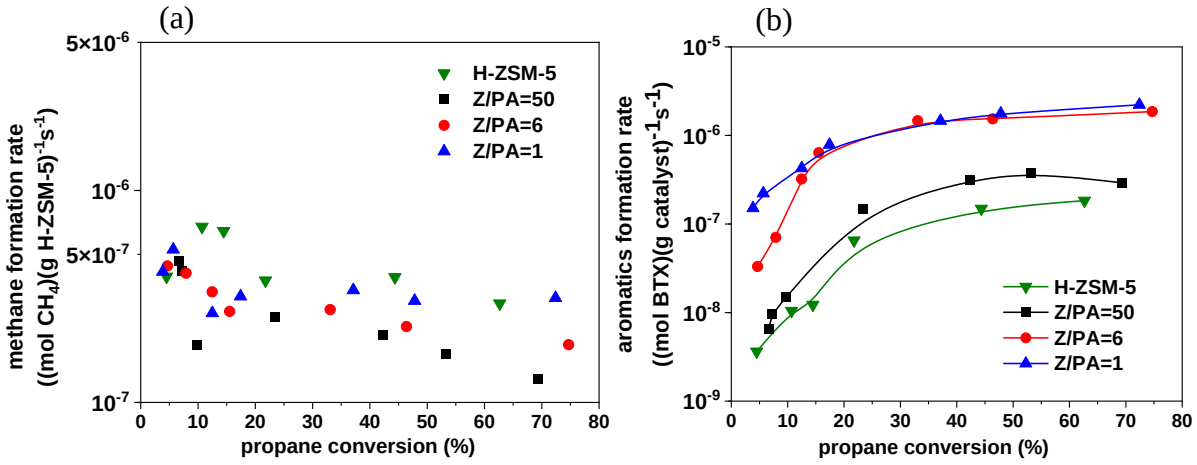


Figure 14. (a) methane formation rate (b) aromatics formation rate as a function of propane conversion on ZSM-5 and PtZn/$SiO_2$+ZSM-5 catalysts

Figure 14b shows BTX formation rate on ZSM-5 and PtZn/$SiO_2$+ZSM-5 catalysts. The BTX formation rate on the former is low ($3.6\times10^{-9}$ (mol BTX)(g catalyst) $^{-1}s^{-1}$) at 10% propane conversion and increases by 200 times ($1.5\times10^{-7}$ (mol BTX)(g catalyst) $^{-1}s^{-1}$) at 50% propane conversion. The Z/PA=50 catalyst has a slightly higher BTX formation rate ($3.8\times10^{-7}$ (mol BTX)(g catalyst) $^{-1}s^{-1}$) at ~50% propane conversion. As the Z/PA ratio decreases to 6, BTX formation rate increases from $3.3\times10^{-8}$ (mol BTX)(g catalyst) $^{-1}s^{-1}$ at 5% propane conversion to $1.5\times10^{-6}$ (mol BTX)(g catalyst) $^{-1}s^{-1}$ at high conversion (~50%), which is 10 times higher than that on ZSM-5. With Z/PA=1, BTX formation rate ($1.5\times10^{-7}$ (mol BTX)(g catalyst) $^{-1}s^{-1}$) is 40 times higher than ZSM-5. At conversion higher than 15%, the rate is nearly the same as that with Z/PA=6.

### 3.3.5 The Effect of Propane Partial Pressure on Product Distribution on Bifunctional PtZn/$SiO_2$+ZSM-5 catalysts

Since the Z/PA=1 catalyst has the lowest methane selectivity (~1%) and highest aromatics formation rate, pure propane (99.99%) at 101 kPa was also evaluated on this catalyst at 550℃. The product distribution is compared to that using 5% propane to understand the influence of propane partial pressure on the product selectivity (Figure 15). A similar product selectivity as a function of propane conversion is observed at two propane partial pressures. However, higher propane partial pressure has a positive impact on propene conversion since the propene selectivity is lower and decreases much faster than that at lower propane partial pressure at the same conversion (Figure 15c). Meanwhile, the selectivities to butenes and BTX are higher at the higher propane pressure (Figure 15d and 15e). A high BTX selectivity (42%) is observed at 65% propane conversion at higher propane partial pressure, which is 10% higher than that using 5% propane at the same conversion (Figure 15e). Figure 15f shows that ethane selectivity also increases by about 2 times that at lower propane pressure above 30% propane conversion. The increased ethane selectivity occurs at about the same propane conversion as the BTX selectivity increases, suggesting that hydrogen, which formed during aromatics formation, hydrogenates ethene. In summary, these results show that high propane partial pressure has a beneficial effect on olefin conversion and aromatics formation rate but also leads to higher selectivity to unfavored ethane.

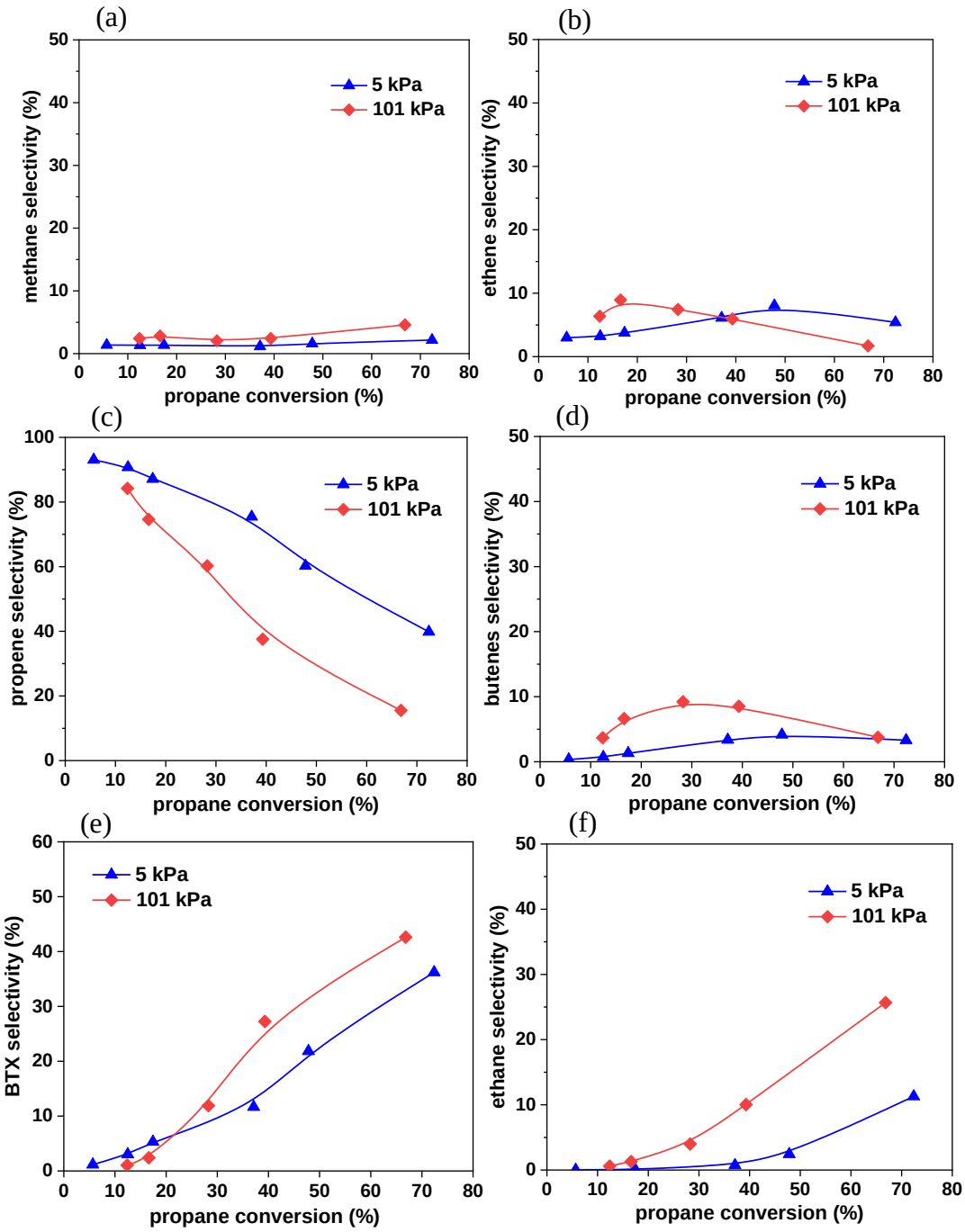


Figure 15. selectivities of (a) methane, (b) ethene, (c) propene, (d) butenes, (e) BTX aromatics, (f) ethane as a function of propane conversion at 5 kPa and 101 kPa propane partial pressure.
Reaction conditions: cat., 0.005-0.1g, temperature, 550°C; total pressure, 101 kPa; Z/PA=1; WHSV=54-1072 $h^{-1}$

### 3.3.6 Cyclohexene Conversion to Aromatics

Naphthenes or cyclic paraffins and olefins, are likely key intermediates for formation of aromatics. To better understand the aromatization pathway, cyclohexene is selected as a model compound, and the relative rates and selectivity to products over $PtZn/SiO_2$, $Ga/Al_2O_3$, and ZSM-5 catalysts were determined.

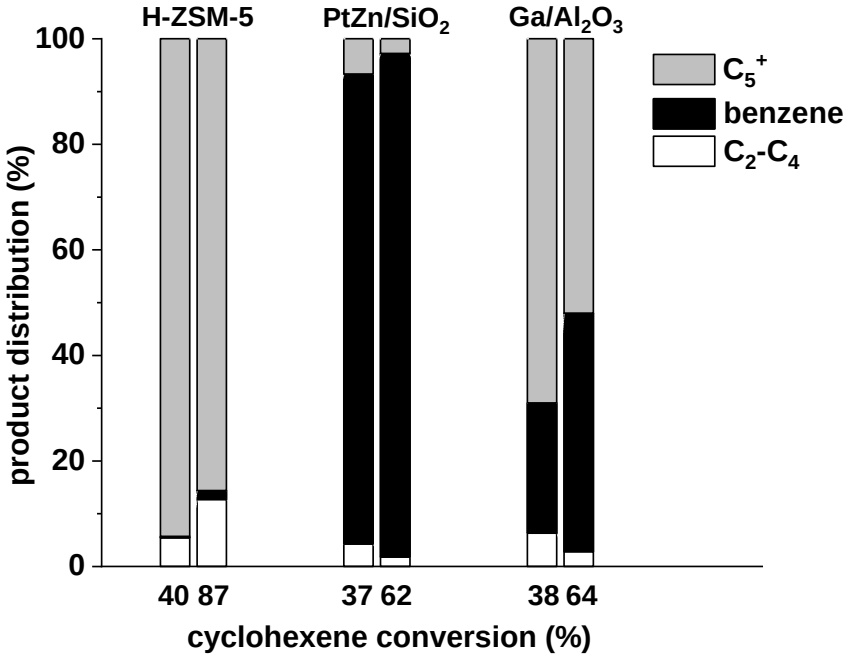


Figure 16. Product distribution of cyclohexene conversion on ZSM-5, $PtZn/SiO_2$ and $Ga/Al_2O_3$ catalysts. Reaction conditions: cat., 0.0015-0.5g, temperature, 550°C; pressure, 101 kPa; cyclohexene partial pressure, 3 kPa[a]; WHSV, 0.3-104 $h^{-1}$

[a] cyclohexene partial pressure is estimated by vapor saturation pressure at 0°C using Antoine equation

Table 5. The apparent rates of cyclohexene conversion and the formation of benzene and $C_2$-$C_5^+$ cracking products over ZSM-5, $PtZn/SiO_2$ and $Ga/Al_2O_3$ catalysts [a]

| Catalysts | Cyclohexene conversion rate (mol $C_6H_{10}$)(g catalyst)$^{-1}s^{-1}$ | Benzene formation rate (mol benzene)(g catalyst)$^{-1}s^{-1}$ | Cracking rate (mol $C_2$-$C_5^+$)(g catalyst)$^{-1}s^{-1}$ |
|---|---|---|---|
| ZSM-5 | $5.4\times10^{-4}$ | $1.3\times10^{-6}$ | $5.3\times10^{-4}$ |
| $PtZn/SiO_2$ | $3.1\times10^{-4}$ | $2.8\times10^{-4}$ | $3.5\times10^{-5}$ |
| $Ga/Al_2O_3$ | $3.8\times10^{-6}$ | $9.5\times10^{-7}$ | $2.9\times10^{-8}$ |

[a] The rates are estimated at 38-40% cyclohexene conversion.

Figure 16 shows that cyclohexene is primarily converted to $C_5^+$ hydrocarbons on ZSM-5 and benzene only formed with low selectivity (2%) at high cyclohexene conversion (87%). Most of $C_5^+$ hydrocarbons are composed of $C_6$ olefins. The detailed product selectivities on each catalyst are listed in Table S2. On the contrary, the $PtZn/SiO_2$ demonstrates higher than 90% selectivity to benzene with less than 10% selectivity to non-aromatic $C_2$-$C_5^+$ hydrocarbons. In comparison with ZSM-5 and $PtZn/SiO_2$, $Ga/Al_2O_3$ demonstrates a combination of dehydrogenation and cracking selectivity with 25% selectivity to benzene at 38% cyclohexene conversion. The benzene selectivity increases to 45% as the cyclohexene conversion increases to 64%.

The cyclohexene conversion rates over each catalyst were further estimated (Table 5). The cyclohexene conversion rates on ZSM-5 and $PtZn/SiO_2$ are similar, $5.4\times10^{-4}$ (mol $C_6H_{10}$)(g ZSM-5)$^{-1}s^{-1}$ and $3.1\times10^{-4}$ (mol $C_6H_{10}$)(g $PtZn/SiO_2$)$^{-1}s^{-1}$ respectively; while $Ga/Al_2O_3$ is $3.8\times10^{-6}$ (mol $C_6H_{10}$)(g $Ga/Al_2O_3$)$^{-1}s^{-1}$, approximately 100 times lower. Benzene formation and cracking rates are estimated by multiplying the cyclohexene conversion rate with the carbon selectivity to benzene and $C_2$-$C_5^+$ hydrocarbons, respectively. $C_2$-$C_5^+$ hydrocarbons are indicative of non-aromatic products. The benzene formation rates on ZSM-5 and $Ga/Al_2O_3$ were similar, $1.3\times10^{-6}$ (mol benzene)(g ZSM-5)$^{-1}s^{-1}$ and $9.5\times10^{-7}$ (mol benzene)(g $Ga/Al_2O_3$)$^{-1}s^{-1}$, respectively. Even though $Ga/Al_2O_3$ has higher selectivity to benzene, the conversion rate is lower than ZSM-5 and, therefore, the benzene formation rate is comparable on the ZSM-5 and $Ga/Al_2O_3$. On the contrary, the benzene formation rate on $PtZn/SiO_2$ is $2.8\times10^{-4}$ (mol benzene)(g $PtZn/SiO_2$)$^{-1}s^{-1}$, which is 200 times higher than that on ZSM-5. However, cracking rate on ZSM-5 ($5.3\times10^{-4}$ (mol $C_2$-$C_5^+$)(g ZSM-5)$^{-1}s^{-1}$) is the same order of magnitude of the benzene formation rate on the $PtZn/SiO_2$.

## 3.4 Discussions

### 3.4.1 The Strategy to Minimize Methane Formation

The propane conversion rate on ZSM-5 is 1.5 times higher than that on the $Ga/Al_2O_3$ (Table 3). Based on the difference in rates, 60% of propane will react with ZSM-5 by propane monomolecular cracking and the remaining 40% will react with $Ga/Al_2O_3$ by dehydrogenation. Based on the selectivities for each catalyst, the primary product mixture on ZSM-5 will consist of ~17%

methane and ~43% light olefins with some higher molecular weight hydrocarbons, while the product for $Ga/Al_2O_3$ will consist of 39% selectivity to propene and less than 1% methane.

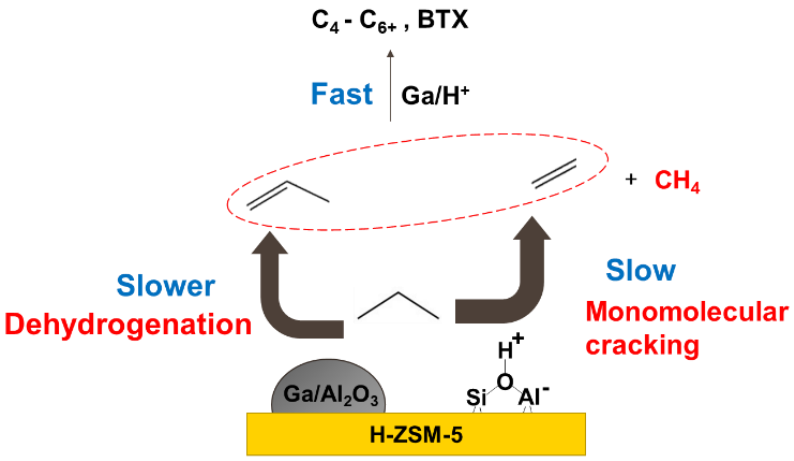


Figure 17. relative kinetics of light gas formation pathways on the $Ga/Al_2O_3$+ZSM-5 catalysts

While Ga has higher propene selectivity, Ga dehydrogenation rates and ZSM-5 monomolecular cracking rates are in the same order of magnitude. As a result, significant amounts of propane will react with the ZSM-5 to form light olefin and unreactive methane simultaneously. By comparing the conversion rates of alkanes and olefins on ZSM-5, olefins are significantly more reactive than alkanes (Figure 6b), and since olefins can be eventually converted to higher molecular weight hydrocarbons with little methane or ethane, these results suggest that the majority of light gas is caused by monomolecular cracking on ZSM-5 on this bifunctional catalyst. The relative kinetics of the steps for dehydroaromatization of propane on the $Ga/Al_2O_3$+ZSM-5 catalyst is summarized qualitatively in Figure 17.

Accordingly, we hypothesize that methane formation can be minimized by significantly enhancing propane conversion rate by dehydrogenation and reducing the propane conversion rate on ZSM-5. The strategy is to balance the alkane and olefin conversion rates on two catalytic functions to ensure that propane will be primarily activated by dehydrogenation catalyst. Since olefin reactivity is much higher than alkane, olefin conversion rate on ZSM-5 is still high even with decreasing amounts of zeolite. Based on this strategy, the bifunctional catalyst requires a highly active

dehydrogenation catalyst with much higher propane conversion rate than ZSM-5. The previous study with Pt/ZSM-5 reported that propene is the only primary product from propane conversion, which suggests propane conversion occurs on Pt sites. However, monometallic Pt has two drawbacks, low dehydrogenation selectivity and fast deactivation. For example, a 20wt% selectivity to methane on the Pt/ZSM-5 was still observed. For Pt/ZSM-5, methane and part of ethane results from hydrogenolysis of propane on Pt sites.[24] In addition, metallic Pt sites deactivates rapidly due to fast coke formation. As a result, very quickly, Pt/ZSM-5 catalysts are very similar to ZSM-5. The $PtZn/SiO_2$ catalyst (PtZn alloy) has much higher dehydrogenation rates, olefin selectivity and stability than monometallic Pt. However, the methane selectivity is still high at 15-20% on the $PtZn/SiO_2$+ZSM-5 (Z/PA=50), i.e., a catalyst with high loading of ZSM-5. As Z/PA ratio decreases, the methane selectivity decreases and BTX selectivity increases. This indicates that the optimal selectivity is dependent on balancing the alkane dehydrogenation and olefin conversion rates, while limiting monomolecular cracking. Accordingly, the product distribution can be controlled by adjusting the loading of each component ($PtZn/SiO_2$ and ZSM-5) in the bifunctional catalyst. Because olefins are much more reactive than alkanes on ZSM-5, the rate of monomolecular cracking can be minimized, while maintaining high olefin conversions with lower loadings of ZSM-5. Figure 12a-12c show that the methane and ethene selectivities decrease and propene selectivity increases at low propane conversion (<5%) when Z/PA ratio decreases from 50 to 1, which is consistent with our hypothesis. As the loading of the $PtZn/SiO_2$ increases (lower Z/PA ratio), propane conversion rate on the $PtZn/SiO_2$ becomes significantly higher relatively to that on ZSM-5. Low methane selectivity (<2%) and high propene selectivity (95%) at 5% propane conversion on the Z/PA=1 catalyst suggests that $PtZn/SiO_2$ propane dehydrogenation dominates over ZSM-5 monomolecular cracking. At high conversions, the decreasing propene selectivity indicates that propene is sufficiently reactive despite the lower levels of ZSM-5 in the catalyst.

Based on the results in Figure 12, methane formation rates normalized by the amount of ZSM-5 in the bifunctional catalyst regardless of Z/PA ratio are similar with those on ZSM-5, which suggests that monomolecular cracking is still occurring in all catalysts. Consequently, the possibility that decreasing methane selectivity on the $PtZn/SiO_2$+ZSM-5 catalysts is due to suppressed monomolecular cracking by higher olefin concentration can be excluded. The low methane

selectivity is resulting from increasing propane conversion rate on the selective dehydrogenation catalyst and decreasing the propane monomolecular cracking on ZSM-5 while maintaining high olefin conversion rates.

### 3.4.2 Comparison of Propane Dehydroaromatization Pathway

Figure 18 compares the dominant reaction pathways for ZSM-5, $Ga/Al_2O_3$+ZSM-5 and $PtZn/SiO_2$+ZSM-5 catalysts. The blue and orange colored-arrows are used to indicate the dominant reaction pathways catalyzed by acid and metal catalysts, respectively, while the width of the colored-arrows exhibit the relative rate of individual reactions qualitatively. Figure 18a shows the typical propane conversion pathway catalyzed by ZSM-5. Propane is converted to methane, ethene and propene by monomolecular cracking. Ethene and propene rapidly undergo oligomerization, cracking and cyclization to produce $C_3$-$C_6$ as well as cyclic hydrocarbons. The cyclohexene cracking rate is significantly higher than benzene formation rate, suggesting most of cyclic hydrocarbons will return to the oligomerization-cracking cycle to produce olefins and only few are converted into aromatics by hydrogen transfer. Thus, aromatics formation by ZSM-5 is kinetically slow.

With addition of Ga, Ga/ZSM-5 bifunctional catalysts have higher propane conversion rates and higher aromatics selectivity.[25–31] The $Ga/Al_2O_3$+ZSM-5 catalyst is used as a representative bifunctional catalyst to demonstrate propane conversion reaction pathway (Figure 18b). Based on conversion rates on ZSM-5 and $Ga/Al_2O_3$ (Table 3), propane is converted at similar rates by ZSM-5 monomolecular cracking and Ga dehydrogenation. Although the methane selectivity of Ga/ZSM-5 is improved relative to ZSM-5, there is still a significant selectivity from monomolecular cracking in this bifunctional catalyst. The light olefins in the reaction mixture go through a similar reaction pathway to those on ZSM-5 to form higher molecular weight olefins, including cyclic olefins. As indicated in the Table 5, the cyclohexene conversion rate on ZSM-5 is significantly higher than on $Ga/Al_2O_3$, suggesting that cyclic olefins primarily crack on the former rather than dehydrogenate to aromatics on the latter. The benzene formation rates on ZSM-5 and $Ga/Al_2O_3$ are similar, suggesting the major role of $Ga/Al_2O_3$ is to form some propene and to facilitate the dehydrogenation step of cyclic olefins to aromatics. This is indicative of higher rate and selectivity to aromatics on the bifunctional Ga/ZSM-5 catalysts.

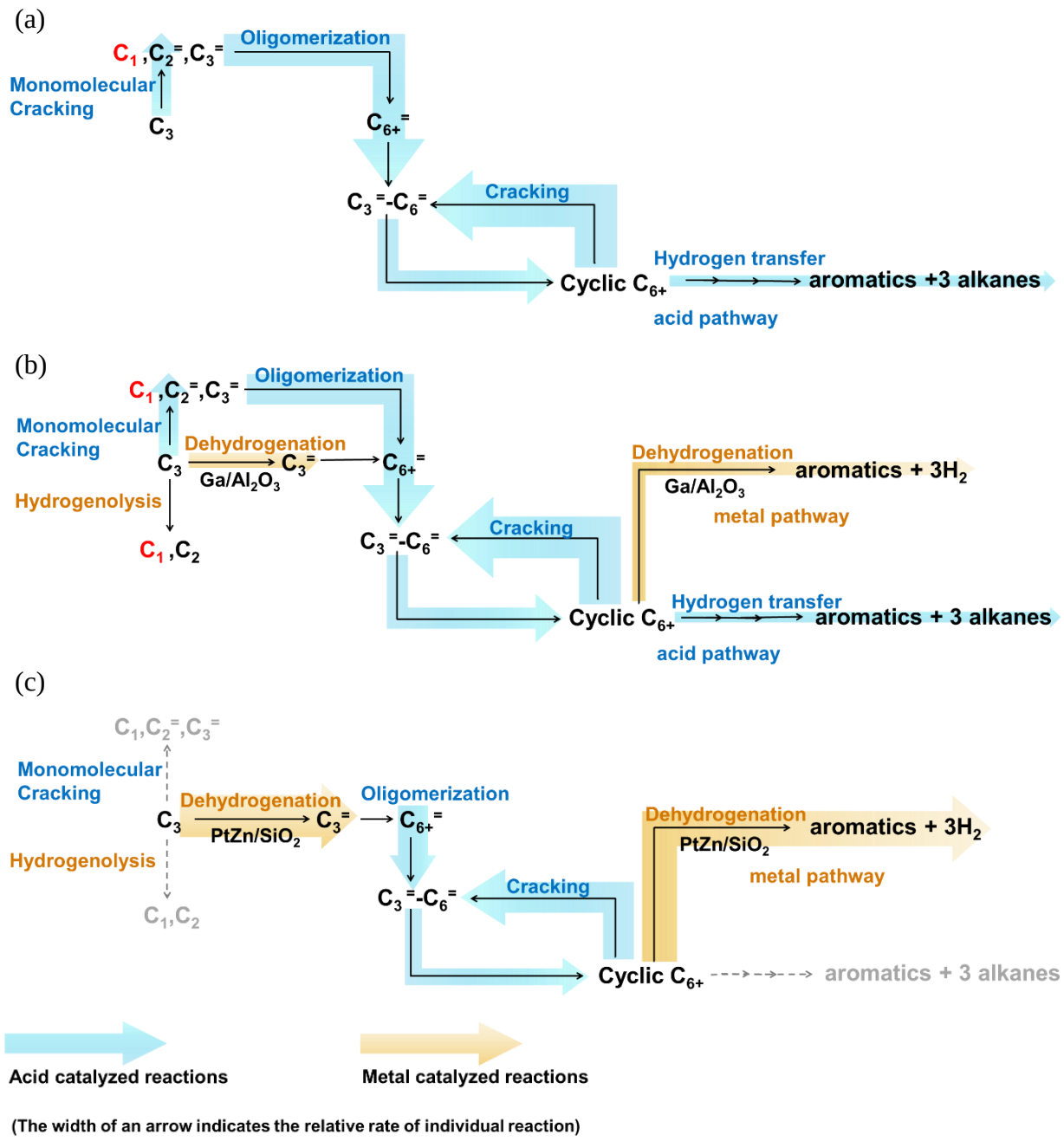


Figure 18. (a) Dominant reaction pathways on (a) ZSM-5 (b) $Ga/Al_2O_3$+ZSM-5 (c) $PtZn/SiO_2$+ZSM-5 catalysts

The $PtZn/SiO_2$+ZSM-5 catalyst not only has a low methane selectivity, but also has a higher rate and selectivity to BTX than ZSM-5 and Ga/ZSM-5. Figure 18c summarizes the effect of the $PtZn/SiO_2$ on the dominant propane conversion pathways over the $PtZn/SiO_2$+ZSM-5 bifunctional

catalyst. The dash arrow is utilized to highlight the reaction pathways that have been minimized. $PtZn/SiO_2$ has a higher propene selectivity; thus, there is little methane formed by hydrogenolysis. In addition, the high dehydrogenation rate has two beneficial effects. First, it increases propene selectivity and allows for a lower loading of ZSM-5, resulting in a much smaller contribution of methane from monomolecular cracking by ZSM-5. Second, it has a much higher selectivity and rate of aromatics formation than ZSM-5 or Ga; thus, the BTX formation rates are higher, suggesting that cyclohexene is primarily converted to benzene by the dehydrogenation pathway.

As Z/PA ratio decreases from 50 to 6, the aromatics selectivity increases at the constant propane conversion. This suggests the dehydrogenation reaction is the rate limiting step for aromatics formation since the aromatics are formed at a higher rate with increasing amounts of $PtZn/SiO_2$ in the bifunctional catalyst. With Z/PA=6, a maximum selectivity of 52% to BTX at about 80% propane conversion is produced without making significant amount of methane (<5%). The BTX selectivity is estimated to exceed 85% at full recycle of all reactive intermediates with byproducts of 5% methane and 10% ethane. However, as Z/PA ratio further decreases from 6 to 1, the BTX selectivity decreases. This indicates that increasing dehydrogenation rate no longer enhances the aromatics formation rate and suggests that aromatics formation is likely limited by acid catalyzed reactions, i.e., oligomerization and cyclization.

The results of product selectivity using higher propane partial pressure suggest the reaction pathway is similar to that using dilute propane. The selectivity of methane and ethene increases slightly, indicating monomolecular cracking is slightly affected by the propane partial pressure (Figure 15a and 15b). The decrease in propene selectivity as a function of propane conversion implies that the olefin oligomerization rate is higher at higher propane pressure (Figure 15c). This result agrees with higher selectivity to butenes and aromatics using higher propane partial pressure (Figure 15d and 15e). Nevertheless, aromatics formation involves oligomerization steps on acid sites and dehydrogenation steps on PtZn sites, which favor high and low pressures, respectively.[7] At higher propane pressure, the ethane selectivity is higher than at lower partial pressure (Figure 15f). Since the methane selectivity is low, it is less likely that ethane is formed by either propane hydrogenolysis on $PtZn/SiO_2$, or monomolecular cracking followed by ethene hydrogenation. Since the ethane selectivity changes in a similar way as the aromatics selectivity, ethane is inferred

to be a secondary product formed along with aromatics and co-produced hydrogen, for example, by aromatics dealkylation along with ethene hydrogenation.[8,63–65]

Generally, activation of light alkane to olefin is thought as the rate limiting step for propane dehydroaromatization.[1,66] As a result, high activity zeolites are utilized in the bifunctional catalysts to enhance not only propane activation but the rate and selectivity to aromatics by rapidly converting generated olefins to aromatics. However, significant monomolecular cracking occurs on catalysts with high loading of ZSM-5, and eventually formation of methane limits the production of aromatics. The selectivity to methane can be reduced by adjusting the Z/PA ratio in the $PtZn/SiO_2$+ZSM-5 to balance the rates of alkane and olefin conversion. With high loading of $PtZn/SiO_2$, the propane conversion gives primarily propene, leading to higher selectivity of higher molecular weight hydrocarbons, including $C_4^+$ paraffins, olefins and BTX. By balancing the dehydrogenation rate with PtZn alloy and the olefin conversion rates by ZSM-5, higher yields of valuable products can be obtained.

### 3.5 Conclusion

Comparison of the relative rate and selectivity of propane conversion on $Ga/Al_2O_3$ and ZSM-5, methane is suggested to form predominantly by monomolecular cracking on ZSM-5. While Ga increases the propene selectivity and rate through propane dehydrogenation, there is still a significant contribution by monomolecular cracking with high methane selectivity from ZSM-5 in the bifunctional catalyst. By utilizing the $PtZn/SiO_2$ (PtZn alloy) with very high dehydrogenation rate and selectivity, significant improvements in the product distribution are observed. Firstly, the methane selectivity decreases to less than 5% because the hydrogenolysis and monomolecular cracking pathways are minimized. Since the rate and selectivity of cyclohexene to benzene on $PtZn/SiO_2$ is significantly higher than that on $Ga/Al_2O_3$ and ZSM-5, aromatics are formed at a higher rate by the metal pathway (dehydrogenation) over the former catalysts instead of acid pathway (hydrogen transfer) over the latter two. To achieve the optimal product selectivity, it is necessary to balance the propane dehydrogenation and olefin conversion rates by changing the ratio of PtZn alloy and ZSM-5. This work also highlights the difference in the reaction pathways for propane dehydroaromatization for ZSM-5, Ga/ZSM-5 and $PtZn/SiO_2$+ZSM-5.

# 4. THE DIFFERENCE IN DEHYDROAROMATIZATION PATHWAYS OF PROPANE ON BIFUNCTIONAL CATALYSTS

This chapter is reproduced from C.-W. Chang, J.M. Miller, “Catalytic Process Development Strategies for Propane to Liquid Hydrocarbons on Bifunctional Catalysts". submitted to Applied Catalysis A: General

## 4.1 Introduction

Since propane activation is highly endothermic and is the rate-limiting step, propane conversion was reported at high temperatures (>500°C) on Ga/MFI catalysts. However, at high temperatures, alkane monomolecular cracking rates are high, leading to high methane selectivity. Additionally, catalyst deactivates rapidly at high temperatures. As a result, the dehydroaromatization pathways were mostly studied on Ga/ZSM-5 catalysts in a limited temperature range, i.e., 550-650°C. The understandings of the temperature effect on propane dehydroaromatization pathways are limited. By utilizing a dehydrogenation catalyst with much higher propane dehydrogenation rate than Ga and converting generated olefins with zeolites, propane conversion can occur at much lower temperatures and give distinctly different product distribution on the PtZn/SiO2+ZSM-5 bifunctional catalyst.

## 4.2 Objective

The objective of Chapter four is to investigate the temperature effect on the propane dehydroaromatization pathways on the PtZn/SiO2+ZSM-5 bifunctional catalysts to better understand how reaction temperature and duel catalytic functions are associated with controlling selectivity to light gas and liquid hydrocarbons as well aromatics distribution. Furthermore, the limitations and opportunities for low temperature propane conversion will be discussed. Eventually, the strategies for optimal bifunctional catalyst compositions and operation ranges depending on the reaction temperatures for propane to valuable liquid hydrocarbons, i.e., aromatics and gasoline-blending hydrocarbons, are also different.

## 4.3 Results

### 4.3.1 Temperature Effect on Propane Conversion Rate and Product Selectivity

Previously in our study, the $PtZn/SiO_2$+ZSM-5 catalyst with Z/PA=1, where Z/PA was defined as the weight ratio of ZSM-5 (Z), with a Si/Al ratio of 100, and 2%$PtZn/SiO_2$ (PA), had the lowest methane selectivity (<5%) and highest BTX formation rate for propane conversions at 550°C [67]. As a result, the Z/PA=1 bifunctional catalyst will be utilized to study the temperature effect on propane conversion rates and product selectivity at lower temperatures. Figure 19 shows the product selectivity as a function of propane conversion and reaction temperature from 350-550℃. At 550℃, the methane selectivity is less than 5% from 12-68% propane conversion (Figure 19a). The propene selectivity is high (85%) at 12% propane conversion (Figure 19c). These results indicate the dominant primary product is propene by dehydrogenation. As propane conversion increases, the propene selectivity decreases, suggesting that propene is subsequently converted to higher molecular weight hydrocarbons. The selectivities to butenes and $C_5^+$ hydrocarbons go through a maximum of 10% and 4% at propane conversions of 30% and 40%, respectively (Figure 19e and 19f). The BTX selectivity is zero and increases rapidly to 44% as propane conversion increases from 12% to 67% (Figure 19g). The ethane selectivity increases in a similar way to that of BTX and is 26% at 67% propane conversion (Figure 19h), implying ethane is likely formed along with BTX. These results suggest that butenes and $C_5^+$ hydrocarbons are formed by propene and further converted to BTX and ethane at high propane conversions.

At a lower temperature of 450℃, the methane selectivity is low (~2%) and the ethene selectivity is 5-7% at 7% propane conversion, indicating propane is predominantly dehydrogenated to propene (Figure 19a and 19b). However, the propene selectivity is only 65% at 7% propane conversion, while the selectivity to butene and $C_5^+$ hydrocarbons are 15% and 5% (Figure 19c, 19e and 19f). The rapid decrease in the propene selectivity at low propane conversions suggests that propene is rapidly converted to higher molecular weight olefins at 450℃. As a result, secondary reactions of propene allow ~56 % propane conversion at 450℃, which is much higher than the equilibrium conversion of 9%. The selectivities to butenes and $C_5^+$ hydrocarbons undergo a maximum at the propane conversion of 13% and 15%, while the butanes selectivity goes through a maximum of 25% at a higher conversion (~40%), suggesting butanes are secondary products

from butenes and $C_5^+$ hydrocarbons (Figure 19d, 19e and 19f). BTX products are observed at propane conversion of 7% and selectivity increases with increasing propane conversions (Figure 19g). The ethane selectivity is zero at below 7% propane conversion and increases significantly to 42% at 58% propane conversion (Figure 19h). The selectivity of ethane and butanes increases rapidly as aromatics are formed, implying that significant amounts of hydrogen formed with aromatics hydrogenates ethene and butenes to make ethane and butanes, respectively.

At 400℃, the maximum propane conversion (38%) on the bifunctional catalyst is significantly higher than the equilibrium conversion of propane dehydrogenation (4%) due to propene secondary reactions. Both methane and ethene selectivity is less than 2% at up to 38% propane conversion, (Figure 19a and 19b). However, the propene selectivity is 32% at ~5% propane conversion. At the same propane conversion, the selectivities to butanes (18%), butenes (18%) and $C_5^+$ (13%) are substantially high, indicative of fast secondary reactions of propene to $C_4^+$ hydrocarbons (Figure 19c-19f).

In addition, the selectivities of propene, butene and $C_5^+$ hydrocarbons decrease rapidly as propane conversion increases, while the butanes selectivity has a maximum of ~37% at 27% propane conversion, suggesting butanes become dominant intermediates formed from higher molecular weight olefins at 400℃ and are eventually converted to BTX at higher propane conversions. At 38% propane conversion, the BTX selectivity is 30% and ethane selectivity is 33% (Figure 19g and 19h). Although higher than 40% propane conversion can be achieved at 400℃ by further lowering the space velocity, significant amounts of undesired ethane will be formed simultaneously. With further decrease in temperature to 350℃, the low methane selectivity (<1%) is identical to that on the PtZn/$SiO_2$, indicating propene is the only primary product and is formed by dehydrogenation (Figure 19a). The propene selectivity is 20% at low propane conversion (~5%) (Figure 19c). The butanes selectivity increases from 40% to 63% as propane conversion increases from 4% to 18% (Figure 19d). The results indicate that tandem reaction of propane to butanes is fast at 350℃. The butanes are likely formed in sequence of propane dehydrogenation on PtZn, propene oligomerization-cracking on ZSM-5 and butenes hydrogenation on PtZn. The BTX selectivity is 6% at low propane conversion (~5%) and increase in the BTX selectivity is low (Figure 19g). The BTX selectivity is 15% at 18% propane conversion.

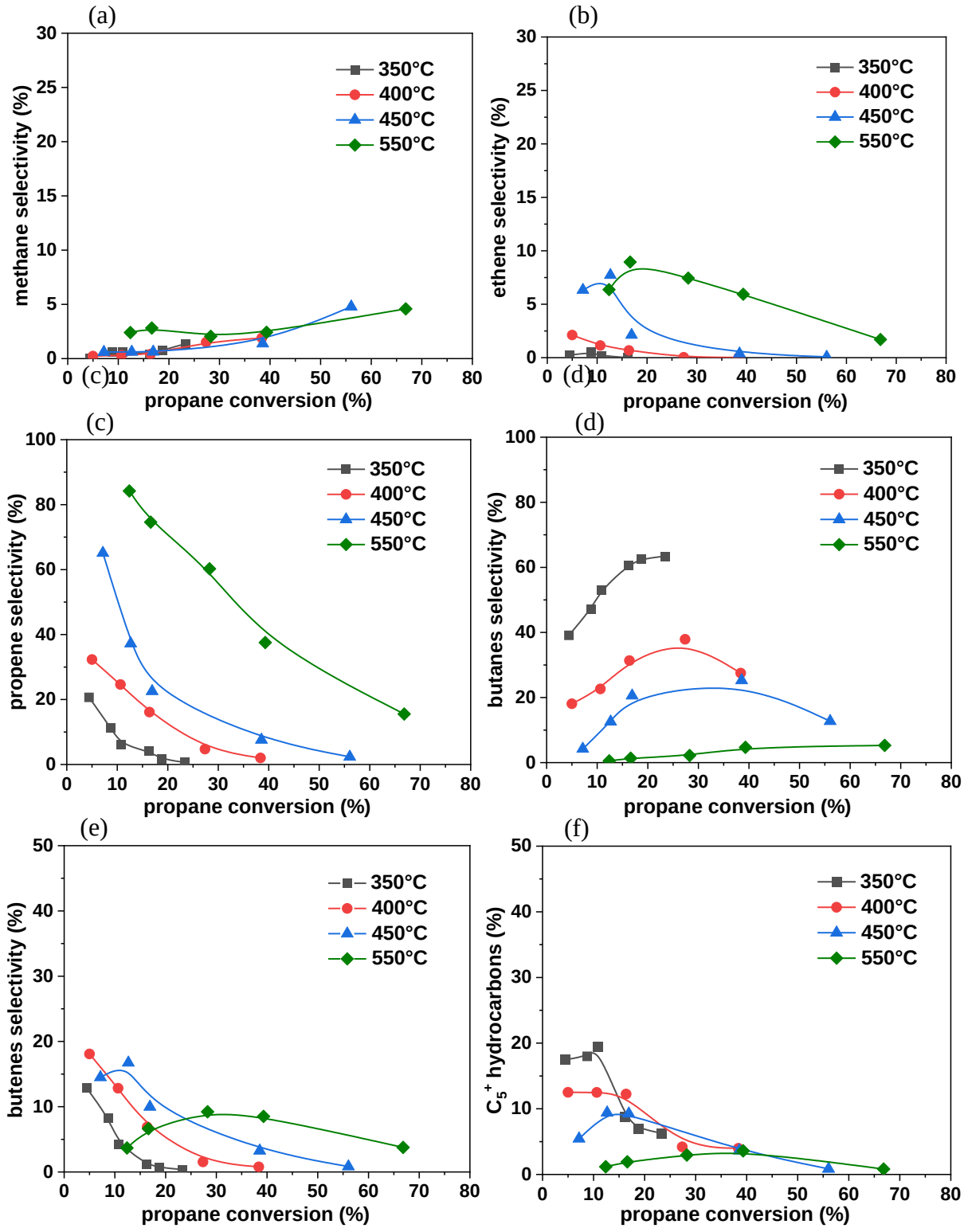


Figure 19. selectivites of (a) methane, (b) ethene, (c) propene, (d) butanes, (e) butenes, (f) $C_5^+$, (g) aromatics (h) ethane as a function of propane conversion and reaction temperature on the $PtZn/SiO_2$+ZSM-5 (Z/PA=1) catalyst Reaction conditions: cat., 0.01-2.0 g; pressure, 101 kPa; WHSV, 0.36-715 $h^{-1}$

Figure 19. Continued

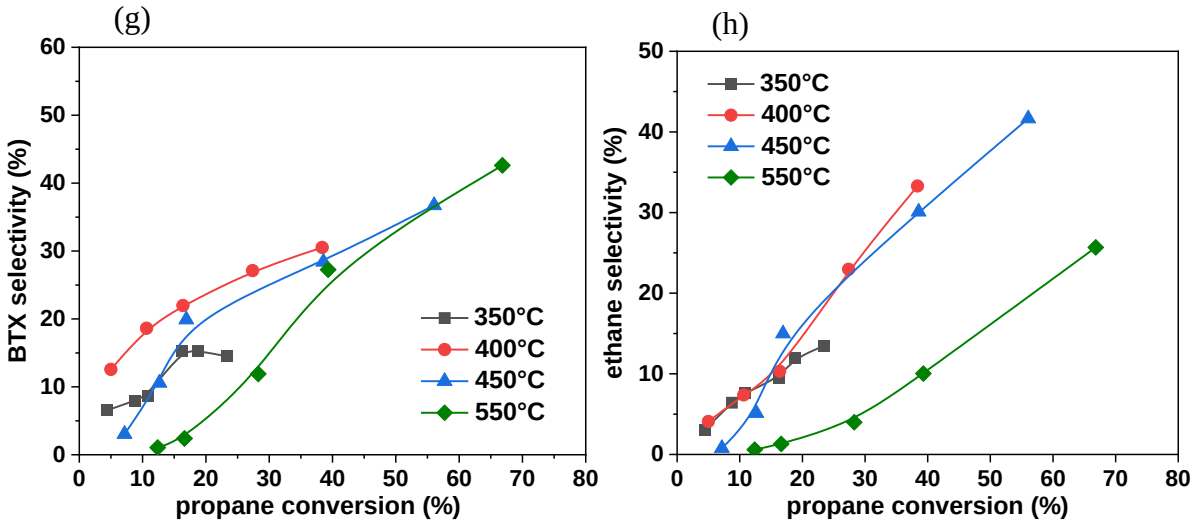


The ethane selectivity increases with increasing propane conversion and is 13% at 24% conversion. The maximum propane conversion is around 25% at 350℃ on this bifunctional catalyst, which is far beyond the equilibrium conversion of propane to propene (<3%). However, the conversion is low even with very low space velocity, implying that 350℃ is unlikely to obtain high propane conversion and BTX yields.

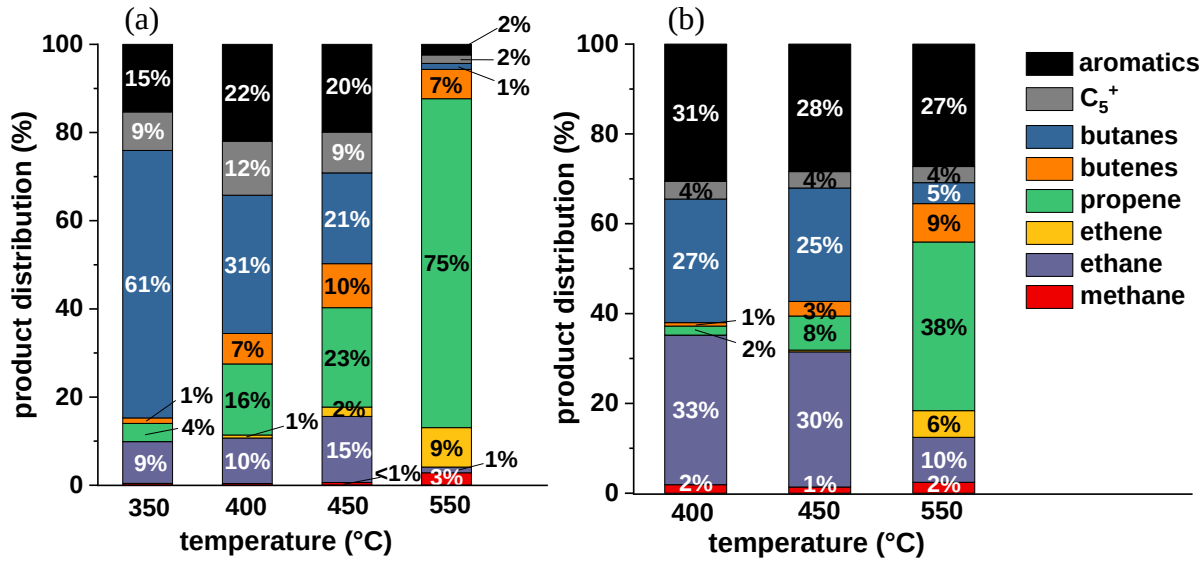


Figure 20. comparison of product selectivity at iso-conversion level of propane on the PtZn/$SiO_2$+ZSM-5 catalysts (Z/PA=1) at $P_{C3H8}$=101 kPa. (a) conversion=16%, (b) conversion=39%

Since the product selectivity changes with propane conversions, the product distributions at different temperatures are compared at two propane conversions (Figure 20). Figure 20a shows the product selectivity at 16% propane conversion from 350℃ to 550℃. At 550℃, the dominant product is propene (75%) with 4% light gas byproducts (3% methane and 1% ethane). The product mixture only consists of 12% of $C_4^+$ hydrocarbons, which mostly consists of 7% butanes. As temperature decreases from 550℃ to 350℃, a few trends can be summarized. Firstly, propene selectivity decreases, while the butanes selectivity increases. In addition, light gas significantly increases but is mainly composed of ethane at lower temperatures. Furthermore, the selectivity to $C_4^+$ hydrocarbons (sum of butenes, $C_5^+$ hydrocarbons and BTX) increases as temperature decreases but mid temperatures (400-450℃) give highest BTX selectivity. Figure 20b shows that at moderate propane conversion (39%), the major products are propene (38%) and BTX (27%) at 550℃, while the product distributions at 400℃ and 450℃ predominantly consist of ethane, butanes and BTX.

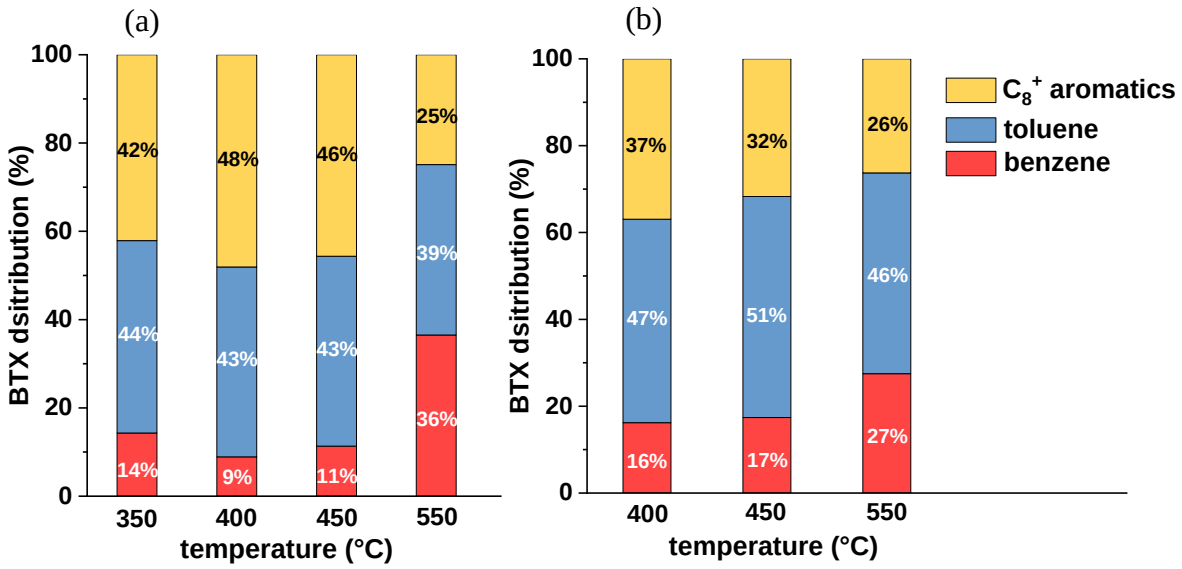


Figure 21. comparison of BTX distribution on the PtZn/SiO2+ZSM-5 (Z/PA=1) catalyst at iso-conversion level of propane at $P_{C3H8}$=101 kPa. (a) conversion=16%, (b) conversion=39%

In addition to BTX selectivity, BTX distribution varies with reaction temperatures. Figure 21a shows the effect of reaction temperature on BTX distribution at 16% propane conversion. At 550℃, the dominant aromatics are benzene and toluene with selectivity of 36% and 39%, respectively. In contrast, the dominant aromatics are toluene and $C_8^+$ aromatics at 350-450℃. At latter three temperatures, the toluene selectivity is similar (~43%), while the lowest benzene selectivity (9%)

and highest $C_8^+$ aromatics selectivity (48%) were observed at 400°C. Higher selectivity to toluene and $C_8^+$ aromatics at lower temperatures (350-450°C) is likely attributed to higher amounts of $C_4^+$ hydrocarbons in the product mixture (Figure 19e and 19f). At moderate propane conversion (39%), the dominant aromatic hydrocarbon at 550°C is toluene (46%), while benzene and $C_8^+$ aromatics are nearly in equal percentage (~26%) (Figure 21b). Compared to the benzene percentage (36%) at 16% propane conversion, lower benzene percentage (27%) at 39% conversion at 550°C is because toluene and $C_8^+$ aromatics formation rates are enhanced as increasing amounts of $C_4^+$ hydrocarbons are formed from propene. At 39% propane conversion, the benzene selectivity is the lowest (16%) and $C_8^+$ aromatics selectivity is the highest (37%) at 400°C. The detailed BTX distributions as a function of propane conversion at various temperatures are shown in Figure. S2.

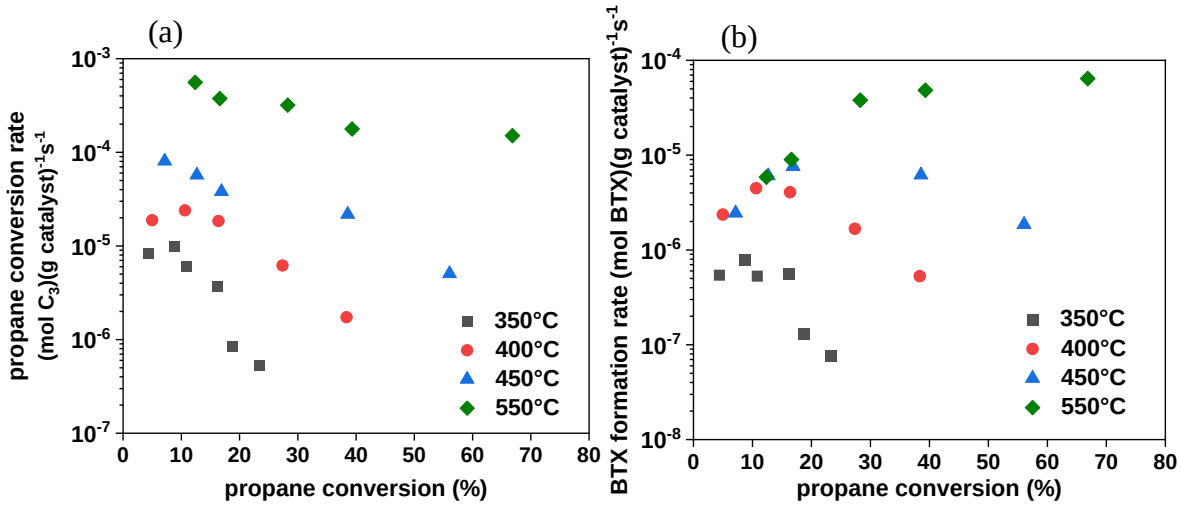


Figure 22. temperature effect on (a) propane conversion rate and (b) BTX formation rate as a function of propane conversion on the $PtZn/SiO_2$+ZSM-5 (Z/PA=1) catalyst
Reaction conditions: cat., 0.01-2.0 g; pressure, 101 kPa; WHSV, 0.36-715 $h^{-1}$

Figure 22a shows the propane conversion rate normalized by the catalyst weight as a function of propane conversion. At 550°C, the propane conversion rate slightly decreases from $6\times10^{-4}$ to $2\times10^{-4}$ (mol $C_3$)(g catalyst)$^{-1}s^{-1}$ as the propane conversion increases from 10% to 70%. The decrease in the propane conversion rates is likely attributed to partial suppression of dehydrogenation rates by hydrogen formed from higher molecular weight hydrocarbons, i.e., aromatics. At 450°C, the propane conversion rate is $8\times10^{-5}$ (mol $C_3$)(g catalyst)$^{-1}s^{-1}$ at 10%

conversion and decreases to $5\times10^{-6}$ (mol $C_3$)(g catalyst)$^{-1}$s$^{-1}$ as propane conversion increases to 56%. The propane conversion rates at 400℃ and 350℃ are similar at ~5% propane conversion, $2\times10^{-5}$ and $9\times10^{-6}$ (mol $C_3$)(g catalyst)$^{-1}$s$^{-1}$, respectively. However, the propane rate at 350℃ decreases much more rapidly to $5\times10^{-7}$ (mol $C_3$)(g catalyst)$^{-1}$s$^{-1}$ compared to higher temperatures likely because increasing amounts of light alkanes (butanes and $C_5^+$ alkanes) formed by hydrogenation hinders propane conversion by competing the PtZn sites (Figure 19).

Although propane conversion rates are lower at 350-450℃, the BTX selectivities are higher than those at 550℃, particularly at low propane conversions, e.g., <10% (Figure 19g). As a result, the BTX formation rates at 400℃, 450℃ and 550℃ at low propane conversions (5-10%) are similar (Figure 22b). However, at 550℃, the BTX formation rate increases by 10 times as propane conversion increases to ~70% due to increasing amounts of high molecular weight olefins formed by propene. On the contrary, the BTX formation rate undergoes a maximum of $8\times10^{-6}$ and $5\times10^{-6}$ (mol BTX)(g catalyst)$^{-1}$s$^{-1}$ at 450℃ and 400℃, respectively. Initial increase in the BTX formation rates at 450℃ and 400℃ is due to higher concentration of higher molecular weight hydrocarbons, e.g., butenes and $C_5^+$ (Figure 19e and 19f), while the decrease in the BTX rates at higher propane conversions are due to saturation of intermediate olefins to less reactive alkanes. With further decrease in temperature to 350℃, the BTX formation rate decreases rapidly by 7 times within 5-20% propane conversion, suggesting propene is primarily oligomerized and hydrogenated to ethane and higher molecular weight alkanes rather than converted to aromatics.

### 4.3.2 Low Temperature Propane Conversion

Since PtZn/$SiO_2$ has high dehydrogenation rates, propane conversion becomes feasible with this bifunctional catalyst at low temperature. Figure 19 shows that pure propane is converted beyond the equilibrium conversion (<5%) at 350℃ and 101 kPa on the Z/PA=1 catalyst and the product selectivity is significantly different from those at higher temperatures [68]. To better understand the individual role of PtZn/$SiO_2$ and ZSM-5 as well as their synergetic effect for low temperature propane conversion, the product distributions for propane conversion on the PtZn/$SiO_2$, ZSM-5 and PtZn/$SiO_2$+ZSM-5 were determined at 350℃ in Table 5. PtZn/$SiO_2$ has ~3% propane conversion with 99.7% propene selectivity at 350℃. ZSM-5 also demonstrates ~3% propane

conversion but with 9 times higher catalyst loading. The results indicate that PtZn/$SiO_2$ has much higher activity than ZSM-5, implying propane is firstly dehydrogenated to propene on the PtZn sites of the bifunctional catalyst at 350℃.

With the same amounts of ZSM-5, propene conversion is high (95.6%), indicating olefins are highly reactive at 350℃ (Table 6). Propene formed on the PtZn sites will rapidly react with ZSM-5. Although both PtZn/$SiO_2$ and ZSM-5 have low propane conversion individually, the bifunctional catalyst can achieve a maximum of ~25% propane conversion at 350℃ (Figure 19), suggesting that propane is converted beyond the equilibrium conversion due to rapid conversion of propene on ZSM-5.

Table 6. product distribution of propane conversion at 350℃

| Catalyst | PtZn/$SiO_2$ | ZSM-5 | | PtZn/$SiO_2$+ZSM-5 |
|---|---|---|---|---|
| Reactant | propane | propane | propene[a] | propane |
| Loading (g) | 0.1 | 0.9 | 0.9 | 1.0[b] |
| Conversion (%) | 3.1 | 2.9 | 95.6 | 9.0 |
| Selectivity (%) | | | | |
| Methane | 0.1 | 12.9 | 0.3 | 0.6 |
| Ethane | 0.2 | 8.7 | 0.3 | 11.5 |
| Ethene | 0 | 10.5 | 2.9 | 0.6 |
| Propane | - | - | 11.5 | - |
| Propene | 99.7 | 12.6 | - | 4.0 |
| Butanes (n-$C_4$, i-$C_4$) | 0 | 44.2 | 35.9 | 62.4 |
| Butenes | 0 | 1.4 | 4.4 | 3.3 |
| Oligomers ($C_5^+$) | 0 | 9.7 | 26.0 | 9.5 |
| BTX Aromatics | 0 | 0 | 18.7 | 8.3 |

[a] 3% propene
[b] catalyst composition: PtZn/$SiO_2$, 0.1g; ZSM-5, 0.9g

The major products for propene on ZSM-5 are composed of propane (11.5%), butanes (35.9%), $C_5^+$ oligomers (26.0%) and BTX (18.7%), which is consistent with propene reactions on ZSM-5 in prior studies [13,14,17,69]. However, on the PtZn/$SiO_2$+ZSM-5, the selectivities to ethane (11.5%) and butanes (62.4%) are high, while $C_5^+$ hydrocarbons (9.5%) and BTX (8.3%) are low. The selectivity differences between propene on ZSM-5 and propane on PtZn/$SiO_2$+ZSM-5 likely results from PtZn hydrogenation of intermediate olefins, i.e., ethene and butenes. Since ethane

remains unreactive at 350℃, ethane formation at higher propane conversions becomes the major yield loss reaction at low temperature. In addition, extremely low space velocity is required to obtain >40% propane conversion at 350℃, and therefore slightly higher temperature, e.g., 400℃, is seemly more practical.

Since propene is very reactive on ZSM-5 at lower temperature, much less ZSM-5 in the bifunctional catalyst is likely sufficient to give higher propane conversion by converting intermediate propene to higher molecular weight olefins without further leading to high amounts of aromatics and hydrogen, which subsequently saturates ethene. The selectivity to ethane, butanes, and aromatics as well as propane conversion rates are investigated on the bifunctional catalysts with Z/PA ratios from 9 to 0.05 at 400℃ (Figure 23).

Figure 23a shows that propane conversion rate is around $8\times10^{-7}$ (mol $C_3$)(g catalyst)$^{-1}s^{-1}$ with Z/PA=0.1 at ~30% propane conversion. At the constant conversion, the conversion rates are $7\times10^{-6}$ and $4\times10^{-5}$ (mol $C_3$)(g catalyst)$^{-1}s^{-1}$ with Z/PA=1 and 9, respectively, indicating higher loadings of ZSM-5 are required to enhance the secondary conversion of intermediate propene in order to obtain higher propane conversions. The butanes selectivity is ~60% with Z/PA= 0.1 and 0.05 at ~17% propane conversion and is ~30% with Z/PA=1, suggesting butenes are hydrogenated more rapidly due to higher loadings of PtZn sites (Figure 23b).

The BTX selectivity is slightly higher on the bifunctional catalyst with Z/PA=1 and both increase and decrease in Z/PA ratio leads to lower BTX selectivity (Figure 23c), which likely results from the imbalance of PtZn dehydrogenation and ZSM-5 oligomerization rates. Higher Z/PA ratio has lower dehydrogenation rates to convert cyclic hydrocarbons to aromatics, while lower Z/PA ratio limits oligomerization rates of light olefins. However, ethane selectivity increases significantly as propane conversion increases and is independent of Z/PA ratio (Figure 23d). The selectivities of BTX and ethane as a function of propane conversion and Z/PA ratio are consistent with the results in our prior study of propane conversion on PtZn/$SiO_2$+ZSM-5 bifunctional catalyst at 550℃,[67] implying the ethane selectivity is dependent on reaction temperature and determined by thermodynamics equilibrium of ethane/ethene, while the relative rates on the individual catalyst

function have a minor effect on controlling ethane selectivity once ethene and hydrogen are present in the product mixture.

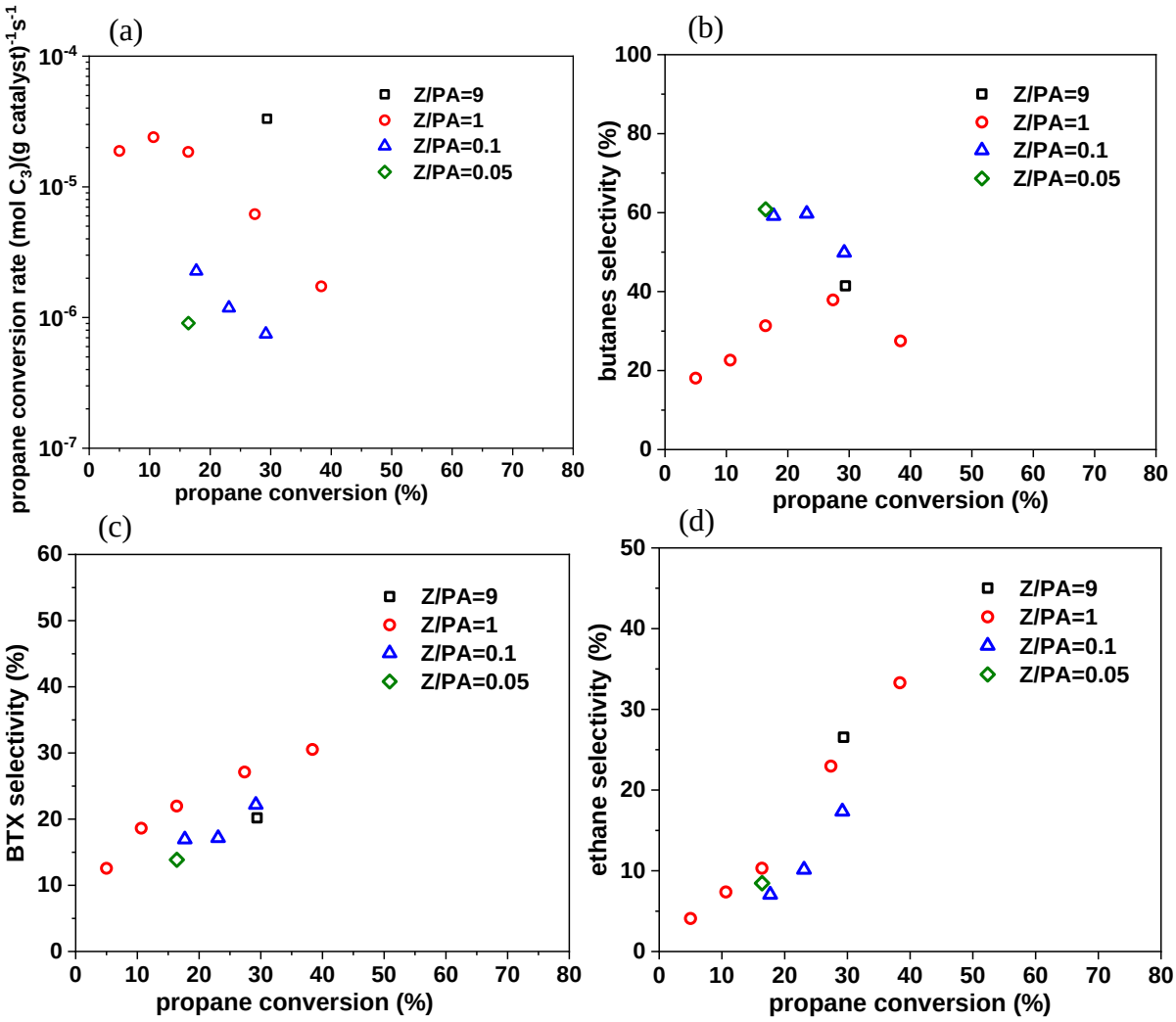


Figure 23. The effect of Z/PA ratio on the (a) propane conversion rate, (b) ethane selectivity, (c) butanes selectivity and (d) BTX selectivity on PtZn/$SiO_2$+ZSM-5 catalyst
Reaction conditions: temperature, 400°C; pressure, 101 kPa; HWSV, 0.72-60 $h^{-1}$

## 4.4 Discussions

### 4.4.1 Temperature Dependence of the Propane Dehydroaromatization Pathway

Based on the product selectivity investigated at different temperatures, the dominant propane conversion pathways at high (550℃), mid (400-450℃) and low (350℃) temperatures on the PtZn/$SiO_2$+ZSM-5 (Z/PA=1) bifunctional catalysts have been proposed in Figure 24. At all temperatures, the methane selectivity is low (<5%), suggesting that propane is primarily dehydrogenated to propene by the PtZn alloy on the bifunctional catalyst (Figure 19a). At 550℃, generated propene oligomerize and cyclize over ZSM-5 to make higher molecular weight olefins/cyclo-olefins, which are dehydrogenated to BTX on the PtZn sites (Figure 24a), as previously proposed.[67]

At mid temperatures (400-450℃), propene selectivity is lower and the selectivities to ethane, butanes, $C_5^+$ hydrocarbons and BTX are higher than those at 550℃ (Figure 19), suggesting that secondary conversion of propene is fast at low propane conversions. Rapid increase in butanes selectivity indicate that propane is firstly dehydrogenated to propene, which rapidly oligomerizes to $C_6^+$ hydrocarbons on ZSM-5. $C_6^+$ hydrocarbons partially crack to butenes, which are subsequently saturated to butanes likely by PtZn alloy hydrogenation, while some $C_6^+$ hydrocarbons are converted into primarily toluene and $C_8^+$ aromatics. The results suggest that $C_2$-$C_5$ olefins are hydrogenated to alkanes, while $C_6^+$ olefins are dehydrogenated to aromatics (Figure 24b). At mid temperatures, the pathways of intermediate olefins on the dehydrogenation/hydrogenation catalyst are different because the thermodynamic equilibrium favors alkanes compared to higher temperatures. For example, cyclohexene dehydrogenation has near 100% conversion at 340 ℃ while butanes has less than 5% conversion at the same temperature.[70,71] At mid temperatures, higher molecular weight olefins and cyclic hydrocarbons have high equilibrium to dehydrogenated products, e.g., aromatics, while lower molecular weight alkanes are more stable than olefins. As a result, the ethane selectivity significantly increases at high propane conversions. Due to low equilibrium of ethane to ethene at 400-450℃, ethane results from immediate saturation of ethene, which is formed by cracking of higher molecular weight hydrocarbons on the ZSM-5 catalyst. Ethane dehydrogenation rate and equilibrium is low and, thus, will not be further converted to BTX. Consequently, the ethane formation at higher propane

conversion limits the aromatic selectivity and becomes the major yield loss reaction on the PtZn/$SiO_2$+ZSM-5 at 400-450℃. In addition, the propane conversion rate decreases at higher propane conversions likely because butanes compete for dehydrogenation sites with propane due to their higher reactivity (Figure 19d and 22a).

At 350℃, the propane conversion is driven by significantly higher secondary propene conversion rates on ZSM-5. For example, the propane/propene equilibrium at 350℃ is low and, thus, the propane conversion is <5% in the absence of secondary reaction of propene conversion to other products. This result is consistent with the lowest propene selectivity among all temperatures at low propane conversions (Figure 19c). However, the BTX selectivity is also lower due to cracking and hydrogenation of intermediate olefins to ethane and butanes (Figure 19d and 19g). Consequently, the dominant pathway at low temperature is propane dehydrogenation, propene oligomerization-cracking and olefins hydrogenation to produce ethane and butane. Butane does react on the bifunctional catalysts at higher propane conversions.

The BTX selectivity is highest at low propane conversions (5-10%) at mid temperatures (400-450℃) because of relatively higher oligomerization rates than cracking rates on ZSM-5 and moderately high dehydrogenation rates on PtZn sites (Figure 24b). In addition, low benzene percentage is also associated with higher amounts of $C_4^+$ hydrocarbons in the mixture due to the balance of oligomerization and dehydrogenation rates. At high temperature, i.e., 550℃, the Z/PA=1 bifunctional catalyst has high dehydrogenation rates and relatively low monomolecular cracking rates, leading to low methane selectivity. However, olefin cracking rates are also high, leading to lower concentration of higher molecular weight olefins for aromatics formation (Figure 24a). At low temperature, i.e., 350℃, PtZn hydrogenation competes with ZSM-5 oligomerization by saturating intermediate $C_2$-$C_5$ olefins. Rapid increase in the selectivity to ethane and butanes and low increase in the BTX selectivity indicate that olefin hydrogenation is more favored than BTX formation (Figure 19b, 19d and 19g). While butanes can be eventaully converted to higher molecular weight hydrocarbons, ethane formation becomes the yield loss reaction on the Z/PA=1 catalyst particular at low and mid temperatures (Figure 24c). The results indicate that the liquid yield is mostly limited by methane formation at high temperature due to monomolecular cracking

but ethane formation at lower temperature due to olefin cracking and ethene hydrogenation on the PtZn/$SiO_2$+ZSM-5 bifunctional catalysts.

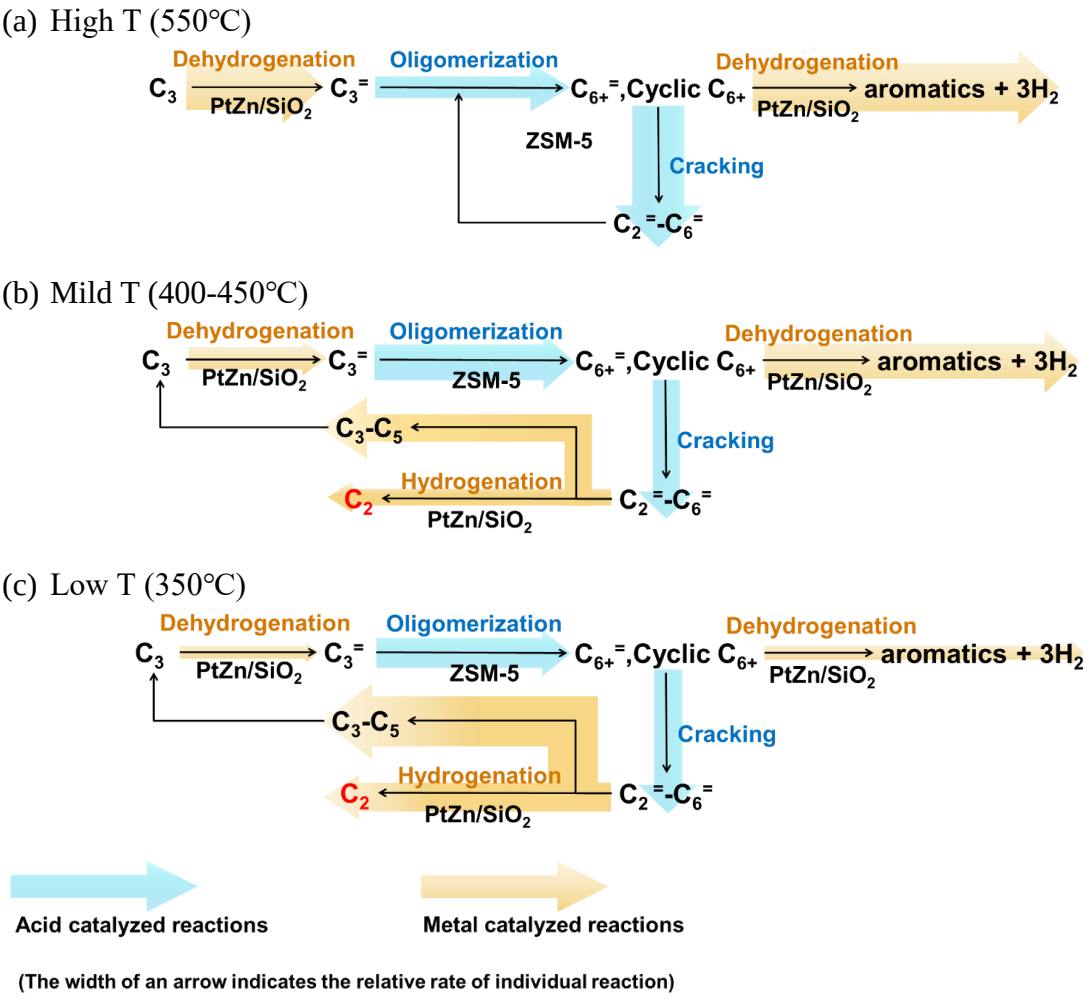


Figure 24. proposed reaction pathways of propane conversion over PtZn/$SiO_2$+ZSM-5 (Z/PA=1) catalyst at (a) T=550℃, (b) T=400-450℃, (c) T=350℃

### 4.4.2 Strategies for Propane to Liquid Hydrocarbons Based on Reaction Temperature

The effects of catalytic function and reaction temperature have been investigated to identify optimal strategies for propane conversion to valuable liquid products, i.e., aromatics and gasoline-blending hydrocarbons. At high temperature (550℃), methane formation by ZSM-5 monomolecular cracking is the major contributor to low BTX yield on Ga/ZSM-5 catalysts.[46] As a result, a selective dehydrogenation catalyst with much higher propane conversion rates than ZSM-5, i.e., PtZn alloy, and low loadings of ZSM-5 are both critical to minimize monomolecular

cracking. Excessively high ratio, i.e., Z/PA= 50, leads to increasing methane selectivity, while lower ratio, i.e., Z/PA=1, limits the conversion rates of higher molecular weight intermediates to BTX.

At low temperature (350℃), propane dehydroaromatization on the Ga/ZSM-5 has not been possible due to low rates on both Ga and ZSM-5. However, ~25% propane conversion at 350℃ is achieved with the combination of highly active PtZn alloy and ZSM-5. There are multiple advantages of converting propane at low temperature. Firstly, monomolecular cracking is insignificant, indicating high loadings of PtZn alloy are unnecessary. Secondly, the single-pass product mixture is abundant in gasoline-range molecules because olefin oligomerization is favored over cracking. Furthermore, benzene percentage is much lower in the BTX distribution, which makes the product mixture more favorable for gasoline blending. However, considering low rates and conversions at 350℃, mid temperature (400-450℃) is more practical for production of gasoline-blending components.

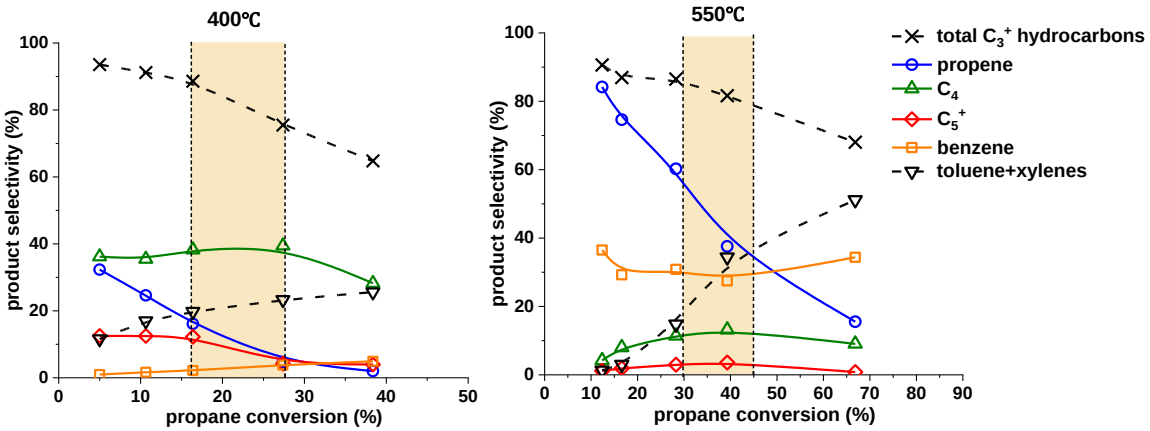


Figure 25. product distribution of propane conversion on the PtZn/$SiO_2$+ZSM-5 (Z/PA=1) bifunctional catalyst at 400℃ and 550℃

Optimal strategies to develop catalytic processes for propane to valuable liquid hydrocarbons can vary based on reaction temperatures. Since the Z/PA=1 bifunctional catalyst has <5% methane selectivity at all temperatures, the distributions of $C_3^+$ hydrocarbons as a function of propane conversion on this catalyst are determined at 400℃ and 550℃ in Figure 25. The $C_3^+$ hydrocarbons

selectivity is the sum of propene, butanes, butenes, $C_5^+$ and BTX. At 400℃, it is possible to make gasoline-blending hydrocarbons due to high selectivity to $C_4^+$ hydrocarbon mixture. The optimal operation range is 15-25% propane conversion, where the $C_3^+$ selectivity is 80-90%, consisting of $C_4$ (~40%), toluene and xylenes (~20%) and $C_5^+$ (~10%). With higher propane conversion (25-35%), the increase in BTX selectivity is low and the total $C_3^+$ selectivity decreases to 65-75%, which is less favored due to unreactive ethane formation. At 550℃, it is practical to convert propane to aromatic chemicals. The $C_3^+$ selectivity is 80-85% in the propane conversion range of 30-45% and consists of propene (35-60%), benzenes (~30%), toluene and xylenes (15-35%), which is the optimal conversion range for the BTX production. By recycling propene from the product mixture back to the reactor or reacting propene with ZSM-5 in a second reactor, >80% BTX yields are possible at 550℃. Higher propane conversion (>45%), however, gives significant amounts of ethane formation, which will limit the overall BTX yield. At all temperatures, while methane formation is minimized on the PtZn/$SiO_2$+ZSM-5 catalyst, ethane formation becomes the major yield-loss reaction especially at lower temperatures.

### 4.5 Conclusion

The temperature dependence of propane dehydroaromatization pathways on the PtZn/$SiO_2$+ZSM-5 (Z/PA=1) catalyst is determined from 350-550℃, and optimal strategies for catalysts and processes development based on reaction temperatures are discussed. At high temperature (550℃), low Z/PA ratio is necessary to give low methane selectivity (<5%) and leads to propene and BTX. As the temperature decreases to 400-450℃, a high selectivity to $C_4^+$ hydrocarbons is attributed to relatively higher oligomerization rates with lower cracking rates as well as moderately high PtZn dehydrogenation rates. However, due to low equilibrium concentration of low molecular weight olefins, ethane is formed by hydrogenation of ethene produced by cracking of higher olefins. As a result, ethene formation limits the aromatics yield at high propane conversions. At 350℃ propane can be converted up to 25% by dehydrogenation on PtZn/SiO2 and the synergetic effect between PtZn/$SiO_2$ and ZSM-5. However, the conversion rates are likely too low for a practical process. In addition, propane is primarily converted to butanes and ethane by the tandem reactions of propane dehydrogenation, propene oligomerization-cracking and olefin hydrogenation. Thus, the products are less desirable for gasoline blending.

The practical implication of this work is to offer insights on catalyst composition formulation and processes development for propane to valuable liquid hydrocarbons by developing molecular-level understandings of reaction pathways at different temperatures. For example, at 550℃, higher than 80% BTX yield is achievable by recycling propene and other reactive intermediates in the range of 30-45% propane conversion per pass with Z/PA=1. At 400℃, there is potential to produce gasoline-blending hydrocarbons at 15-25% propane conversion per pass with Z/PA=0.1-1.

# 5. FUTURE WORK: ETHANE CONVERSION ON PTZN/$SIO_2$+ZSM-5 CATALYSTS IN A SINGLE STEP

## 5.1 Introduction

Zeolite catalysts with different metal promoters, e.g., Zn, Ga and Pt, have been reported for ethane conversion at high temperatures (>600℃). However, the BTX yields are low due to the methane formation. It remains unclear how methane is formed for ethane conversion since the proposed ethane dehydroaromatization pathways are mostly identical regardless of the type of metal promoters. In addition, the proposed dehydroaromatization pathways of ethane and propane are similar in the prior work despite of the differences between ethane and propane. The differences of the yield-loss reaction and the dehydroaromatization pathways between ethane and propane has never been systematically investigated and discussed in the literature. Based on these understandings, the strategies for converting ethane and propane to valuable liquid hydrocarbons are likely different.

## 5.2 Objective

The objective of chapter five is to convert ethane to high yields of higher molecular weight hydrocarbons utilizing the PtZn/$SiO_2$+ZSM-5 bifunctional catalysts. In chapter three and four, the PtZn/$SiO_2$+ZSM-5 bifunctional catalysts have shown high propane rates, low methane selectivity and high BTX selectivity. Due to high dehydrogenation rates, ethane can also be dehydrogenated on PtZn/$SiO_2$, while ethene can be further converted to higher molecular weight hydrocarbons on ZSM-5. The effect of ZSM-5 to PtZn/$SiO_2$ ratio (Z/PA) and temperature will be studied on the bifunctional catalysts for ethane conversion and further compared to those of propane to offer insights on their differences in the light gas formation and dehydroaromatization pathway and the catalytic process development strategy for converting ethane and propane.

## 5.3 Preliminary Results and Discussions

### 5.3.1 The Effect of Z/PA Ratio on Product Selectivity

Ethane dehydrogenation is firstly evaluated on $PtZn/SiO_2$ catalyst at 600°C and >99% ethene selectivity indicates that ethane dehydrogenation is highly selective even in presence of hydrogen (Figure 26).

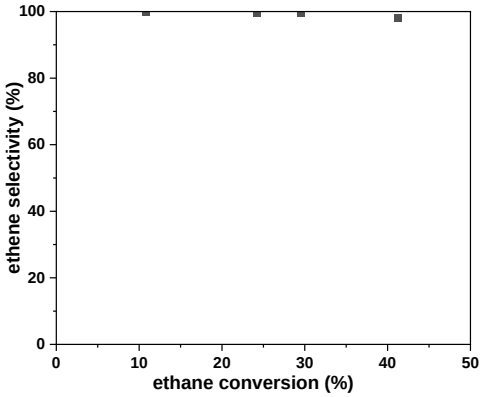


Figure 26. ethene selectivity as a function of ethane conversion on $PtZn/SiO_2$
Reaction conditions: temperature, 600°C; pressure, 101kPa; concentration, 5% $C_2H_6$

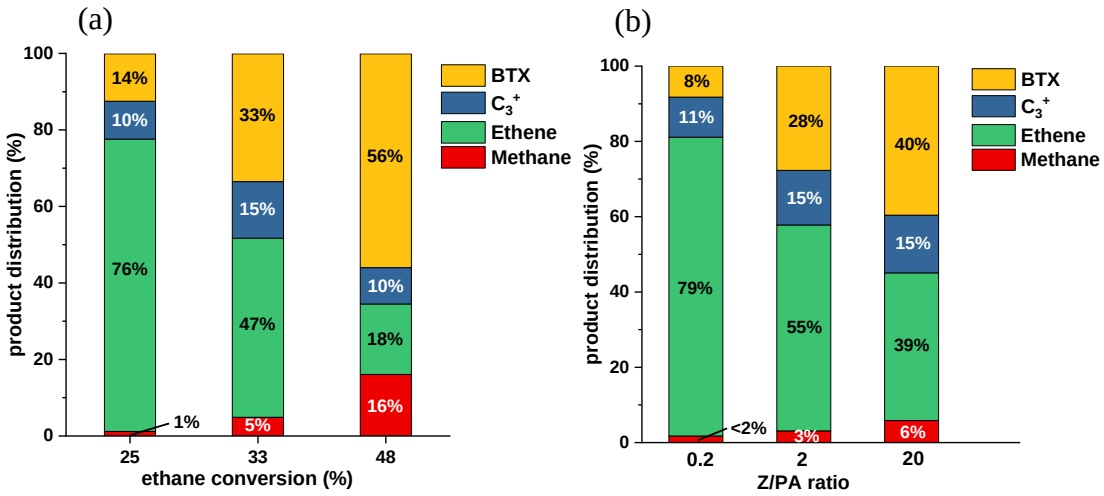


Figure 27. (a) product selectivity and (b) BTX distribution as a function of ethane conversion on $PtZn/SiO_2$+ZSM-5 (Z/PA=2) catalyst (c) product selectivity and (d) BTX distribution as a function of Z/PA ratio at 28% ethane conversion on $PtZn/SiO_2$+ZSM-5 catalysts
Reaction conditions: temperature, 600°C; pressure, 101kPa; concentration, 100% $C_2H_6$

With a highly active and selective $PtZn/SiO_2$ catalyst, $PtZn/SiO_2$+ZSM-5 catalyst was prepared by physical mixing of ZSM-5 and $PtZn/SiO_2$ with different weight ratio (Z/PA). The product selectivity on $PtZn/SiO_2$+ZSM-5 catalyst with Z/PA=2 using pure ethane at 600°C is investigated to further understand the ethane dehydroaromatization pathways (Figure 27a). The methane selectivity is 1% at 25% ethane conversion, suggesting that ethane monomolecular cracking is not occurring and therefore ethane is dominantly dehydrogenated to ethene on $PtZn/SiO_2$. As ethane increases to 48%, the methane selectivity is 16%. These results imply that methane is a secondary product for ethane conversion, in contrast to a primary product for propane conversion (Figure 12a). As ethane conversion increases from 25% to 48%, the ethene selectivity decreases from 76% to 18%, indicating ethene undergoes secondary reactions to produce higher molecular weight hydrocarbons, i.e., $C_3^+$ and BTX, on ZSM-5. This is consistent with that the $C_3^+$ selectivity goes through a maximum of 15% at 33% ethane conversion and the BTX selectivity is high (56%) at 48% ethane conversion, suggesting $C_3^+$ hydrocarbons are intermediates from ethene and eventually converted to BTX at higher ethane conversions.

To understand the individual contribution of two catalytic components to ethane dehydroaromatization, the effect of Z/PA ratio is also investigated at the same ethane conversion (28%). Figure 27b shows that the methane selectivity slightly increases from <2% to 6% as the Z/PA ratio increases from 0.2 to 20, indicating that Z/PA ratio has a minor impact on the methane selectivity for ethane conversion. The ethene selectivity decreases from 79% to 39%, while the BTX selectivity increases from 8% to 40% as the Z/PA ratio increases by 100 times, implying that ethene is converted to BTX more rapidly due to higher ZSM-5 loadings.

### 5.3.2 The Temperature Effect on Product Selectivity

Since $PtZn/SiO_2$+ZSM-5 (Z/PA=2) bifunctional catalyst has low methane selectivity (<5%) while moderately high BTX selectivity (28%), the temperature effect on the product distribution for ethane conversion is further studied on this catalyst at 500-600°C (Figure 28).

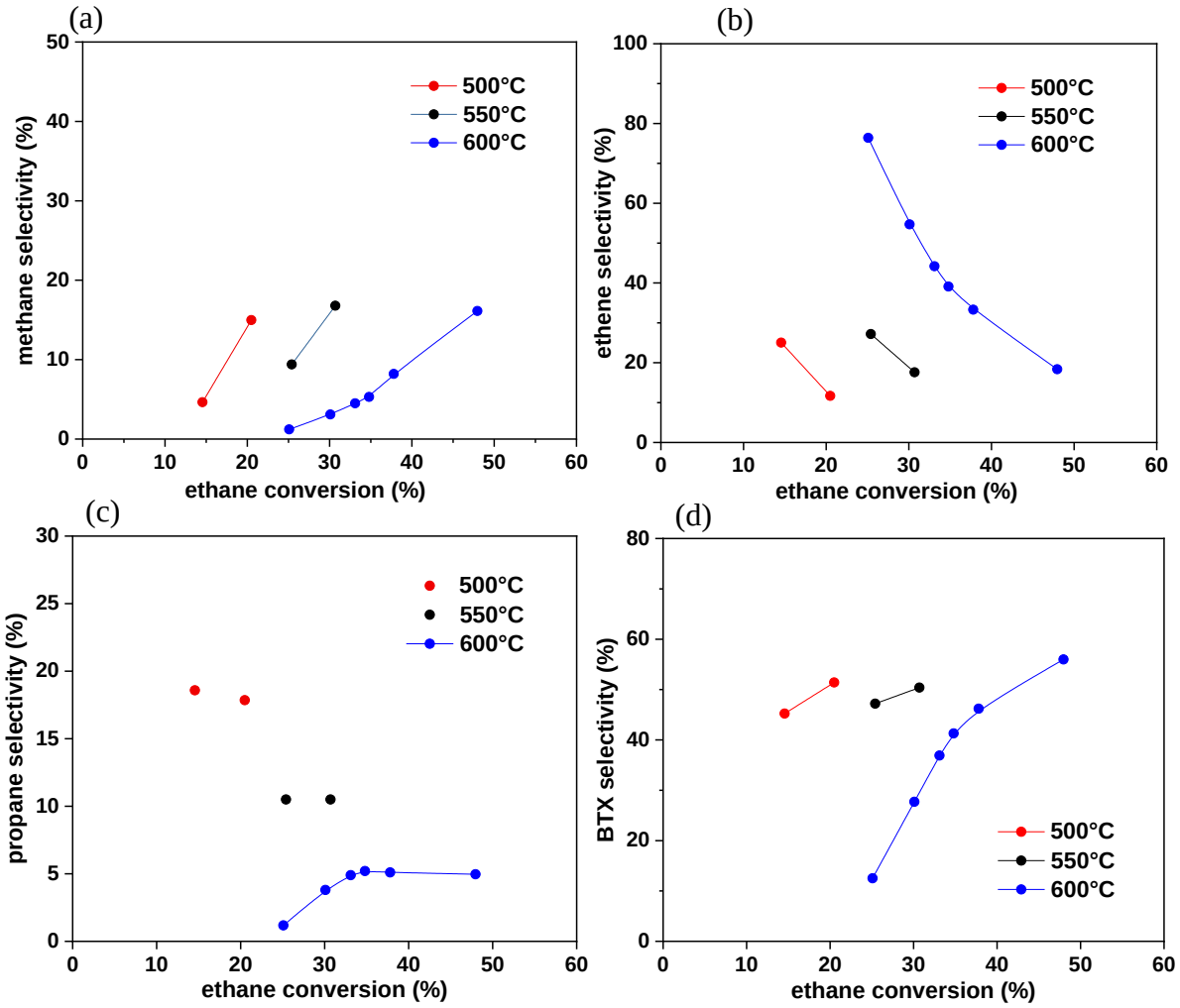


Figure 28. selectivities of (a) methane, (b) ethene, (c) propane, (d) BTX as a function of ethane conversion on PtZn/$SiO_2$+ZSM-5 (Z/PA=2) bifunctional catalyst
Reaction conditions: $P_{C2H6}$=1.01bar, WHSV=3-110 $h^{-1}$

At 600°C and 550°C, the methane selectivity is <5% and 17%, respectively, at 30% ethane conversion (Figure 28a). With further decrease in temperature to 500°C, the methane selectivity is high (16%) at lower ethane conversion (20%), suggesting that the methane selectivity increases more rapidly as temperature decreases. The ethene selectivity decreases more rapidly as temperature decreases, implying the secondary reactions of ethene to higher molecular weight hydrocarbons is faster at lower temperatures (Figure 28b). This result is consistent with increasing propane selectivity as temperature decreases (Figure 28c), indicative of fast tandem reaction of ethane dehydrogenation, ethene oligomerization-cracking and propene hydrogenation at 500°C.

Figure 28d also shows that BTX selectivity is 50% at 550°C, while it is 28% at 600°C at the same ethane conversion (30%). This result indicates that lower temperature is conductive to BTX formation because olefin oligomerization is more favored and dehydrogenation rate is moderately high.

### 5.3.3 Hypotheses for Methane Formation Pathways for Ethane

Although both ethane and propane undergo similar reaction pathways, i.e., dehydrogenation, oligomerization-cracking, isomerization, cyclization, and aromatization to produce higher molecular weight olefins and BTX on bifunctional catalysts, there are two major differences concerning the catalytic behavior between two alkanes. Firstly, ethane monomolecular cracking is not possible since there are no stable $C_1$ monomolecular cracking products. Secondly, ethane has much lower rate and equilibrium compared to propane. As a result, the reaction pathways of ethane and propane are slightly different.

It was shown that methane formation from propane monomolecular cracking can be significantly minimized to <5% by increasing dehydrogenation rates with PtZn alloy and lowering the rates on ZSM-5 (Figure 12a). However, the Z/PA ratio has no apparently positive effect on minimizing methane for ethane at 600℃ (Figure 27b). At 500℃, methane selectivity is still high even with low Z/PA ratio. In addition, the methane selectivity as a function of the conversion is different for ethane and propane. The methane selectivity is low at all propane conversions and all temperatures (350-550°C) on the Z/PA=1 catalyst. In contrast with propane, the methane selectivity increases more rapidly with the ethane conversion as temperature decreases. Lower temperature results to higher methane selectivity at the same ethane conversion. These results imply that methane formation pathways for ethane and propane are different, and methane is not primarily formed by monomolecular cracking of either ethane or propane for ethane conversion.

Nevertheless, there exists a similar trend regarding the dehydroaromatization pathways of ethane and propane with reaction temperature. As reaction temperature decreases, the BTX selectivity both increases for ethane and propane likely because oligomerization is more favored and dehydrogenation rate is moderately high (Figure 12e and 28d). For the conversion of propane, the ethane selectivity increases significantly with BTX at the same conversion, suggesting ethene

formed from higher molecular weight olefins consumes hydrogen by hydrogenation, which enables propane dehydrogenation to proceed without being limited by the thermodynamic equilibrium of propane, propene, and hydrogen. For the conversion of ethane, the methane selectivity increases as the BTX selectivity increases at all temperatures (500-600°C) in the similar way of ethane formation for propane (Figure 28a and 28d). This implies that methane formation from ethane is related to hydrogen formed along with BTX. Hydrogen co-produced at high ethane conversions saturates $C_3^+$ olefins to make $C_3^+$ paraffins (Figure 28c). However, $C_3^+$ hydrocarbons have higher rates and higher equilibrium than $C_2$ hydrocarbons. At high ethane conversion, the equilibriums of $C_2^+$ paraffin/olefin are established, and eventually excessive hydrogen can't be consumed by hydrogenation of $C_2^+$ olefins. As a result, it is postulated that hydrogen likely undergoes irreversible reactions, i.e., alkane hydrogenolysis, to make methane at ethane conversions beyond the equilibrium.

## 5.4 Conclusions and Future Work

Since ethane monomolecular cracking is not possible and ethane has low rates and equilibrium, the dehydroaromatization pathways of ethane and propane are slightly different. The effect of space velocity, Z/PA ratio and temperature on product selectivity of ethane and propane were compared and discussed on the PtZn/$SiO_2$+ZSM-5 bifunctional catalysts to understand the differences in the light gas formation pathways. For propane, methane formed by propane monolecular cracking is the dominant yield-loss reaction at high temperature, while ethane formed by olefin cracking and ethene hydrogenation limits the liquid yields at lower temperatures. For ethane, methane is likely not formed by ZSM-5 monomolecular cracking but is related to hydrogen formed with BTX. One of the future works will focus on understanding the methane formation pathway for ethane conversion. It is postulated that methane formation is likely correlated to the hydrogen in the reaction mixture. Consequently, the effect of hydrogen concentration on methane formation will be investigating by cofeeding hydrogen with varied ethane to hydrogen ratio. In addition, the change of product distribution with the conversion of ethane and propane is also different. As a result, the revolution of product distribution will be also investigated by varying ethane to propane ratio in the feed ($C_2/C_3$).

Regarding catalytic process development, it was shown in chapter four that propane can be converted to high yields of either gasoline-blending hydrocarbons or BTX aromatics based on reaction temperature. However, lower temperature leads to more methane for ethane conversion in a single step, implying the strategy for ethane is different from propane. The future work will also focus on identifying the optimal catalysts, reactor configurations and process conditions. Figure 29 shows that two potential ways to configurate catalyst in the reactors. A dual layer bed contains the ZSM-5 downstream to the $PtZn/SiO_2$+ZSM-5 bifunctional catalyst is shown in Figure 29a. By adjusting the space velocity in each layer, an improved liquid yield for ethane is achievable. For example, ethane is firstly converted to ethene, $C_3^+$ and BTX with <5% methane at 25-33% conversion on the $PtZn/SiO_2$+ZSM-5 bifunctional catalyst in the first layer, while the remaining ethene and $C_3^+$ are further aromatized to BTX on ZSM-5 in the second layer. A two-bed configuration is also shown in Figure 29b, where ethane is firstly dehydrogenated to ethene, which is subsequently converted into BTX at lower temperature (200-400°C). Compared to the dual layer configuration in Figure 29a, the two-bed configuration requires higher temperature (650-700°C) to obtain high ethane conversion in the first bed due to the lack of synergetic effect of the bifunctional catalyst system. However, there is higher flexibility for controlling the product distribution to make higher molecular olefins or BTX and higher tolerance to hydrogen concentration in the reaction mixture. Although $PtZn/SiO_2$ is one of the most selective catalysts for alkane dehydrogenation, its deactivation is significant at higher than 600°C. As a result, $Pt-Mn/SiO_2$ is a better option for the dehydrogenation catalyst in the two-bed system due to higher thermal stability and high ethene selectivity (>95%) at 650°C and 700°C.

The chapter five shows that the methane selectivity is lower at 600°C than 500°C at the constant ethane conversion, implying that higher temperature than 600°C is preferred for ethane conversion to higher yields of liquid hydrocarbons. Since $PtZn/SiO_2$ deactivates rapidly at higher than 600°C, an alternative dehydrogenation catalyst with high ethene selectivity and high stability at higher temperatures is preferred. For example, the $PtMn/SiO_2$ alloy catalyst has been reported to show high ethane selectivity (>98%) and high stability even at 700°C for ethane dehydrogenation in prior work. Nevertheless, high temperature, e.g., 700°C, is not favored for olefin oligomerization. Unlike propane, ethane dehydroaromatization is likely more practical in a two-step process, where ethane is dehydrogenated to ethene at higher than 600°C to obtain high ethene yields in one reactor

(a)

and then reacts ethene with ZSM-5 in a second reactor at lower temperatures, i.e., 200-400°C, to produce higher molecular weight hydrocarbons (Figure 29b).

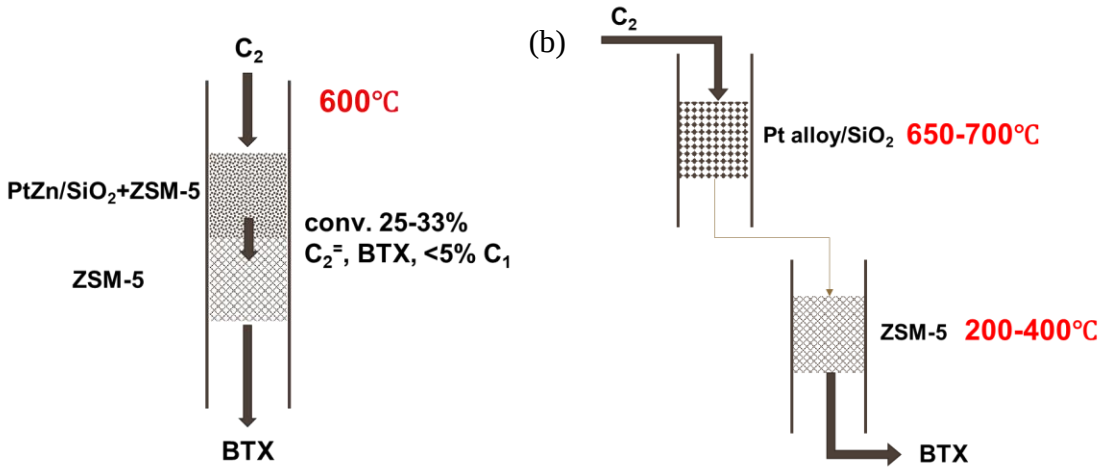


Figure 29 catalyst configuration in the reactors (a) single step, two-bed, (b) two-step

# 6. SUMMARY

The yield loss reaction on Ga/MFI catalysts has been identified due to the imbalance of the propane dehydrogenation and olefins rates between two catalytic functions. Accordingly, an improved bifunctional catalyst composition has been proposed. By utilizing the PtZn alloy and lowering the ZSM-5 loadings to increase dehydrogenation rates and decrease propane monomolecular cracking rates while maintain moderate olefin conversion rates, two distinct differences in the product distribution are observed for propane conversion: (1) less than 5% selectivity to methane (2) higher rate and selectivity to aromatics. These results suggest that methane formation was minimized because the monomolecular cracking pathway is suppressed and aromatics are formed at a higher rate through the metal pathway over the PtZn alloy instead of acid pathway over ZSM-5.

The temperature dependence of propane conversion shows that low temperature (350℃) propane conversion is feasible over PtZn/$SiO_2$+ZSM-5 catalysts because secondary olefins are converted. In addition, higher selectivity to $C_4^+$ hydrocarbons is reported at mid temperature (400-450℃), which makes perfect gasoline-blending products. It is unprecedented that propane can be converted lower temperature and makes paraffin and aromatics as major products with little light gases formation. Light olefins hydrogenation on PtZn alloy is particularly influential in the product distribution at lower temperature.

Eventually, although ethane appears as the dominant byproduct for propane particularly at lower temperature, PtZn/$SiO_2$+ZSM-5 catalysts can convert ethane into approximate 60% BTX selectivity at 50% ethane conversion. The differences in the methane formation pathway between ethane and propane has been proposed, which implies different catalytic processes development strategies for ethane and propane conversion. In summary, PtZn/$SiO_2$+ZSM-5 catalysts successfully overcame two major limitations in the Cyclar process, improving the product yield and reaction of ethane, and can even convert propane at low temperature.

# APPENDIX A. SUPPORTING INFORMATION

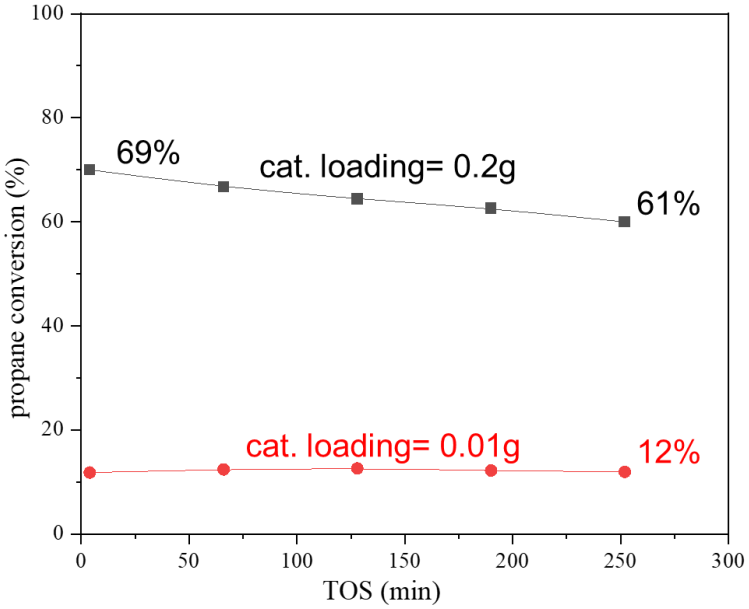


Figure S1. Propane conversion as a function of time on steam (TOS) on $PtZn/SiO_2$+ZSM-5 catalyst
*Reaction conditions: temperature, 550℃, pressure, 101 kPa, propane concentration, 99.9%, flow rate, 67ccm

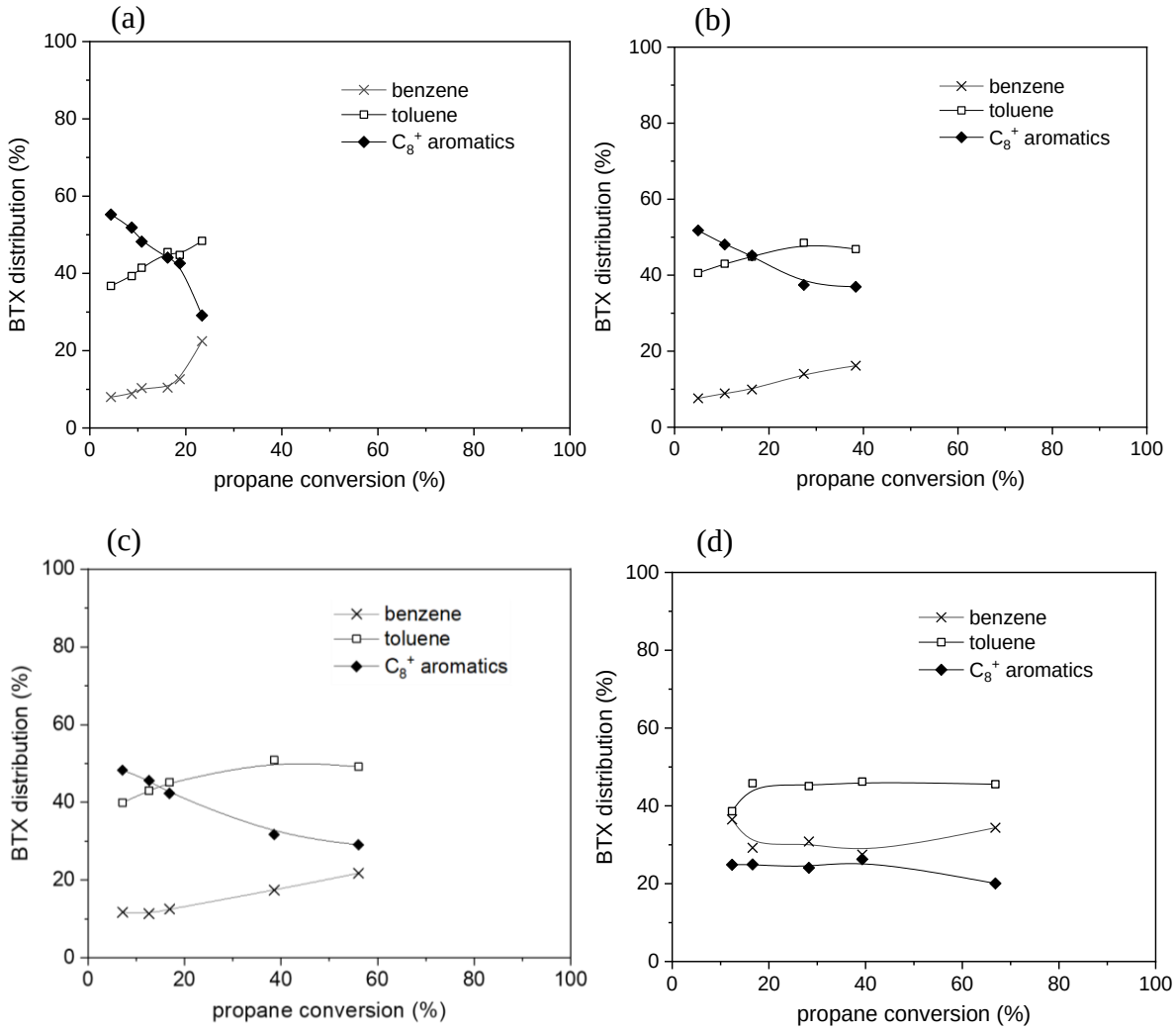


Figure S2. BTX distribution as a function of propane conversion at (a) 350℃, (b) 400℃, (c) 450℃ and (d) 500℃ at $P_{C3H8}$=101 kPa on the PtZn/$SiO_2$+ZSM-5 (Z/PA=1) catalyst

Table S1. Product selectivity of propene conversion on ZSM-5

| Catalyst | ZSM-5 | | |
|---|---|---|---|
| Conversion (%) | 19.4 | 32.0 | 73.6 |
| Selectivity (%) | | | |
| Methane | 0.4 | 0.5 | 3.1 |
| Ethane | 0.2 | 0.4 | 1.0 |
| Ethene | 37.7 | 44.7 | 43.0 |
| Propene | 5.1 | 5.3 | 7.2 |
| Butanes | 0.9 | 1.3 | 2.4 |
| Butenes | 40.8 | 32.7 | 8.8 |
| $C_5^+$ paraffins and olefins | 8.9 | 6.9 | 1.5 |
| Benzene | 1.3 | 1.9 | 12.1 |
| Toluene | 3.1 | 4.2 | 15.3 |
| $C_8^+$ aromatics | 1.7 | 2.2 | 5.7 |

Table S2. Product selectivity of cyclohexene conversion on ZSM-5, $PtZn/SiO_2$ and $Ga/Al_2O_3$

| | ZSM-5 | | $PtZn/SiO_2$ | | $Ga/Al_2O_3$ | |
|---|---|---|---|---|---|---|
| Conversion (%) | 40.3 | 86.8 | 37.1 | 62.1 | 37.8 | 64.4 |
| Selectivity (%) | | | | | | |
| Methane | 0.1 | 0.3 | trace | trace | 0.2 | 0.4 |
| Ethane | trace | trace | trace | trace | trace | trace |
| Ethene | 1.7 | 3.5 | 1.8 | 1.0 | 2.0 | 0.8 |
| Propane | trace | trace | trace | trace | trace | trace |
| Propene | 0.4 | 4.3 | 0.2 | trace | 0.3 | 0.2 |
| Butanes | trace | trace | trace | trace | trace | trace |
| Butenes | 3.2 | 4.6 | 3.3 | 1.8 | 3.8 | 1.4 |
| $C_5^+$ paraffins and olefins | 94.3 | 85.6 | 6.7 | 2.8 | 69.0 | 52.0 |
| Benzene | 0.2 | 1.7 | 89.0 | 95.4 | 24.7 | 45.2 |

*trace indicates less than 0.05%

# REFERENCES


(1) National Academies of Sciences. Engineering and Medicine. *The Changing Landscape of Hydrocarbon Feedstocks for Chemical Production: Implications for Catalysis: Proceedings of a Workshop*; 2016. https://doi.org/10.17226/23555.

(2) Csicsery, S. M. Dehydrocyclodimerization I. Dehydrocyclodimerization of Butanes over Supported Platinum Catalyst. *Journal of catalysis* **1970**, *17*, 207–215.

(3) Csicsery, S. M. Dehydrocyclodimerization. *Industrial and Engineering Chemistry Process Design and Development* **1979**, *18* (2), 191–197. https://doi.org/10.1021/i260070a001.

(4) Csicsery, S. M. Dehydrocyclodimerization II . Dehydrocyclodimerization over Supported of Propane and Pentane over Supported Platinum Catalyst. *Journal of catalysis* **1970**, *17*, 216–218.

(5) Csicsery, S. M. Dehydrocyclodimerization V. The Mechanism of the Reaction. *Journal of catalysis* **1970**, *18*, 30–32.

(6) Lukyanov, D. B.; Gnep, N. S.; Guisnet, M. R. Kinetic Modeling of Ethene and Propene Aromatization HZSM-5. *Ind. Eng. Chem. Res* **1994**, *33*, 223–234. https://doi.org/10.1021/ie00026a008.

(7) Quann, R. J.; Green, L. A.; Tabak, S. A.; Krambeck, F. J. Chemistry of Olefin Oligomerization ZSM-5 Catalyst. *Ind. Eng. Chem. Res.* **1988**, *27*, 565–570. https://doi.org/10.1021/ie00076a006.

(8) Ono, Y. Transformation of Lower Alkanes into Aromatic Transformation of Lower Alkanes into Aromatic Hydrocarbons over ZSM-5 Zeolites. *Catalysis Reviews* **1992**, No. 34(3), 179–226. https://doi.org/10.1080/01614949208020306.

(9) Giannetto, G.; Monque, R.; Galiasso, R.; Galiass, R. Transformation of LPG into Aromatic Hydrocarbons and Hydrogen over Zeolite Catalysts. *Catalysis Reviews—Science and Engineering* **1994**, *36(2)*, 271–304. https://doi.org/10.1080/01614949408013926.

(10) Kitagawa, H.; Sendoda, Y.; Ono, Y. Transformation of Propane into Aromatic over ZSM-5 Zeolites. *Journal of catalysis* **1986**, *101*, 12–18.

(11) Guisnet, M.; Gnep, N. S. Mechanism of Short-Chain Alkane Transformation over Protonic Zeolites Alkylation, Disproportionation and Aromatization. *Applied Catalysis A: General* **1996**, *146*, 33–64.

(12) Caeiro, G.; Carvalho, R. H.; Wang, X.; Lemos, M. A. N. D. A.; Lemos, F.; Guisnet, M.; Ramˆ, F. Activation of C2–C4 Alkanes over Acid and Bifunctional Zeolite Catalysts. *Journal of Molecular Catalysis A: Chemical* **2006**, *255*, 131–158. https://doi.org/10.1016/j.molcata.2006.03.068.

(13) Guisnet, M.; Gnep, N. S.; Aittaleb, D.; Doyemet, Y. J. Conversion of Light Alkanes into Aromatic Hydrocarbons VI. Aromatization of C2-C4 Alkanes on H-ZSM-5 - Reaction Mechanisms. *Applied Catalysis A, General"* **1992**, No. 87, 255–270.

(14) Guisnet, M.; Gnep, N. S. Aromatization of Short Chain Alkanes on Zeolite Catalysts. **1992**, *89*, 1–30.

(15) Haag, W. O.; Dessau, R. M. Proceedings, 8th International Congress on Catalysis, Berlin, 1984; Vol. Vol 2, p Dechema, Frankfurt-am-Main, 305.

(16) Haag, W. O. Catalytic Conversion of Propane to Aromatics, Effects of Adding Ga and or Pt to HZSM-5. *Journal of catalysis* **1994**, No. 149, 465–473.

(17) Bhan, A.; Delgass, W. N. Propane Aromatization over HZSM-5 and Ga/HZSM-5 Catalysts. *Catalysis Reviews* **2008**, No. 50:1, 19–151. https://doi.org/10.1080/01614940701804745.

(18) Krannila, H.; Haag, W. O.; Gates, B. C. Monomolecular and Bimolecular Mechanisms of Paraffin Cracking: N-Butane Cracking Catalyzed by HZSM-5. *Journal of catalysis* **1992**, No. 135, 115–124.

(19) Mole, T.; Anderson, J. R.; Creer, G. The Reaction of Propane over ZSM-5-H and ZSM-5-Zn Zeolite Catalyst. *Applied catalysis* **1985**, *17*, 141–154.

(20) Sirokman, G.; Sendoda, Y.; Ono, Y. Conversion of Pentane into Aromatics over ZSM-5 Zeolites. *ZEOLITES* **1986**, *6*, 299–303.

(21) Biscardi, J. A.; Iglesia, E. Reaction Pathways and Rate-Determining Steps in Reactions of Alkanes on H-ZSM5 and Zn/H-ZSM5 Catalysts. *Journal of catalysis* **1999**, *182*, 117–128.

(22) Price, G. L.; Kanazirev, V.; Dooley, K. M.; Hart, V. I. On the Mechanism of Propane Dehydrocyclization over Cation-Containing, Proton-Poor MFI Zeolite. *Journal of catalysis* **1998**, *173*, 17–27.

(23) Noh, G.; Shi, Z.; Zones, S. I.; Iglesia, E. Isomerization and β-Scission Reactions of Alkanes on Bifunctional Metal- Acid Catalysts: Consequences of Confinement and Diffusional Constraints on Reactivity and Selectivity. *Journal of Catalysis* **2018**, *368*, 389–410. https://doi.org/10.1016/j.jcat.2018.03.033.

(24) Gnep, N. S.; Doyemet, J. Y.; Ribeiro, F. R.; Guisnet, M. Conversion of Light Alkanes into Aromatic Hydrocarbons: 1-Dehydrocyclodimerization Propane on PtHZSM-5 Catalysts. *Applied catalysis* **1987**, *35*, 93–108.

(25) Price, G. L.; Kanazirev, V. Ga2O3/HZSM-5 Propane Aromatization Catalysts: Formation of Active Centers via Solid-State Reaction. *Journal of catalysis* **1990**, *126*, 267–278.

(26) Jacobs, P. A.; Chemistry, Z.; Henares, F. De. DEHYDROCYCLODIMERIZATION OF SHORT CHAIN ALKANES ON Ga/ZSM-5 AND Ga/BETA ZEOLITES. *Zeolite Chemistry and Catalysis* **1991**, No. 5, 409–416.

(27) Dooley, K. M.; Chang, C.; Price, G. L. Effects of Pretreatments on State of Gallium and Aromatization Activity of Gallium/ZSM-5 Catalysts. *Applied Catalysis A: General* **1992**, *84*, 17–30.

(28) Biscardi, A.; Iglesia, E. Structure and Function of Metal Cations in Light Alkane Reactions. *Catalysis Today* **1996**, *31*, 207–231.

(29) Choudhary, V. R.; Kinage, A. K.; Choudhary, T. V. Simultaneous Aromatization of Propane and Higher Alkanes or Alkenes over H-GaAlMFI Zeolite. *Chemical Communication* **1996**, 2545–2546.

(30) Yashima, T.; Fujita, S.; Komatsu, T. Reaction Scheme of Aromatization of Butane over Ga Loaded HZSM-5 Catalyst. *石油学会誌 Sekiyu Gakkaishi* **1998**, *41* (1), 37–44.

(31) Ishaq, M.; Khan, M. A.; Yashima, T. Mechanism of Butane Transformation. *Journal of the Chinese Chemical Society* **2000**, *47*, 1137–1143.

(32) Gnep, N. S.; Doyemet, J. Y.; Seco, A. M.; Ribeiro, F. R.; Guisnet, M. Conversion of Light Alkanes to Aromatic Hydrocarbons II. Role of Gallium Species in Propane Transformation on GaHZSM5 Catalysts. *Applied catalysis* **1988**, *43*, 155–166.

(33) Choudhary, T. V.; Kinage, A. K.; Banerjee, S.; Choudhary, V. R. Effect of Temperature on the Product Selectivity and Aromatics Distribution in Aromatization of Propane over H-GaAlMFI Zeolite. *Microporous and Mesoporous Materials* **2004**, *70* (1–3), 37–42. https://doi.org/10.1016/j.micromeso.2004.01.010.

(34) Scurrell, M. S. Factors Affecting the Selectivity of the Aromatization of Light Alkanes on Modified ZSM-5 Catalysts. *Applied Catalysis* **1988**, *41* (C), 89–98. https://doi.org/10.1016/S0166-9834(00)80384-X.

(35) Viswanadham, N.; Pradhan, A. R.; Ray, N.; Vishnoi, S. C.; Shanker, U.; Prasada Rao, T. S. R. Reaction Pathways for the Aromatization of Paraffins in the Presence of H-ZSM-5 and Zn/H-ZSM-5. *Applied Catalysis A: General* **1996**, *137* (2), 225–233. https://doi.org/10.1016/0926-860X(95)00287-1.

(36) Xiang, Y.; Wang, H.; Matsubu, J. Progress and Prospects in Catalytic Ethane Aromatization. *Catalysis Science & Technology* **2018**, *8*, 1500–1516. https://doi.org/10.1039/C7CY01878A.

(37) Saito, H.; Sekine, Y. Catalytic Conversion of Ethane to Valuable Products through Non-Oxidative Dehydrogenation and Dehydroaromatization. *RSC Advances* **2020**, *10* (36), 21427–21453. https://doi.org/10.1039/d0ra03365k.

(38) Hagen, A.; Roessner, F. Ethane to Aromatic Hydrocarbons: Past, Present, Future. *Catalysis Reviews - Science and Engineering* **2000**, *42* (4), 403–437. https://doi.org/10.1081/CR-100101952.

(39) Ono, Y.; Nakatani, H.; Kitagawa, H.; Suzuki, E. *The Role of Metal Cations in the Transformation of Lower Alkanes into Aromatic Hydrocarbons*; 1989; Vol. 44. https://doi.org/10.1016/S0167-2991(09)61303-3.

(40) Hagen, A.; Roessner, F.; Reschetilowski, W. Conversion of Ethane on Modified Zsm-5 Zeolites: A Study of Aromatization as a Function of Reaction Media. *Chemical Engineering & Technology* **1995**, *18* (6), 414–419. https://doi.org/10.1002/ceat.270180608.

(41) Mehdad, A.; Lobo, R. F. Ethane and Ethylene Aromatization on Zinc-Containing Zeolites. *Catalysis Science and Technology* **2017**, *7* (16), 3562–3572. https://doi.org/10.1039/c7cy00890b.

(42) Lauritzen, A. M.; Madgavkar, A. M. PROCESS FOR THE CONVERSION OF ETHANE TO AROMATIC HYDROCARBONS, US 8871990 B2, 2014.

(43) Lauritzen, A. M.; Madgavkar, A. M. PROCESS FOR THE CONVERSION OF ETHANE TO AROMATIC HYDROCARBONS, US 9144790 B2, 2014.

(44) Lauritzen, A. M.; Madgavkar, A. Madhav. PROCESS FOR THE CONVERSION OF ETHANE TO AROMATIC HYDROCARBONS, 2014.

(45) Chen, N. Y.; Yan, T. Y. M2 Forming — A Process for Aromatization of Light Hydrocarbons. *Industrial and Engineering Chemistry Process Design and Development* **1986**, No. 25, 151–155. https://doi.org/10.1021/i200032a023.

(46) Al-Zahrani, S. M. Catalytic Conversion of LPG to High-Value Aromatics : The Current State of the Art and Future Predictions. *Dev. Chem. Eng. Mineral Process* **1998**, *6*, 101–120.

(47) Rodrigues, V. D. O.; Júnior, A. C. F. On Catalyst Activation and Reaction Mechanisms in Propane Aromatization on Ga / HZSM5 Catalysts. *Applied Catalysis A, General"* **2012**, *435–436*, 68–77. https://doi.org/10.1016/j.apcata.2012.05.036.

(48) Jentoft, F. C.; Gates, B. C. Solid-Acid-Catalyzed Alkane Cracking Mechanisms : Evidence from Reactions of Small Probe Molecules. **1997**, *4*, 1–13.

(49) Choudhary, V. R.; Panjala, D.; Banerjee, S. Aromatization of Propene and n -Butene over H-Galloaluminosilicate ( ZSM-5 Type ) Zeolite. **2002**, *231*, 243–251.

(50) de Jong, K. P. *Synthesis of Solid Catalysts*; Wiley-VCH Verlag GmbH & Co. KGaA: Weinheim, 2009.

(51) Miller, J. T.; Schreier, M.; Kropf, A. J.; Regalbuto, J. R. A Fundamental Study of Platinum Tetraammine Impregnation of Silica: 2. The Effect of Method of Preparation, Loading, and Calcination Temperature on (Reduced) Particle Size. *Journal of Catalysis* **2004**, *225* (1), 203–212. https://doi.org/10.1016/j.jcat.2004.04.007.

(52) Ressler, T. WinXAS: A Program for X-Ray Absorption Spectroscopy Data Analysis under MS-Windows. *Journal of Synchrotron Radiation* **1998**, *5* (2), 118–122. https://doi.org/10.1107/S0909049597019298.

(53) Cybulskis, V. J.; Bukowski, B. C.; Tseng, H. T.; Gallagher, J. R.; Wu, Z.; Wegener, E.; Kropf, A. J.; Ravel, B.; Ribeiro, F. H.; Greeley, J.; Miller, J. T. Zinc Promotion of Platinum for Catalytic Light Alkane Dehydrogenation: Insights into Geometric and Electronic Effects. *ACS Catalysis* **2017**, *7* (6), 4173–4181. https://doi.org/10.1021/acscatal.6b03603.

(54) Cybulskis, V. J.; Pradhan, S. U.; Lovón-Quintana, J. J.; Hock, A. S.; Hu, B.; Zhang, G.; Delgass, W. N.; Ribeiro, F. H.; Miller, J. T. The Nature of the Isolated Gallium Active Center for Propane Dehydrogenation on Ga/SiO2. *Catalysis Letters* **2017**, *147* (5), 1252–1262. https://doi.org/10.1007/s10562-017-2028-2.

(55) LiBretto, N. J.; Xu, Y.; Quigley, A.; Edwards, E.; Nargund, R.; Vega-Vila, J. C.; Caulkins, R.; Saxena, A.; Gounder, R.; Greeley, J.; Zhang, G.; Miller, J. T. Olefin Oligomerization by Main Group Ga3+ and Zn2+ Single Site Catalysts on SiO2. *Nature Communications* **2021**, *12* (1), 1–9. https://doi.org/10.1038/s41467-021-22512-6.

(56) Szeto, K. C.; Jones, Z. R.; Merle, N.; Rios, C.; Gallo, A.; Le Quemener, F.; Delevoye, L.; Gauvin, R. M.; Scott, S. L.; Taoufik, M. A Strong Support Effect in Selective Propane Dehydrogenation Catalyzed by Ga(i-Bu)3 Grafted onto γ-Alumina and Silica. *ACS Catalysis* **2018**, *8* (8), 7566–7577. https://doi.org/10.1021/acscatal.8b00936.

(57) Sattler, J. J. H. B.; Ruiz-Martinez, J.; Santillan-Jimenez, E.; Weckhuysen, B. M. Catalytic Dehydrogenation of Light Alkanes on Metals and Metal Oxides. *Chemical Reviews* **2014**, *114* (20), 10613–10653. https://doi.org/10.1021/cr5002436.

(58) Den Hollander, M. A.; Wissink, M.; Makkee, M.; Moulijn, J. A. Gasoline Conversion: Reactivity towards Cracking with Equilibrated FCC and ZSM-5 Catalysts. *Applied Catalysis A: General* **2002**, *223* (1–2), 85–102. https://doi.org/10.1016/S0926-860X(01)00745-1.

(59) Zhu, X.; Liu, S.; Song, Y.; Xu, L. Catalytic Cracking of C4 Alkenes to Propene and Ethene: Influences of Zeolites Pore Structures and Si/Al2 Ratios. *Applied Catalysis A: General* **2005**, *288* (1–2), 134–142. https://doi.org/10.1016/j.apcata.2005.04.050.

(60) Jun, J. W.; Kim, T. W.; Il Hong, S.; Kim, J. W.; Jhung, S. H.; Kim, C. U. Selective and Stable Production of Ethylene from Propylene over Surface-Modified ZSM-5 Zeolites. *Catalysis Today* **2018**, *303* (May 2017), 86–92. https://doi.org/10.1016/j.cattod.2017.10.004.

(61) Shibata, M.; Kitagawa, H.; Sendoda, Y.; Ono, Y. Transformation of Propene into Aromatic Hydrocarbons over ZSM-5 Zeolites. *Studies in Surface Science and Catalysis* **1986**, *28*, 717–724. https://doi.org/10.1016/S0167-2991(09)60939-3.

(62) Lei, Y.; Jelic, J.; Nitsche, L. C.; Meyer, R.; Miller, J. Effect of Particle Size and Adsorbates on the L3, L2 and L1 X-Ray Absorption near Edge Structure of Supported Pt Nanoparticles. *Topics in Catalysis* **2011**, *54* (5–7), 334–348. https://doi.org/10.1007/s11244-011-9662-5.

(63) Bjørgen, M.; Joensen, F.; Lillerud, K. P.; Olsbye, U.; Svelle, S. The Mechanisms of Ethene and Propene Formation from Methanol over High Silica H-ZSM-5 and H-Beta. *Catalysis Today* **2009**, *142* (1–2), 90–97. https://doi.org/10.1016/j.cattod.2009.01.015.

(64) Bjørgen, M.; Svelle, S.; Joensen, F.; Nerlov, J.; Kolboe, S. Conversion of Methanol to Hydrocarbons over Zeolite H-ZSM-5 : On the Origin of the Olefinic Species. **2007**, *249*, 195–207. https://doi.org/10.1016/j.jcat.2007.04.006.

(65) Svelle, S.; Joensen, F.; Nerlov, J.; Olsbye, U.; Lillerud, K. P.; Kolboe, S.; Bjørgen, M. Conversion of Methanol into Hydrocarbons over Zeolite H-ZSM-5: Ethene Formation Is Mechanistically Separated from the Formation of Higher Alkenes. *Journal of the American Chemical Society* **2006**, *128* (46), 14770–14771. https://doi.org/10.1021/ja065810a.

(66) Corbetta, M.; Manenti, F.; Pirola, C.; Tsodikov, M. V; Chistyakov, A. V. Aromatization of Propane : Techno-Economic Analysis by Multiscale " Kinetics-to-Process " Simulation. *Computers and Chemical Engineering* **2014**, *71*, 457–466. https://doi.org/10.1016/j.compchemeng.2014.10.001.

(67) Chang, C.-W.; Pham, H. N.; Alcala, R.; Datye, A. K.; Miller, J. T. Dehydroaromatization Pathway of Propane on PtZn/SiO2+ZSM-5 Bifunctional Catalyst. *ACS sustainable chemistry and engineering* **2022**, *10* (1), 394–409.

(68) Yaws, C. L. *Yaws' Handbook of Thermodynamic and Physical Properties of Chemical Compounds*; Knovel, 2003.

(69) Guisnet, M.; Lukyanov, D. Aromatization of Short Chain Alkanes on Ga MFI Catalysts. *Studies in Surface Science and Catalysis* **1994**, *90* (C), 367–378. https://doi.org/10.1016/S0167-2991(08)61847-9.

(70) Ahmed, K.; Chowdhury, H. M. Dehydrogenation of Cyclohexane and Cyclohexene over Supported Nickel and Platinum Catalysts. **1992**, *50*, 165–168.

(71) Caspary, K. J.; Gehrke, H.; Heinritz-Adrian, M.; Schwefer, M. Dehydrogenation of Alkanes. In *Handbook of Heterogeneous Catalysis*; 2008; pp 3206–3229.